2021

Geological Survey Paper 7:

Structural Geology of the Central Tyennan Region, Tasmania

Authors: D. R. Gray
M. J. Vicary
Date: 28/09/2021
Email: info@mrt.tas.gov.au
Website: www.mrt.tas.gov.au

REPORT No: GSP7

Southwestern part of the Central Tyennan region at Mt. McCall. The view is looking northwards with quartzites of the low-grade Fincham-Mary metamorphic sheet in the foreground. The Andrew River Valley bounded to the north by the Engineer Range is in the right background. The quartzites are west-dipping on the western limb of the Devonian Mt Mcall Anticline.

Tasmanian Government

Mineral Resources Tasmania
mrt

CONTENTS

Abstract

The large-scale structure of the Central Tyennan region is a laterally tapered, bulbous, macro-fold "wedge" elongated in the direction of the fold plunge. It is cored by high-grade schists and garnet quartzite of the Franklin-Joyce metamorphic sheet, in-folded and bounded by low-grade quartzites and phyllites of the Fincham-Mary metamorphic sheet. The gross geometry is that of a series of regional-scale, recumbent isoclinal folds (fold-nappes) bounded by high strain zones of platy quartzite, quartz-mica phyllite and phyllite. The structurally highest Franklin fold-nappe dominates the macro-fold "wedge" with a ~40 km axial surface strike-length, a maximum ~7 km thickness and a minimum down-plunge extent of ~20 km. It has an extremely attenuated, flattened and elongated form towards the south and some apparent attenuation to the east. Much of the macro-fold geometry shows a reclined fold form (i.e. fold plunge in the dip direction of the axial surface). Scarce younging data suggests the western limb of Fincham Quartzite is overturned.

Three apparent fold-nappes involving high-grade Franklin-, Joyce and low-grade Fincham-Mary Metamorphic sheets sit on the underlying low-grade Scotchfire Metamorphics. The most continuous recumbent fold is the structurally highest south-facing and closing Franklin synformal fold-nappe to the west, underlain by a north-facing and closing antiformal closure of the Redan Hill recumbent fold, and then the south-facing and closing synformal Collingwood Plain recumbent fold to the east. The structurally lowest recumbent fold is segmented into a series of high-grade fold hinge-cores as pods bounded by intensely foliated, retrograde quartz-mica phyllite. These include the Collingwood Plain and Joyce Creek closures.

The Franklin fold-nappe shows an along strike transition from 1) an isoclinal fold stack in a thicker bedded quartzite-schist sequence (Raglan Range) to 2) a higher strain, hinge domain with conical, sheath-like hinges (closed loop outcrop patterns at Mt Madge and Mt Maud), to 3) attenuated tapering hinge form (Engineer Range and Mt McCall). The closed loop outcrop patterns and curvilinear fold hinges reflect bulbous hinge projections of downward penetrating, synformal closures in the high-grade Franklin-Joyce metamorphic sheet interpenetrating with upward projecting, antiformal hinges in the underlying low-grade Fincham-Mary metamorphic sheet.

Both the high-grade (Franklin-Joyce metamorphic sheet) and the low-grade (Fincham-Mary metamorphic sheet) sheets are internally isoclinally folded and show a consistent mineral stretching lineation and marked rodding to mullion structure in fold hinges. There is a consistent west-northwest to northwest stretching lineation that is clustered about a vector mean of 32°/302°, within a bimodal contoured population where modes of 24°/293° and 24°/309° largely reflect the mineral lineation orientation change from limb to limb of the recumbent isoclinal macro-folds. Other influences may include the younger Devonian refolding and possible folding about a vertical axis. Fold hinges in general are sub-parallel to the mineral stretching lineation (Lm) but do fan about the axial surface traces of the major recumbent macro-folds.

Restored shear sense indicators (shear bands) give calculated Central Tyennan transport directions of towards 110° (Mt McCall), 115° (Frenchmans Cap) and 136° (Collingwood Plains). In all cases data have been rotated to 1) remove the plunge of the younger Devonian folding, and 2) return the foliation Sm to the horizontal.

The Central Tyennan domain prior to fold-nappe formation is considered a series of stacked metamorphic sheets from top to bottom as 1) high-grade Franklin-Joyce Metamorphic sheet with garnet schists and schistose garnet quartzites enveloping lenses of eclogite and amphibolite at the highest level in the sheet, underlain by 2) low-grade Fincham-Mary quartzites, schistose quartzites and phyllites, underlain by 3) low-grade Scotchfire dolomitic schist/phyllite incorporating dolomite. Interfaces between the sheets are commonly intensely foliated, retrograded quartz-mica phyllites.

Tasmanian Government

Mineral Resources Tasmania

Department of State Growth
www.mrt.tas.gov.au

Structural Geology of the Central Tyennan Region, Tasmania

David R. Gray[1] and Michael J. Vicary[2]
1. Consultant Structural Geologist to Mineral Resources Tasmania
2. Geological Survey Branch - Mineral Resources Tasmania

ARTICLE INFO

Published: 28 September 2021
Publisher: Mineral Resources Tasmania
Report No.: GSP7

KEYWORDS

Structural Geology
Frenchmans Cap
Central Tyennan Region

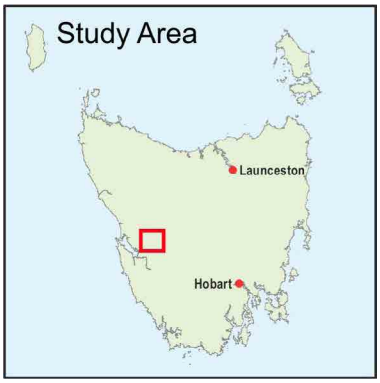

1.0 INTRODUCTION

This Tasmanian Geological Survey Paper is the second in a series of Papers revisiting the structural geology of parts of the Tyennan Block (after Carey, 1953; Turner 1989, fig. 2.10) or Proterozoic nucleus of Tasmania (Figure 1).

The Tyennan nucleus is the belt of Early Neoproterozoic quartzite and phyllite (quartz-chloritic pelite assemblage and garnetiferous schist-quartzite ± amphibolite assemblage after Spry, 1962a, 1963a) that extends from Cradle Mountain in the north, to Southwest Cape in the south (Figure 1b). The Tyennan region represents the major part of the Internal Zone of Berry (2014, fig. 4.2).

The Central Tyennan domain part of the Tyennan nucleus is the northernmost part of the contiguous outcrop belt extending to the southern coastline (Figure 1b). The region is bounded on the north by the Eldon River and extends to Mt McCall in the south, the King William Range in the east and Lake Burbury on the west (see Figure 2).

The aim of this Structural Geology series reappraisal has been to re-examine the structure of the Tyennan Proterozoic rocks in the context of ophiolite obduction and continental margin subduction-obduction (see Berry & Crawford, 1988; Berry 2014, fig. 4.10).

The main elements of this model are:

1. the former passive continental margin (now preserved as the Rocky Cape autochthon);
2. the widespread mafic and ultramafic complexes in Tasmania (relicts of an early Cambrian allochthonous sheet analogous to the Oman ophiolite);
3. high P metamorphism of parts of the subducted margin,;
4. the resultant stacked high-grade and low-grade metamorphic sheets that comprise the Tyennan region (internal zone); and
5. the para-autochtonous, non-metamorphosed to very low-grade overlying sheets (external zone).

Deformation of the Rocky Cape margin beneath the advancing ophiolite sheet has involved crustal-scale stacking of parts of the margin as sheets of different metamorphic grade, isoclinal folding and internal deformation of the sheets, and deformation or welding along their contacts as shear zones ±brittle faulting. The Tyennan region of Tasmania provides a 50-100 km wide window into these underlying rocks, their internal deformation and the nature of their contacts due to the subsequent erosion and removal of the obducted ophiolite sheet.

2.0 BACKGROUND

The structural geology of the Central Tyennan domain (Figure 2) is treated in 3 parts/regions including:

1. the northern part from the Lyell Highway south incorporating the Raglan Range, Mt Mary, Mt Maud to Mt Fincham;
2. the Frenchmans Cap area including Clytemnestra and Agamemnon; and
3. the southernmost part the Mt McCall area.

Each region contributes to the overall geometry and structural understanding of this part of the Tyennan and the Tyennan massif overall.

The Raglan Range-Mt Mary-Mt Maud-Mt Fincham domain (dashed Box 1, Figure 2) provides definition of the geometry of the Franklin fold-nappe, the Collingwood Plains fold-nappe, the Franklin and Joyce parts of the high-grade Franklin-Joyce metamorphic sheet, the low-grade Fincham-Mary metamorphic sheet and the structurally lowest Scotchfire metamorphic sheet.

Frenchmans Cap (dashed Box 2, Figure 2) provides a vertical section through quartzite of the low-grade Fincham-Mary sheet and across the contact with the underlying low-grade Scotchfire metamorphic sheet. It shows the structure in the lower part of the Finchman-Mary sheet and the geometry and character of recumbent macro-folds transitional into high strain zones towards the base of the sheet. The structure of the Frenchmans Cap region is presented in a separate publication (Geological Survey Paper 6: Gray & Vicary, 2021).

Mt McCall (dashed Box 3, Figure 2) provides a section through the high-grade Franklin metamorphic sheet incorporating the hinge of the Franklin fold-nappe, as well as the contacts with the Fincham-Mary metamorphic sheet.

2.1 Mapping

Regional mapping in the 1950's by Mather (1955), McLeod (1955, 1956), Spry (1957) and Spry & Zimmerman (1959) was undertaken as part of the dam-site selection process for the central-northern river catchments and

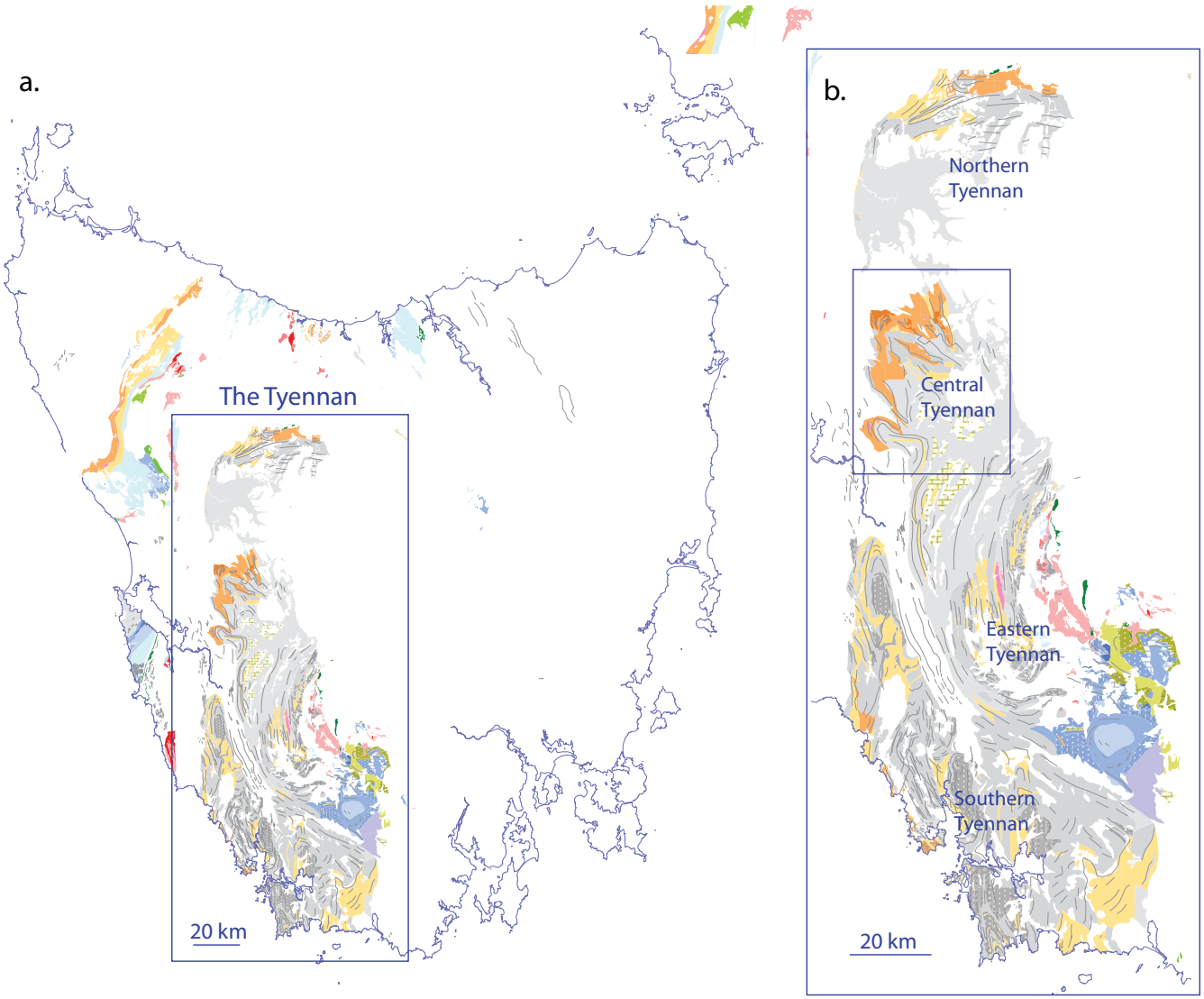

Figure 1. The Tyennan Proterozoic region of Tasmania shown in a). Map base is Mineral Resources Tasmania 1:25000 and 1:250000 digital geological atlas. b) Enlarged map with the location of the Central Tyennan region. The divisions within the Tyennan are after Berry (2014). The approximate Central Tyennan map sheet polygon boundaries are 5345400mN (northern boundary), 5300000mN (southern boundary), 390000mE (eastern boundary) and 429000mE (western boundary).

the then proposed Franklin above Gordon dam (Figure 3). In the 1960's Honours thesis mapping was undertaken by Gee (1962) along the Raglan Range and McIntyre (1964) in the Collingwood Plain area, and also with the PhD completion by Spry (1962b). In the 1970's Honours thesis mapping was undertaken by Turner (1971) at Flat Bluff-Mt Madge and by Williams (1971) at Mt McCall. The Frenchmans Cap area (dashed box 2, Figure 2) was mapped and described by Duncan (1974) with mapping undertaken in 1964 and 1965 as part of a PhD at the University of Tasmania (Duncan, 2021).

Mapping by Gee (1962, 1963) recognised the macro structure on the Raglan Range (Figure 3) as a stack of isoclinal folds. Spry and Gee (1964) showed that these folds were recumbent isoclinal folds by unfolding or removing the effects of the younger Devonian folding. The overall regional structure was interpreted by Spry (1963a) as a series of fold-nappes involving both the low-grade and high-grade sequences. Spry argued for a major large-scale recumbent fold (the Pillinger fold) with fold-nappe geometry similar to the slides in the Scottish Highlands, but chose an east-closing geometry for this fold.

Some of the early work was incorporated into the compilation of the 1:50000 Lyell mapsheet (Calver et al, 1987) with limited filed traverses by Turner, 1986, and on subsequent 1:25000 digital geological compilations: Green and Everard (1998); Green and Everard (2003); Vicary (2004a, 2004b).

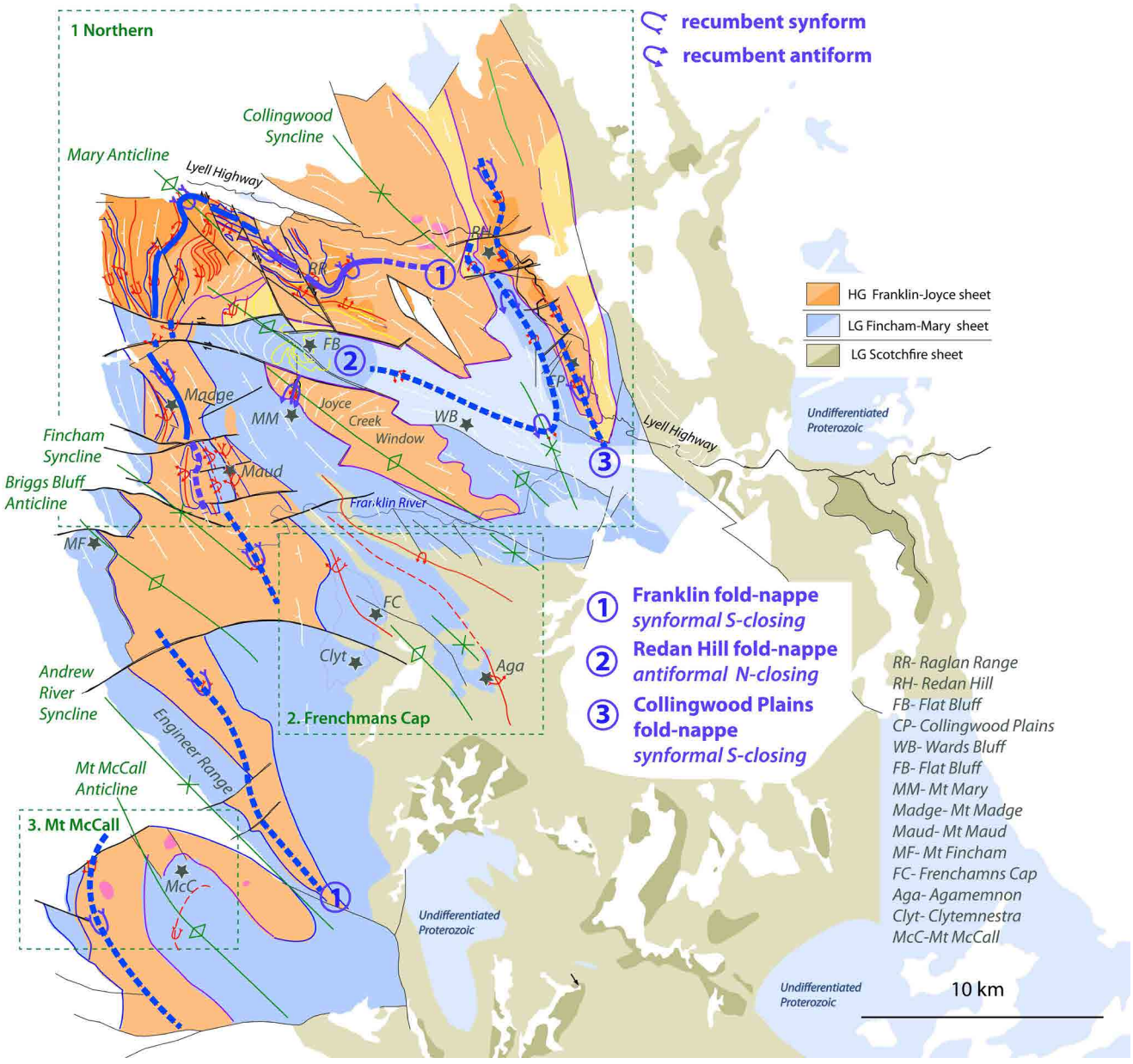

Figure 2. Central Tyennan litho-structural summary map with axial surface traces of regional fold-nappes (heavy blue and blue dashed lines.) Map base is the Mineral Resources Tasmania 1:25000 and 1:250000 Digital Geological Atlas. Orange: high-grade Franklin Metamorphic sheet; Dark orange: garnet quartzite; blue: low-grade quartzite-phyllite sequences of Fincham-Mary Metamorphic sheet; olive green: Scotchfire sheet; light blue: undifferentiated Proterozoic rocks. Dashed boxes are regions that are treated separately within the Central Tyennan chapter or published separately. These are: 1. the Northern domain, 2. the Frenchmans Cap domain and 3. the Mt McCall domain in the south.

2.2 Nature of the Layering, Foliations and Lineations

The schists, quartzites and phyllites of the Central Tyennan region show high strain fabrics typified by strong to intense foliation and transposition layering/ foliation (Sm), rodding fabrics within the transposition layering, mesoscopic isoclinal folds, rootless isoclinal fold pairs, and multiple crenulation cleavages.

There are five types of layering and foliation:

1. So/Sm: compositional banding sub-parallel to a strong to intense foliation that is folded by recumbent isoclinal folding
2. Intense foliation (dominant Sm) which is axial surface to the major recumbent isoclinal macro-folds. Associated with this layering is a marked rodding fabric within the Sm layering. This is the regional foliation that envelopes macro- to meso- fold "pods". The pods occur at all scales up to the scale of the Frenchmans Cap recumbent isoclinal fold.
3. Crenulation cleavages (Scc) associated with development of transposition layering in the basal high strain zones or lower limb to the recumbent folds.
4. Shear Band (S-C') foliation (Sb) as a form of extensional crenulation cleavage that reflects shear-induced, foliation-oblique late stage flattening. These zones areessentially secondary shear zones that record the overall shear sense and/or emplacement direction.
5. Spaced cleavage (Scl) a younger Devonian cleavage that overprints all three foliations listed above.

There are four types of lineations:

1. A mineral lineation (Lm) generally defined by mica and/or elongated quartz grains in the quartzite;
2. An elongation or stretching lineation (Lelong) most commonly shown by elongated quartz grains;
3. A rodding lineation (Lrod) that changes from an initial intersection lineation at high angle to the regional stretching direction, to a "herringbone" pattern where flattened mesoscopic fold hingelines become curvilinear and pulled apart, to eventually develop a strong, sub-parallel alignment with the regional stretching direction (Lstretch);
4. A crenulation lineation (Lcren) as tiny puckers or wrinkles within the foliation.

2.3 Structural Petrology

Structural petrology by Spry (1957, 1963a, 1969), with influences on Gee (1963), Williams (1971) and Turner (1971), provided links between the deformation sequence, the structural fabrics and the metamorphism. The work of Allan Spry had a considerable influence on the understanding of the structural and metamorphic history of the Tasmanian Proterozoic rocks.

The work demonstrated that:

1. The first fabric S1 is either parallel or at a low angle to bedding and not associated with folds (Spry, 1963a).
2. Mesoscopic isoclinal folds are within the S1/So layering and have an axial surface S2 crenulation cleavage.
3. Visible isoclinal folds of all scales are attributed to F2 (Spry, 1957, 1963a).
4. Apart from within F2 fold hinges there is a difficulty in recognising S-surfaces S0, S1 and S2 as they are essentially sub-parallel along the limbs of the isoclinal folds.
5. Lamination in many schists and phyllites is S2 and not S0, where the contacts between quartzite and schist/phyllite are strongly transposed layering.
6. The isoclinal folding (F2) is part of a retrograde metamorphic event involving decompression (Turner, 1971).

For the low-grade rocks Spry (1963a) argued that the quartz-sericite content of siliceous rocks in the low-grade Fincham-Mary metamorphic sheet and Scotchfire metamorphic sheet dictated their deformation behaviour.

Massive quartzites with low sericite content appear only partly deformed, commonly with discernable bedding and visible quartz grains. Under the microscope they show mortar texture with large xenoblastic grains with undulose extimction surrounded by a quartz matrix of small grains showing slight elongation (Figure 4a).

In platy quartzite and quartz -mica schist there is visible sericite on foliation planes where the foliation is defined by strong elongation and flattening of quartz and tiny parallel sericite flakes (Figure 4b).

The low-grade phyllites are mineralogically simple consisting of alternating layers of sericite and quartz (Figure 4c). They are however structurally complex and have the attributes of phyllonites. They contain cm-scale, tight contortions as tiny recumbent isoclinal folds with sheared out limbs, fold mullions, quartz-rods and quartzite boudins (Spry, 1963a, p.110).

For the high-grade rocks of the Franklin and Joyce Metamorphics (including muscovite schists, knotted albite schists, garnet-muscovite schists, fine-grained dark biotite schists, coarse gneissic schists and graphitic phyllites) the main fabric is an S2 schistosity. This schistosity consists of alternating mica-rich and quartz rich layers. An older foliation S1 is "visible as contorted relicts between the layers of S2 and also within porphyroblasts" (Spry, 1963b, p.204). Mica and quartz tend to be elongate along S1 and also along S2 (Figure 5).

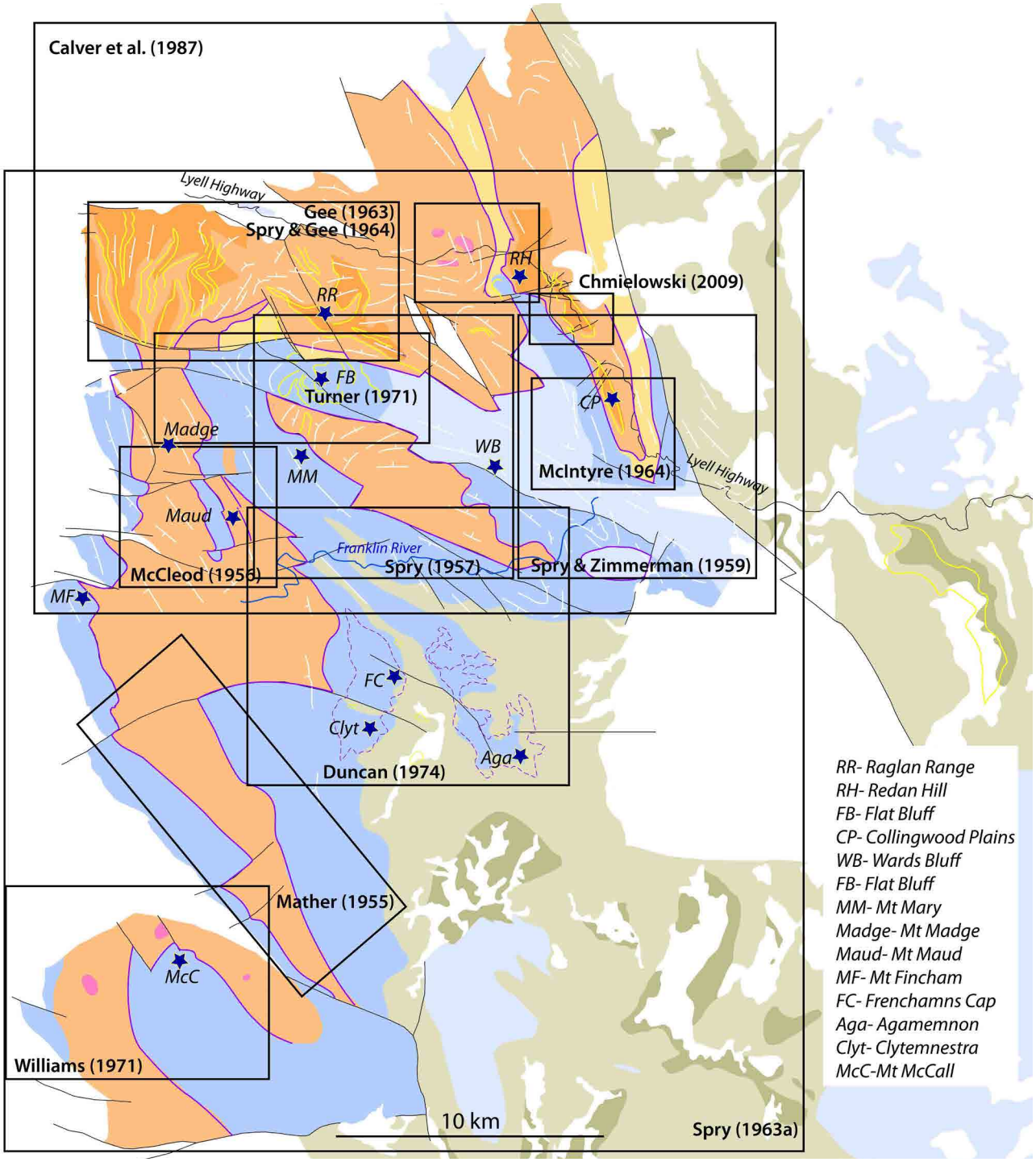

Figure 3. Index map for structural data sources for the Central Tyennan. All of the structural work was done in the 1960's and 1970's, with some mapping for the Hydro in the 1950's for the then proposed dam on the Franklin River. Compilation of the Lyell 1:50000 Geological Map sheet was completed in 1987. Map base is the 1:250000 and 1:25000 digital geological atlas from Mineral Resources Tasmania.

The high-grade rock fabric-porphyroblast relationships and mineralogical associations (Spry, 1963a, b; Gee, 1963; Turner, 1971) show:

1. The dominant schistosity Sm is formed by crenulation of an earlier fabric (S1). Figure 5a shows hinges in S1 layering within S2 microlithons. Figure 5b shows relict hinges and limbs oblique to Sm (S2) and albite porphyroblasts with Si (internal foliation) oblique to Sm the dominant fabric.
2. Garnet and albite porphyroblasts are both wrapped by the S2 foliation.
3. Garnet porphyroblasts display two textural habits: i. "snowball" garnets with inclusions of quartz arranged in symmetrical sigmoidal lines, some with "massive" rims free of inclusions, ii. fractured, massive, idioblastic crystals strung out along the S2 foliation (Gee 1963, p.13).
4. Albite porphyroblasts occur in two forms that differ in size, type of inclusions and twinning. Smaller albites are untwinned and contain curved helicitic trails of small opaques. Large albites, up to 1 cm, are commonly twinned, with abundant inclusions of quartz, muscovite and garnet in straight or slightly curved lines with Si (internal foliation) discordant to Se (external foliation Sm) (see Figure 5c).

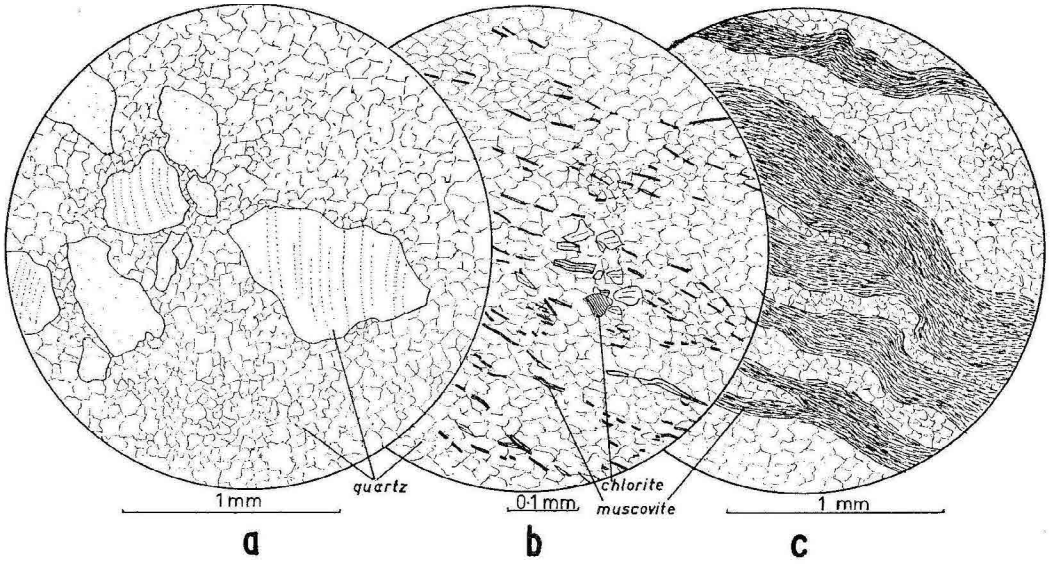

Figure 4. Microstructural fabric relationships in low-grade Mary metamorphic sheet rocks shown in camera lucida sketches from Spry (1963a, fig.3). a) Massive quartzite with mortar texture. b) Quartz schist. c) Phyllite with So and S1 essentially parallel.

Medium-grade quartzites generally contain a single foliation marked by elongate quartz and mica, where occasional relict garnets have web-like crystals with "snowball" structure. Macroscopically the quartzites contain thin layers of schist and have a colour banding "with the strong, single foliation sub-parallel to the schist layers and colour banding" (Spry, 1963b, p.205).

2.4 Metamorphic Petrology and Metamorphism

The Franklin Metamorphic Complex (after Meffre et al, 2000) of the Central Tyennan, defined here as the Franklin-Joyce metamorphic sheet (Figures 2 and 6), has the highest metamorphic grades in Tasmania (Meffre et al., 2000; Chmielowski & Berry, 2012; Palmeri et al., 2009).

The Franklin-Joyce metamorphic sheet consists largely of pelitic schist, minor quartzite and pod-like lenses of amphibolite and eclogite (Meffre et al., 2000), apart from the Raglan Range where "thick slabs of intensely internally folded quartzite and quartz-muscovite-albite-garnet schist occur in approximately equal proportions" (Gee, 1963, p.11). Garnet-, kyanite- and albite-bearing schists are common.

Metamorphic petrology by Chmielowski (2009), Chmielowski and Berry (2012), Palmeri et al. (2009) and Brown et al. (2021) show that:

1. Eclogite lenses within metapelites underwent early metamorphic conditions of ~560°C at ~0.56GPa with peak metamorphism at ~600-650°C and pressures >1.5GPa (Palmeri et al., 2009);
2. Peak conditions for the schists are 700°C and 1.4GPa, but garnet zonation indicates that initial garnet growth occurred at ~560°C (Chmielowski and Berry, 2012);
3. The white schists occur as an alteration rind about a possible mafic boudin (Chmielowski 2009, Chmielowski and Berry 2012). Minerals of the white schists include talc, kyanite, garnet and quartz and give 540°C and 1.96Ga (Chimeloswki, 2009).

A general discussion of the Franklin Metamorphic Complex (the Franklin-Joyce metamorphic sheet), in relation to the other Tyennan metamorphic complexes, is provided by Turner (1989) and Meffre et al. (2000).

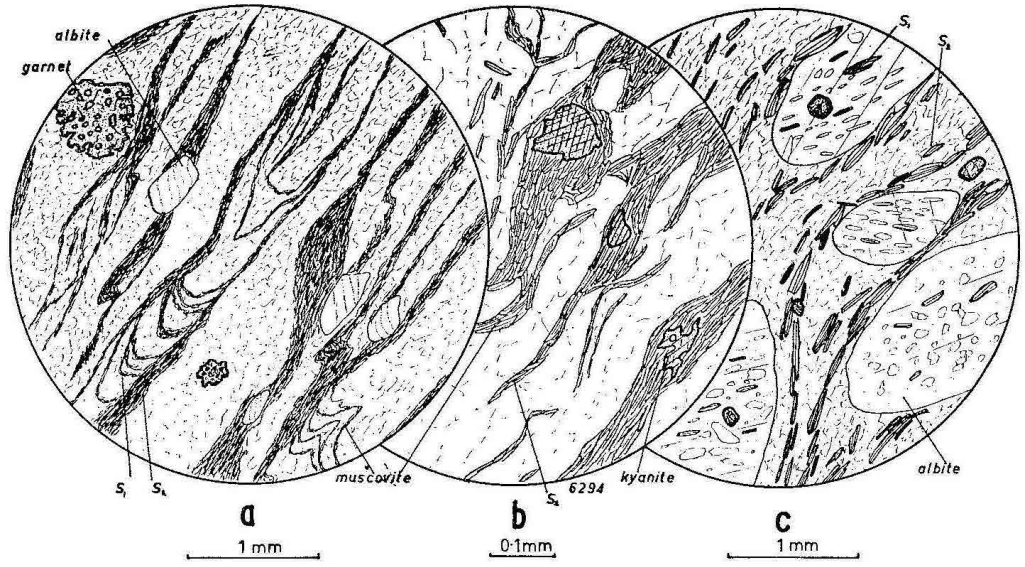

Figure 5. Microstructural fabric relationships in high-grade Franklin Metamorphics (camera lucida sketches from Spry, 1963a, fig.5). a) Garnet-mica schist with two fabrics, a crenulated S1 with mica-rich limb zones as a spaced S2 crenulation cleavage/schistosity. b) Muscovite-quartz schist with domainal schistosity with kyanite in the mica domains. c) albite-muscovite schist with domainal schsitosity wrapping around albite prophyroblasts containing S1 as inclusion trails.

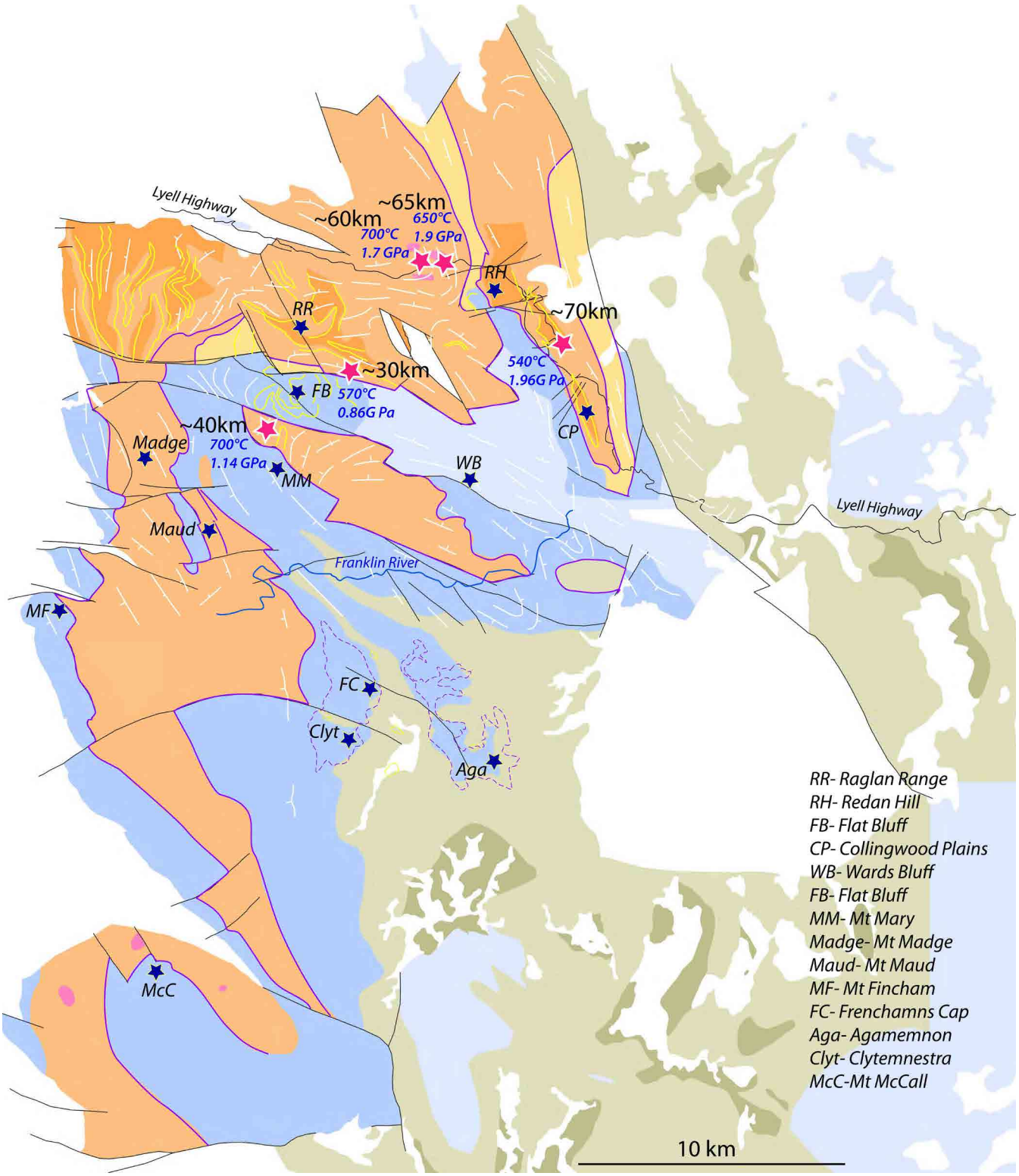

Figure 6. Franklin Metamorphic complex (orange) with metamorphic PT data from Chmielowski (2009). Sample locations are highlighted by red stars. T and P estimates are shown in blue. Inferred crustal depths (km) for the metamorphism(s) are shown in black. Map base is the 1:25000 and 1:250000 digital geological atlas from Mineral Resources Tasmania.

2.5 Significance of Metamorphism for the structural evolution of the Central Tyennan Region

Chmielowski & Berry (2012) present a tectonic model involving 1) rapid compression in a subduction zone setting followed by 2) an even more rapid, decompression that brought various fault-bounded metamorphic complexes back to the surface in less than 5 Ma.

They proposed two models to explain differences in pressure between the various entities in the Franklin-Joyce metamorphic sheet:

1. Different parts of the segmented margins were subducted to different levels;
2. Subduction zone geometry resulted in significantly different pressures occurring similtaneously within portions of the channel, which are not far removed from one another.

Further to this, Palmeri et al. (2009) suggest two possibilities for the eclogite pods/boudins and host schists:

1. The mafic rocks and hosting schists underwent the same P-T evolution (including high pressure) but the enclosing schists were totally re-equilibrated during retrogression;
2. The mafic rocks and hosting schists attained peak metamorphism at different crustal levels, at nearly the same age, but the mafic rocks were rapidly uplifted and coupled with the schist host-rocks at shallower crustal levels, and then developed a common history from amphibolite facies conditions.

From the perspective of structural petrology the deformation history has been interpreted by:

1. Gee (1963) defined deformation phases as:

   First phase: produced the bedding schistosity and the mineral lineation with the "regional" peak metamorphism producing chlorite, biotite and almandine in a zonal arrangement: "stacked sheets" concept?

   Second Phase: involved retrograde metamorphism accompanied by large scale recumbent folding with development of a basal phyllonite (Governor River Phyllite of the Franklin Group). This equates to the base of the Franklin Joyce sheet. Gee (1963) describes the Governor River Phyllite as a tectonic slice that developed with emplacement of the Franklin Group over the Mary Group.

2. Turner (1971, 1989) re-interpreted the porphyroblast relationships using criteria from Bell et al (1986) to argue for a single prograde metamorphic event initiated at the start of the second deformation and persisting until maximum S2 foliation development.

2.6 Current Structural Compilation

This Central Tyennan region investigation and reappraisal is based on:

1. Structural data collected by the authors on traverses along the Lyell Highway and the Mt McCall road, and a helicopter day-trip into Frenchmans Cap, involving a traverse from Lions Head ridge down to Lake Tahune and visits to Clytemnestra and Agamemnon; and
2. Analysis, re-interpretation and compilation of all existing data primarily from mapping by Gee (1963), Spry (1963a, 1963b), Spry & Gee (1964) for the Raglan Range, Mt Mary area by Spry (1957), Mt Mullen area by Spry & Zimmerman (1959) and McIntyre (1964), Mt Madge and Flat Bluff area by Turner (1971), Mt McCall by Williams (1971), Frenchmans Cap by Duncan (1974), and metamorphic petrology by Chmielowski (2009), Chmielowski and Berry (2012), and Palmeri et al. (2009) (see Figure 3).

All measurements/ orientations cited in the text are true unless stated as magnetic. Structural data is presented in Appendix 2.

All map grids and grid references in the text have a GDA94 datum with MGA coordinates in Zone 55.

3.0 CENTRAL TYENNAN REGION GEOLOGY OVERVIEW

The Central Tyennan region consists of the high-grade Franklin-Joyce metamorphic sheet, previously referred to as the Franklin Metamorphics by Spry (1963a) and the Franklin Metamorphic Complex by Meffre et al. (2000). This high-grade metamorphic sheet is structurally interleaved and folded with lower grade rocks of the Fincham-Mary metamorphic sheet (after Spry, 1963b, fig.2), which is infolded with the underlying low-grade Scotchfire Metamorphic sheet (Figures 2 and 7).

The high-grade rocks of the Franklin-Joyce metamorphic sheet consist of massive and schistose quartzite (commonly containing phengite, almandine and chlorite) intercalated with thinly banded, pelitic, garnetiferous quartz-mica schists (commonly containing phengite, biotite, almandine, albite and chlorite) and lenses of amphibolite and eclogite (Spry, 1963c; Meffre et al., 2000; Chmielowski & Berry 2009). The eclogites and amphibolites have continental rift tholeiite affinity (Meffre et al., 2000). Garnet-, kyanite- and albite-bearing schists are common (Meffre et al., 2000; Chmielowski, 2009).

These high-grade and low-grade metamorphic sheets have been isoclinally folded as part of a large, regional scale fold-nappe cored by high-grade units of the Franklin-Joyce metamorphic sheet (the Franklin Metamorphics of Spry, 1963a). The form and taper of the high-grade rocks in the Raglan Range fold stack require a south-facing and closing synformal geometry (Figure 7).

Both the Franklin-Joyce metamorphic sheet and the low-grade Fincham-Mary metamorphic sheet are internally isoclinally folded, show a consistent mineral stretching lineation and marked rodding to mullion structure in fold hinges (Gee, 1962, 1963; Turner, 1971).

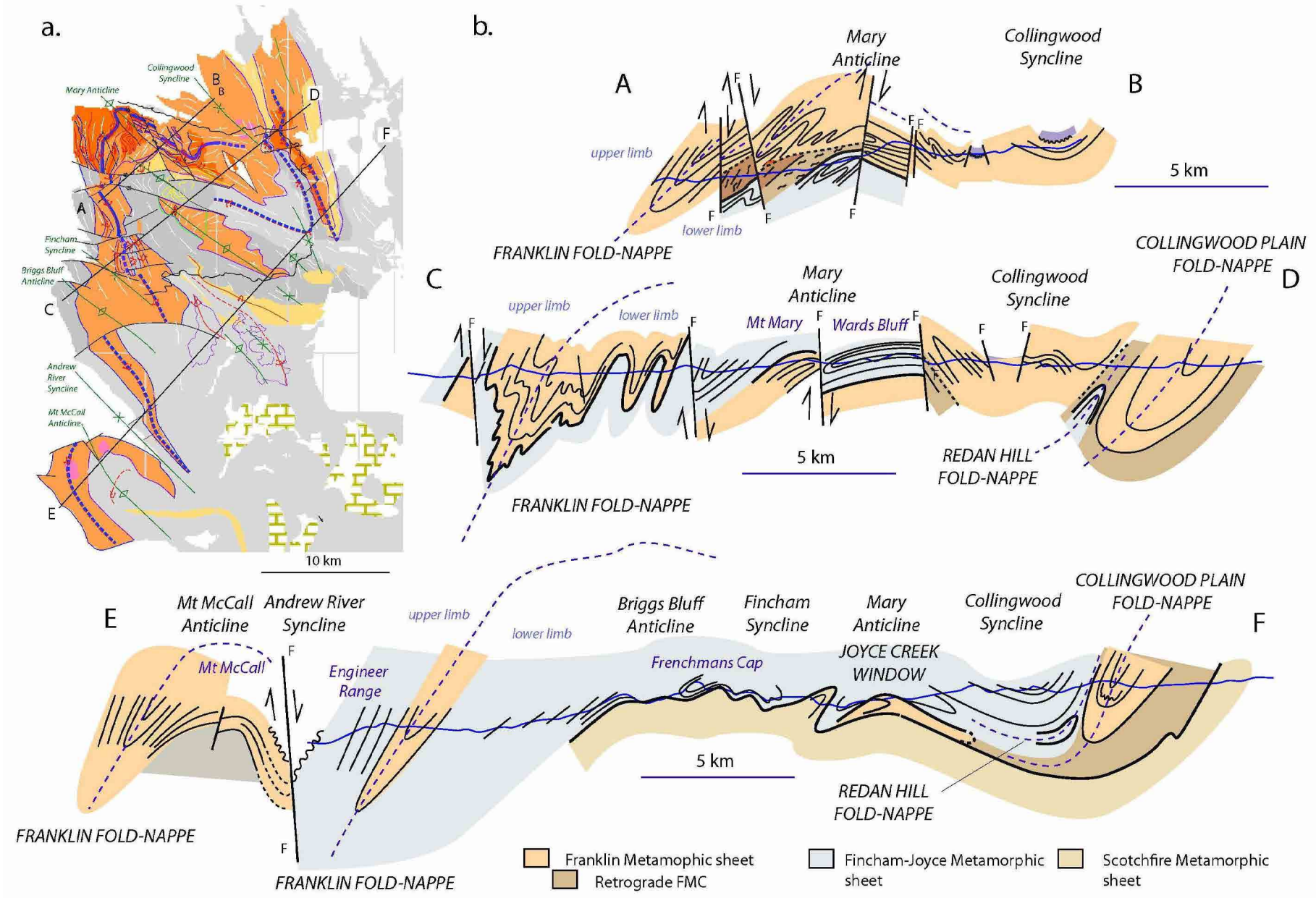

Figure 7. Central Tyennan region cross-sections a) Location map of section lines. Legend: Orange: high-grade sequences; grey: low-grade quartzite, schist -phyllite sequences ; yellow: low-grade dolomitic schist-phyllite. b). Cross sections A-B, C-D and E-F through the Central Tyennan region with the section lines shown in the inset.

Three fold-nappes in the high-grade Franklin- Joyce and low-grade Mary-Fincham metamorphic sheets sit on the underlying low-grade Scotchfire metamorphic sheet (Figures 2 and 7). The most continuous recumbent fold is the structurally highest south-facing and closing Franklin synformal fold-nappe to the west (Figure 7a), underlain by a north-closing antiformal closure (the Redan Hill recumbent fold), and then the south-closing synformal Collingwood Plain recumbent fold to the east (Figures 7b and 7c).

The Central Tyennan region prior to fold-nappe formation is considered as a series of stacked sheets from top to bottom as 1) high-grade Franklin-Joyce metamorphic sheet with garnet schists and schistose garnet quartzites enveloping lenses of eclogite and amphibolite at the highest level in the sheet, underlain by 2) low-grade Fincham-Mary metamorphic sheet with quartzites, schistose quartzites and phyllites, underlain by 3) low-grade Scotchfire metamorphic sheet with dolomitic phyllite and dolomite.

3.1 Map Pattern and Regional Relations

The Central Tyennan map pattern is dominated by the Franklin fold-nappe complex and macro- to mesoscopic isoclinal folding within both the high-grade and low-grade units (Figures 2 and 8). The Franklin, and associated Redan Hills and Collingwood Plain fold-nappes define the Central Tyennan fold-nappe complex (Figures 2 and 7). This fold-nappe complex is re-folded by younger northwest-trending and gently northwest-plunging anticlines and synclines with the Mary Anticline and Collingwood Syncline the largest of these folds (green axial surface traces, Figure 8).

Both the early fold-nappes and the younger northwest-trending folds are offset by steeply dipping

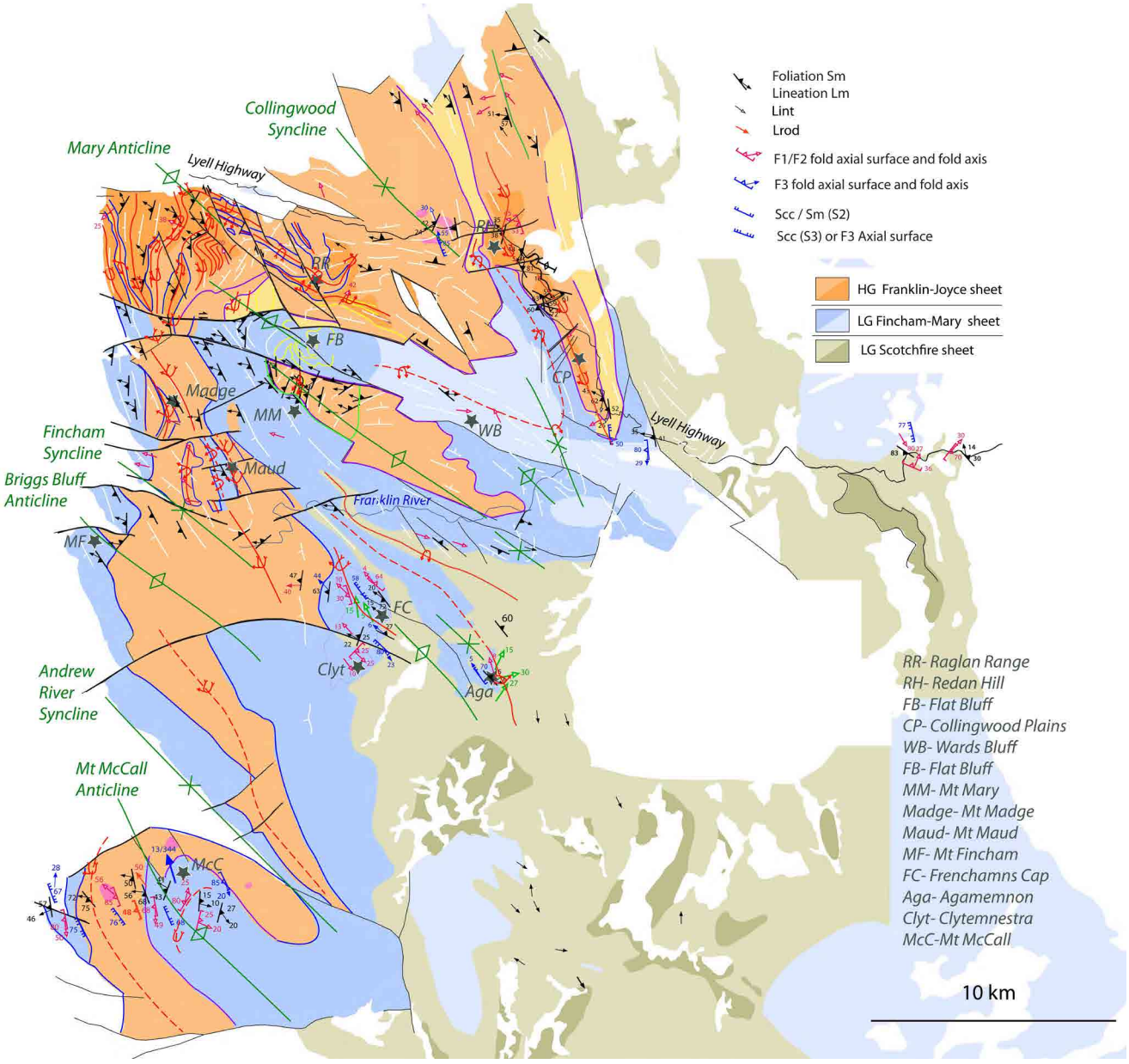

Figure 8. Central Tyennan structural map showing foliation Sm and lineation Lm data, and early recumbent (red traces) and late (green traces) fold axial surface traces, The high-grade rocks are shown as deep orange (garnet quartzite) and orange (garnet schist). The low-grade rocks are shown in blue (quartzite-schist/phyllite), khaki (phyllite/ dolomitic schist), dark olive (dolomite) and light blue (undifferentiated Proterozoic rocks). Map base is the 1:25000 and 1:250000 digital geological atlas from Mineral Resources Tasmania. An A3 version of Figure 8 is attached in Appendix 1.

west-northwest-trending and east-west trending Late Silurian-Devonian brittle faults (black traces, Figure 8). These faults have oblique slip movements with dextral strike slip component in plan and south-side up or north-side down components (Gee, 1963; Spry and Gee, 1964). In-folded and fault-bounded graben-like elements containing Ordovician limestone and Silurian strata occur at Bubs Hill and north of Franklin Hills. These reflect basin-controlling normal-faulting along the Linda Zone (Seymour, 2014, p.291), but with later reactivation of these faults in the Devonian.

3.2 Early Fold Hinge Pattern

The high-grade and low-grade sheets all show tight to isoclinal recumbent folds generally less than metre scale but up to 10's of metres (Spry, 1957, 1963a; Gee, 1963; Spry and Gee, 1964; Turner, 1971). Meso-folds show attenuated limbs, mullion structure in fold hinges and boudinage on fold limbs (Spry, 1963a; Gee, 1963; Spry and Gee, 1964). Isoclinal folds are commonly asymmetric Z-folds (down plunge), disharmonic with respect to the dominant layering Sm and have similar style due to limb attenuation (Gee, 1963, p.23). Spry (1957, p.104) argued that these folds were 'incongruent flow folds" and not parasitic drag folds related to the limbs of the larger scale recumbent folds.

Most of the macro-fold hinges are sub-parallel to the stretching/mineral lineation, although there are variations (compare the orientation of the blue lines for lineations Lm and the pink lines for the fold axes (FA) in Figure 9).

Rotation relationships between FA and Lm can be used to help elucidate the positions of regional fold hinges and to map out axial surface traces. With curving hinge lines typical of conical to sheath-like macro-folds the rotation direction changes across the axial surface trace ("fold hinge line vergence" of Alsop & Holdsworth, 1999). For the Central Tyennan where data is available the rotation direction changes across the inferred axial surface trace for the Franklin fold-nappe (Raglan Range and Mt McCall) and the Collingwood Plain fold-nappe

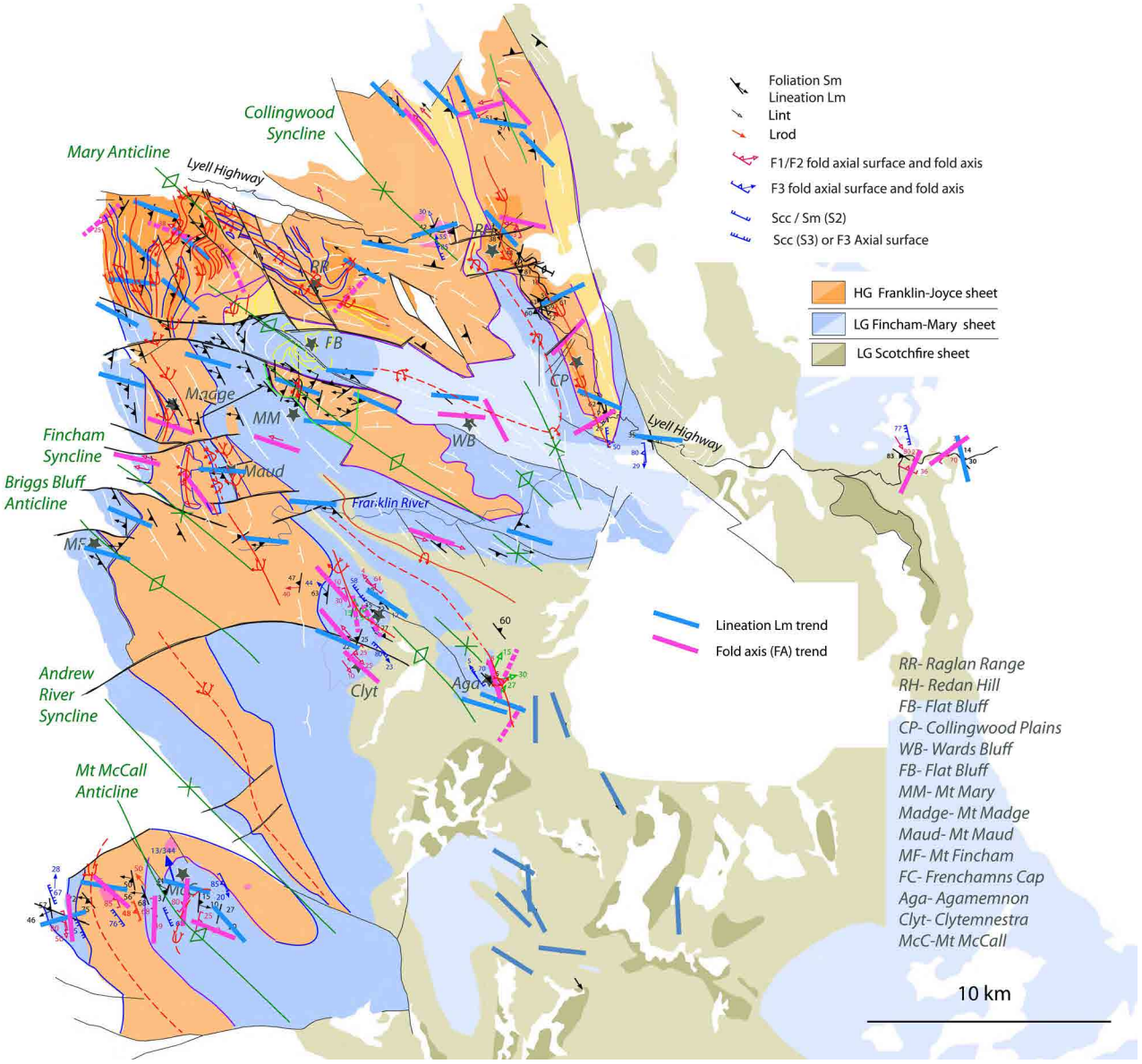

Figure 9. Central Tyennan summary structural map with colour-coded fold axis trends (FA) in pink and mineral lineation Lm trends in blue. Map base is the 1:25000 and 1:250000 digital geological atlas from Mineral Resources Tasmania.

(Figure 10). A change from clockwise to counter-clockwise rotation (blue curved arrows in Figure 10) across the inferred axial surface traces (heavy blue and heavy blue dashed lines in Figure 10) further support the presence of the regional scale fold-nappes.

3.3 Transport Direction Pattern

Shear sense indicators provide the kinematics of fold-nappe transport and development, and the kinematic evolution of the enveloping shear zones. These give the shear sense and displacement direction (i.e. overall transport direction).

Transport directions for the Central Tyennan (Figure 11) have been determined using shear band and foliation measurements from locations on the Lyell Highway, Frenchmans Cap and Mt McCall. In all cases data have been rotated to 1) remove the plunge of the younger Devonian folding, and 2) return the foliation Sm to the horizontal.

The calculated transport directions range from towards 110° (Mt McCall), 115° (Frenchmans Cap) and 136° (Collingwood Plains) with a gradual swing northwards from an east-southeast direction to a more south-east direction with an implied clockwise rotation about a vertical axis (Figure 11). **Significantly these data come from different levels in the fold-nappe pile.**

Reversals in shear sense or opposed shear sense at Mt McCall require the presence of both antithetic and synthetic shear bands, but these will have different angular relationships to Sm. The antithetic shear bands make angles of 50-60° to Sm, whereas the synthetic make angles ~20-30° to Sm. Unfolding Sm and rotating to the horizontal enables calculation of the angle between the shear band and the foliation (Sb^Sm).

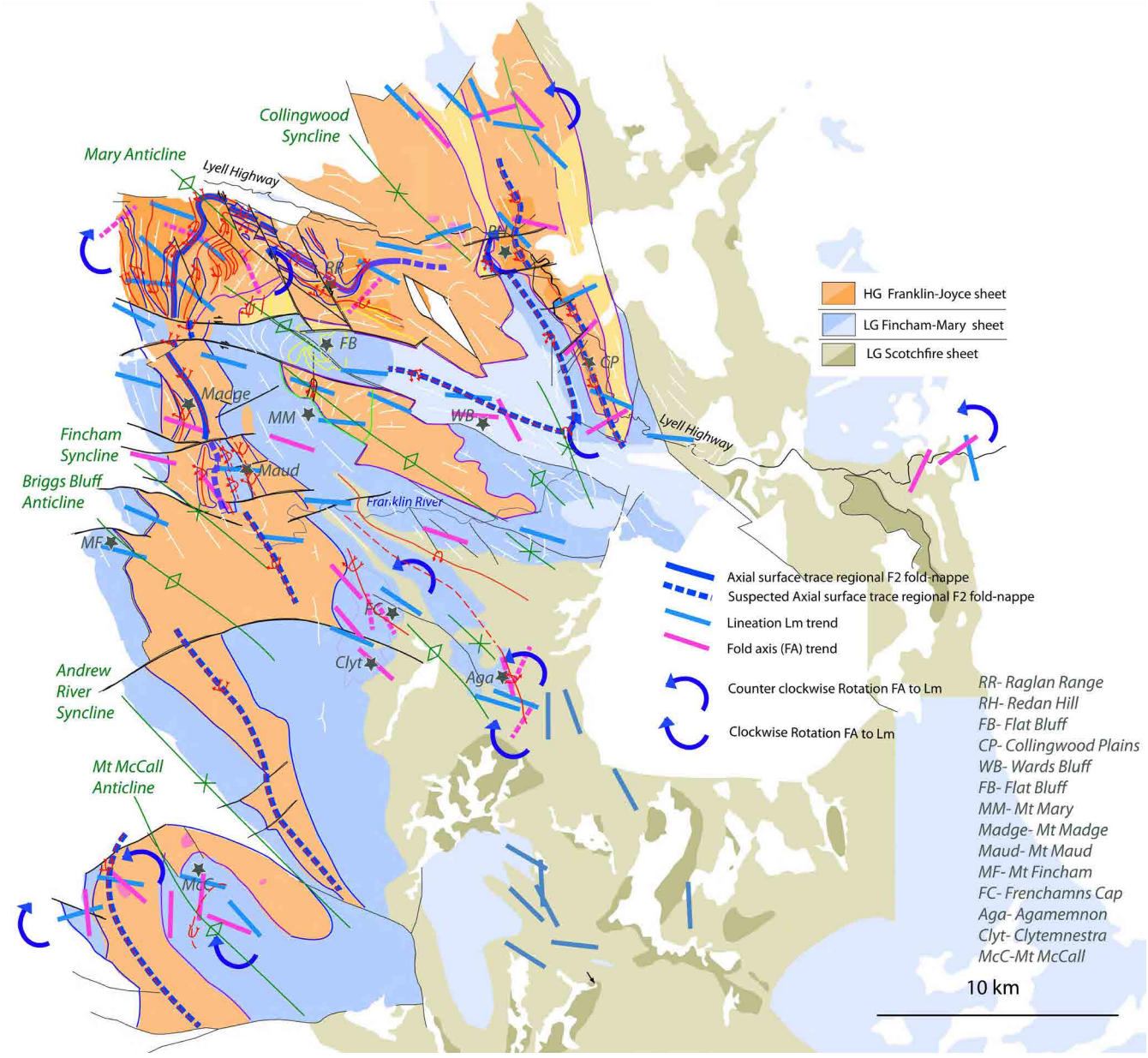

Figure 10. Central Tyennan summary map showing rotation relationships between the local fold axis trend (pink lines) and the mineral/stretching lineation Lm trend (blue lines). The rotation direction (dark blue semi-circle with direction arrow) is defined by rotating the fold axis towards the lineation through closing the acute angle between them. Map base is the 1:25000 and 1:250000 digital geological atlas from Mineral Resources Tasmania.

At Mt McCall one shear band determination occurs within the high-grade schist on the inferred overturned western limb, whereas the other occurs in quartzite on the inferred right-way-up eastern limb (see discussion in Section 5.5). In the high-grade schist the angle between the restored Sm to the shear band is 50° suggesting that these shear bands are antithetic with opposite shear sense (i.e. transport to the northwest at 292°). The vector azimuth for Mt McCall is 110° (Figure 11).

3.4. Fold-nappe Geometry

3.4.1 Regional Cross Sections

The Central Tyennan region is dominated by the regional-scale, Franklin Fold-nappe a major, SW-closing recumbent fold (Figures 2 and 7). It has an extremely attenuated, flattened and elongated form towards the south and some apparent attenuation to the east (compare Figures 12, 13 and 14). Much of the macro-fold geometry shows a reclined fold form (i.e. fold plunge in the dip direction of the axial surface). Scarce younging data suggests the western limb with Fincham Quartzite is largely overturned.

The regional extent of the Franklin fold-nappe is supported by the change from clockwise to counter-clockwise rotation of mesoscopic fold axes (FA) towards the lineation (Lm) across the inferred hinge lines of macro-folds at the Collingwood River (Collingwood Plain recumbent fold), the Raglan Range and Mt Mc-

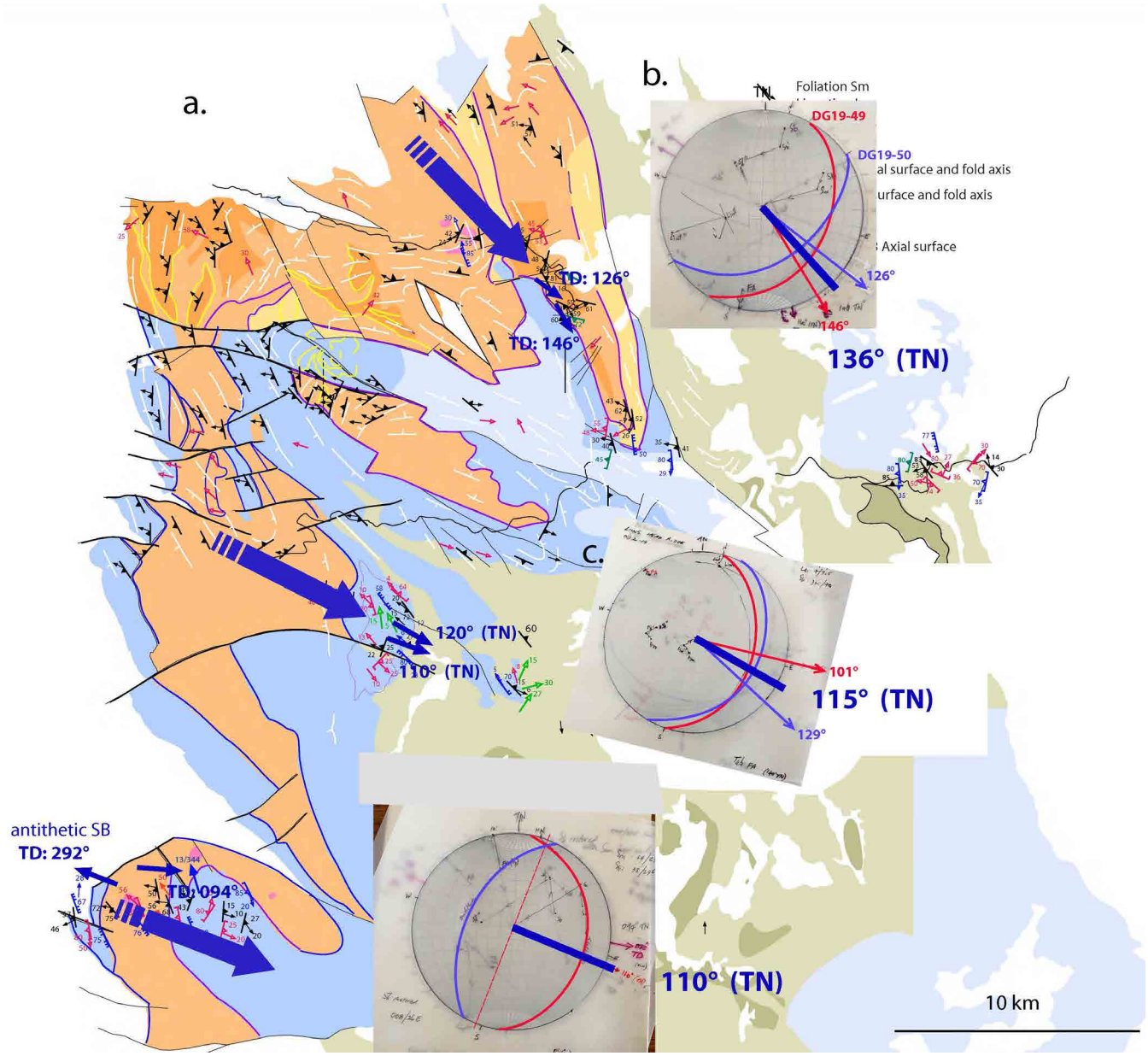

Figure 11. Transport direction vector map for the Central Tyennan. a) Litho-structural map base simplified from the 1:25,000 and 1:250,000 digital geological atlas from Mineral Resources Tasmania. b) Stereonets from Lyell Highway outcrops showing rotated data and final shear band (Sb) attitudes at locations DG 19-49 and DG19-50. c) Stereonets from Frenchmans Cap area showing rotated data and final shear band (Sb) attitudes at locations DG 20-18 and DG20-21. d) Stereonet from Mt McCall showing rotated data and final shear band (Sb) attitudes at locations DG 19-61 (blue great circle trace) and DG19-68 (red great circle trace).

Call (Franklin Fold-nappe) (see Figure 10). Section A-B (Figure 12) through the Raglan Range shows the west-facing and closing Franklin fold-nappe geometry (western and middle part of section) folded by the younger Mary Anticline (middle part of section), and the Collingwood Syncline (eastern part of section).

Section C-D (Figure 13) through Mt Madge, Mt Mary and Flat Bluff, shows: 1) a broader south-closing and upward facing Franklin fold-nappe hinge zone with parasitic folds in the interface between the high-grade Franklin-Joyce sheet and the low-grade Fincham-Mary sheet (west side of section), 2) the lower limb in low-grade Mary metamorphic sheet above the high-grade Joyce metamorphic sheet in two fault blocks and as the hinge of the younger Mary Anticline (middle of section), and 3) the down-dropped high-grade Franklin metamorphic sheet core of the fold-nappe folded by the Collingwood Syncline with a north-closing isoclinal reclined fold nose in low-grade Mary metamorphic sheet (Redan Hill fold-nappe) juxtaposed with the south-closing, reclined, isoclinal fold in high-grade Franklin sheet (Collingwood Plain fold-nappe).

Section E-F (Figure 14) through Mt McCall, Frenchmans Cap and Mt Alma shows a fault-duplicated (Andrew River Fault) Franklin fold-nappe hinge (western part of section), the lower limb of the fold-nappe with low-grade quartzite infolded with low-grade Scotchfire dolomitic phyllite and a fold pod of high-grade Joyce Metamorphics (middle part of section), and the Collingwood Plain synformal south-closing fold pod in the high-grade Franklin-Joyce metamorphic sheet (eastern part of the section).

3.4.2 Geometry through Section Reconstruction- Restored State

The sections have been restored in two steps, firstly by removing the fault offsets, and secondly by unfolding the late-stage Devonian open folds. By unfolding the open Devonian folds the restored section shows the recumbent, isoclinal nature and extent of the early F1/F2 folds. Fault offsets were removed by matching the major contacts between the high-grade and low-grade sequences on opposite sides of the faults. Removing the Devonian folding was achieved by simple rotation of the folded So/Sm surfaces about the major Devonian fold axes to achieve approximate planar form.

The restored states in the three profiles (Figures 12c, 13c and 14c) show the extent and the attenuated fold-nappe geometry of the Franklin fold-nappe in the high-grade Franklin-Joyce metamorphic sheet (orange) with the crosscutting retrograde phyllite (pale green) overlying the low-grade Fincham-Mary sheet quartzites and phyllites.

The sections can be devolved into a series of geometric elements that comprise the large-scale fold-nappe structure (Figure 15).

All the blocks can be assembled to draw the complete geometry: as the major flattened and elongated fold-nappe (compare Figure 15b with Figure 7). It essentially closes and/or pinches out to the south along the Engineer Range through to Mt McCall. At Mt McCall all the meso-folds in the high-grade rocks are reclined and moderately- to steeply west-plunging. Changes in the rotation relationsips between the local fold axis trend and the mineral lineation trend at Mt. McCall (Figure 10), suggest crossing a fold hinge between the high-grade rocks and the quartzite there. The presence of a strongly deformed quartzite "above" the high-grade rocks match the position of the Fincham quartzite at Mt Fincham. This suggests the macro-fold has continued in a highly attenuated form to Mt McCall.

The interpreted geometry in schematic, cartoon form provides a geometric model for the Central Tyennan region (Figure 16). The reconstruction suggests nappe dimensions are ~40 km axial surface strike length (elements 6 to 3 unfolded in Figure 15), with a maximum thickness of ~6-7 km (element 4 in Figure 15: core within Mary Anticline) and a minimum plunge extent of ~20 km (length of Raglan Range; Element 3 in Figure 15).

3.4.3 Key elements of the Central Tyennan Structural Model

1. The Central Tyennan region structural model (Figure 16) has a stacking order from top to bottom of:
    - high-grade Franklin -Metamorphic sheet (garnet quartzite and schists);
    - low-grade Fincham-Mary Metamorphic sheet (quartzite and phyllite);
    - low-grade Scotchfire Metamorphic sheet (dolomite and phyllite ± quartzite) (lowest structural level).
    - The eclogite and amphibolite pods occur within the structurally highest exposed part of the high-grade Franklin-Joyce Metamorphic sheet within a high strain zone (see also Chmielowski, 2009, figs. 2.1 and 2.6) Contacts between the sheets are high strain zones many with younger brittle fault reactivation.
2. The Central Tyennan structural geometry is dominated by the Franklin fold nappe with attenuation of the fold hinge to the southwest and development of lithological "pods" as noses of pinching sheath folds:
    - high-grade Ptug pod (sheath nose closing out of the page) at Mt Madge;
    - low-grade Ptpp and Ptsq pods at Mt Maud (sheath noses closing into the page).

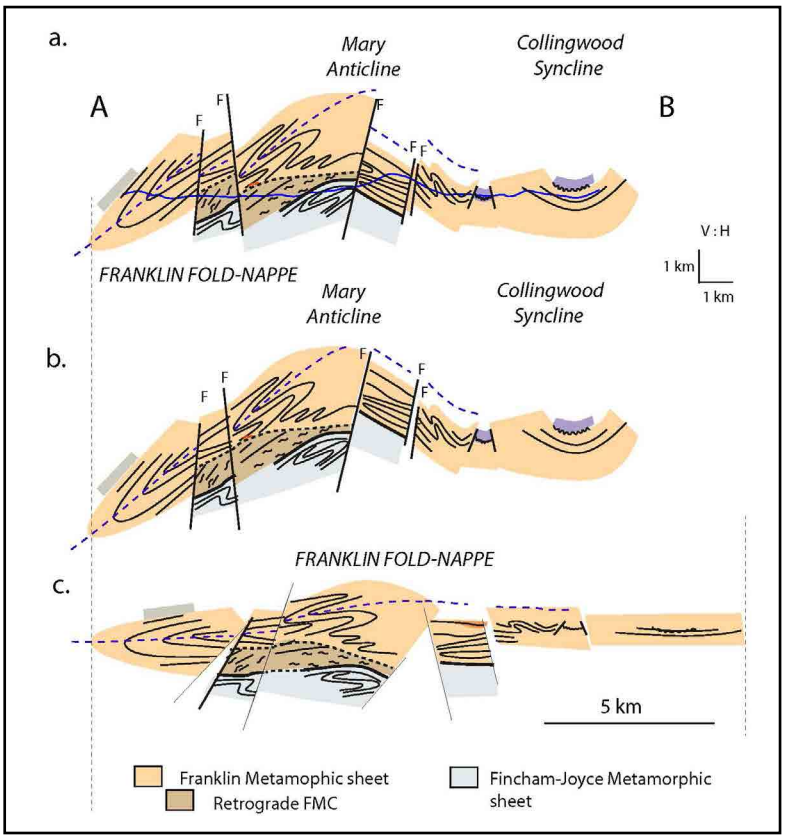

Figure 12. Restored Central Tyennan region profile A-B across the Raglan Range. a) Profile A-B (deformed state). Purple unit is Palaeozoic sediments sitting unconformably on the Tyennan rocks. b) Partly restored profile with late faulting offsets removed. c) Fully restored profile with the younger open Devonian folding removed from the profile in (b) showing the recumbent, isoclinal nature of the Franklin fold-nappe.

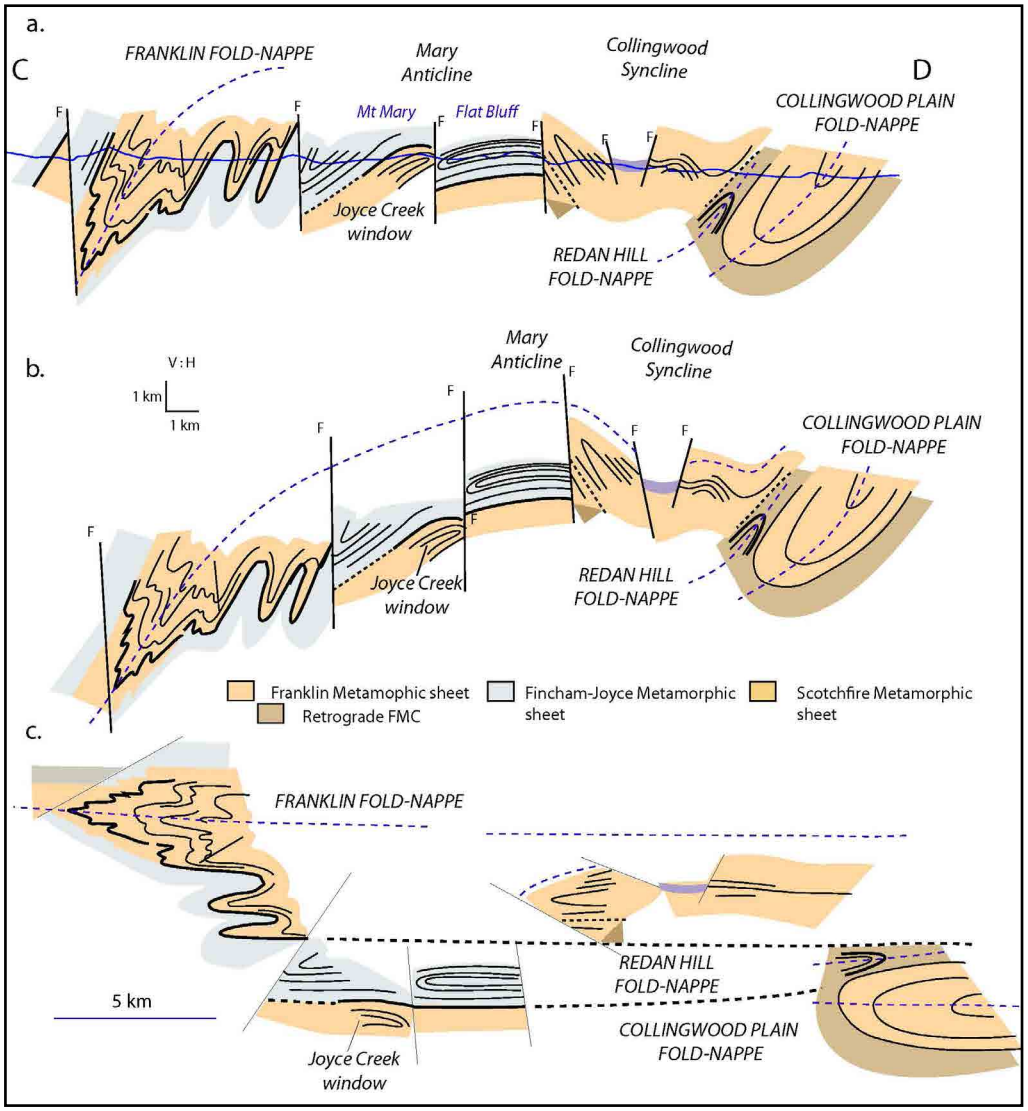

Figure 13. Restored Central Tyennan region profile C-D showing the fold-nappe stacking order. a) Deformed profile. Purple unit is Palaeozoic sediments sitting unconformably on the Tyennan rocks. b) Partly restored profile with late faulting offsets removed. c) Fully restored profile with the younger, open Devonian folding removed from the fault-restored profile in (b).

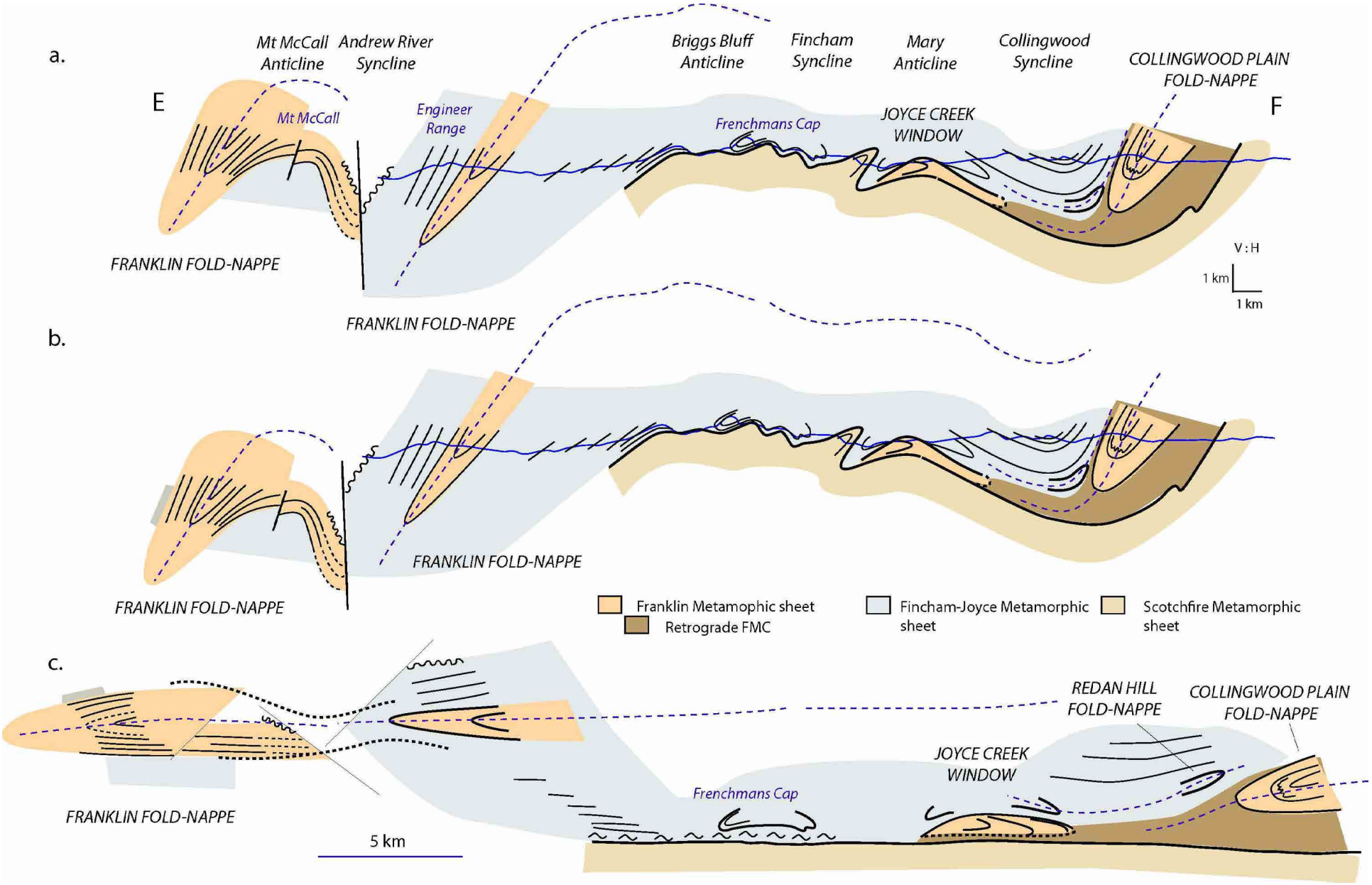

Figure 14. Restored Central Tyennan region profile E-F showing the extremely attenuated and elongated form of the uppermost Franklin Fold-nappe, as well as the dismembered pod-like form of the lowermost Collingwood Plain fold-nappe. a) Deformed profile. b) Partly restored profile with late faulting offsets removed. c) Fully restored profile with the younger, open Devonian folding removed from the fault-restored profile in (b).

3. The Franklin Metamorphics high-grade core is preserved as an isoclinal fold stack at Raglan Range and is associated with marked retrogression/albitisation with tapering and thinning to the south and east.
4. Further folding of the high-grade/low-grade layer system is required by the Redan Hill and Collingwood Plain closures below the Franklin fold-nappe.
5. The Collingwood Plain and the Joyce Creek recumbent folds appear as once contiguous macro-folds that are now relict pods enveloped by schistose and retrogressed zones (turquoise unit).
6. The structurally lowest Scotchfire schists are in-folded (pink unit) with the Fincham-Mary metamorphic sheet quartzites (yellow and grey units). **Implication:** units of differing metamorphic grade were brought together, underwent folding together, and retrograde metamorphism, particularly along interfaces or unit contacts and within the high-grade Franklin Metamorphics as part of the attenuated fold-nappe care.
7. The Central Tyennan region is an isoclinal fold stack with isoclinal folds in all units.
8. The Joyce metamorphics and Collingwood Plains synformal recumbent fold are at same structural level and appear as relict fold-hinge pods in-folded within Fincham-Mary sheet low-grade quartzites and phyllites.
9. F1/F2 fold axis variations (Figure 8) require curved regional fold hinge-lines (Figure 9).
10. Changes in fold geometry from the north to the south:
    - North: attenuated, flattened, reclined isoclinal folds in the low-grade Fincham-Mary sheet sit beneath the retrograded Franklin Metamorphics of the Governor River Phyllite (Raglan Range part of profile, Figure 16);
    - South: main hinge in Franklin Group is occupied by retrogressed (Ptuil) with relict fold cores in high-grade quartzite (Ptug) and low-grade quartz-phengite phyllite (Ptpp) and foliated phengitic quartzite (Ptsq) (Mt Madge and Mt Maud part of profile, Figure 16). Fold hinges are moderately to steeply plunging into the map.

3.4.4 Evidence/Arguments for Regional Fold-Nappes in the Central Tyennan Structural Model

What is a fold-nappe?

A recumbent fold with an overturned limb exceeding 5 km in length.

The Franklin fold-nappe has an apparent overturned limb length of ~35 km and therefore fold-nappe status.

What is the evidence for regional-scale fold nappes?

1. Repeated litho-tectonic "stratigraphy" and younging data linked with inferred macro-fold closures requires overturned limbs of recumbent folds. Upside down Sm/So in low-grade quartzite at Mt Fincham, west of the inferred closure in high-grade Franklin Metamorphics, suggests the presence of an overturned limb as well as continuity of the Fincham Quartzite with the Mary Quartzite (Fincham-Mary metamorphic sheet) across a large-scale recumbent fold (see also Spry, 1963a, p.123-125). The extent of this repeated stratigraphy and overturned limb is ~25 km in length and if extended across late faulting to Mt McCall is ~35 km in length (see Figure 2). The Collingwood Plain recumbent fold has an inferred "overturned" limb length of ~15 km, and the Redan Hill recumbent fold an inferred "overturned" limb length of ~9km (Figure 2). Therefore, these macro-fold structures are fold-nappes with overturned or inferred "overturned" limbs >5 km in length.

   Overturned quartzite at Mt McCall and at the east end of the high-grade Joyce Creek Window, further support the presence of large-scale recumbent folds within the low-grade quartzite of the Fincham-Mary metamorphic sheet.

2. Lineation (Lm) and Fold Axis (FA) data variations and relationships (see section 3.2). Note curved hinge-lines are reflected by the fold axis divergences and convergences, as well as their clockwise or counter-clockwise rotation relative to the regional stretching lineation Lm (Figures 9 and 10). These rotation domains define the opposite limbs of these regional recumbent sheath-like macro-folds (Figure 9).

3. Changes in Lm orientation across suspected or inferred macro-fold hinges. Such changes occur at Collingwood River (see section 4.4.2) and the Mt Madge and Mt Maud area (see section 4.5.6). Small-scale examples also show these limb-to-limb Lm orientation changes (e.g. meso-scale isoclines at Donaghys Lookout: see section 4.4.2).

   Variations in lineation and foliation data along the Collingwood River from Chmielowksi (2009, fig. 2.5) can be explained geometrically by isoclinal folding of the early lineation Lm about an inferred fold axis of ~70°/215° (see discussion in Section 4.2.2 and Figure 22d). These data from across the suspected hinge zone of the Collingwood Plain fold-nappe support the presence of this south-closing, reclined, isoclinal macro-fold.

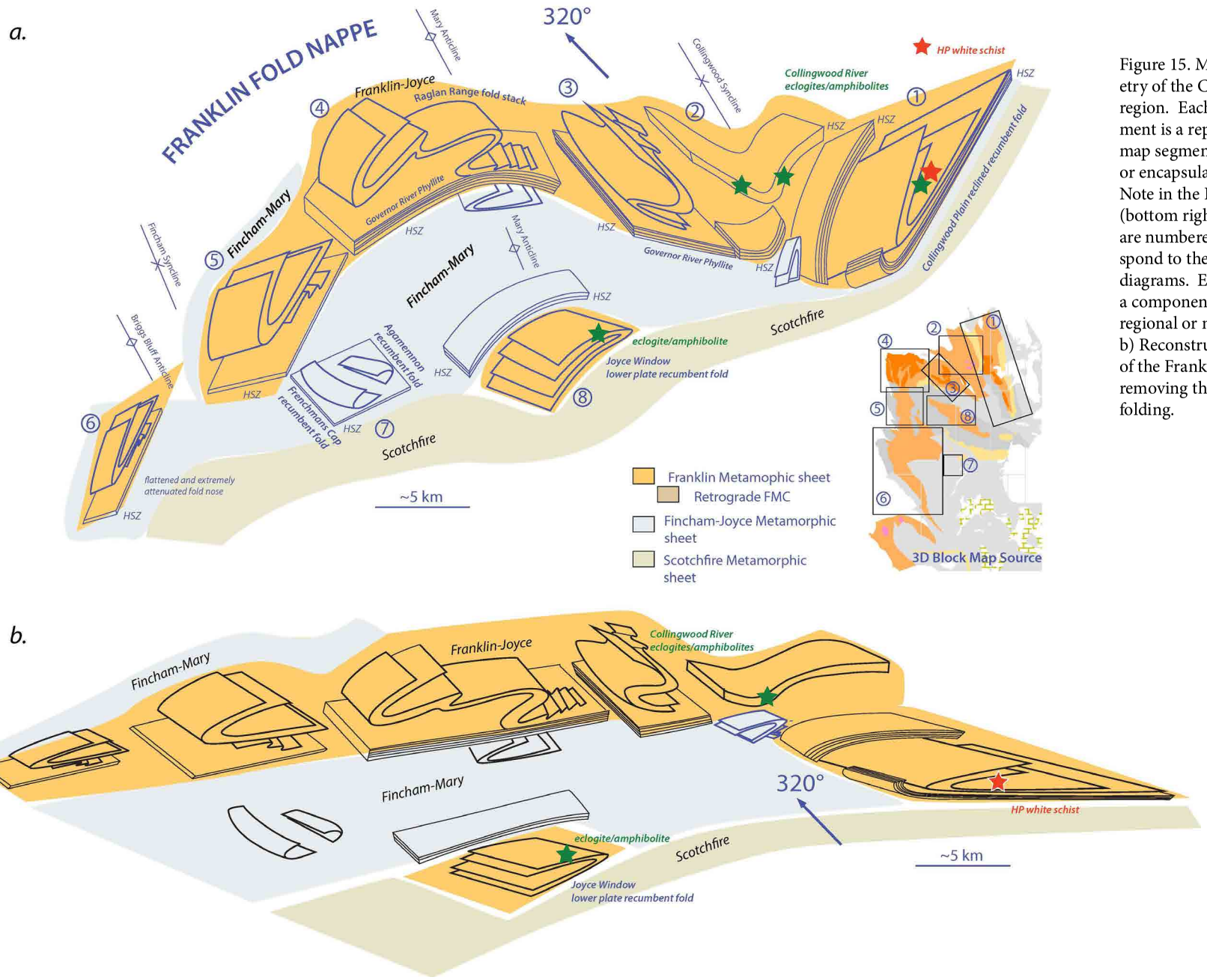

Figure 15. Macro-fold geometry of the Central Tyennan region. Each 3D block element is a representation of a map segment that was drawn or encapsulated into 3D form. Note in the Inset Map Source (bottom right) the map pieces are numbered and correspond to the numbered block diagrams. Each represents a component-part of the regional or macro structure. b) Reconstructed geometry of the Franklin fold-nappe by removing the younger open folding.

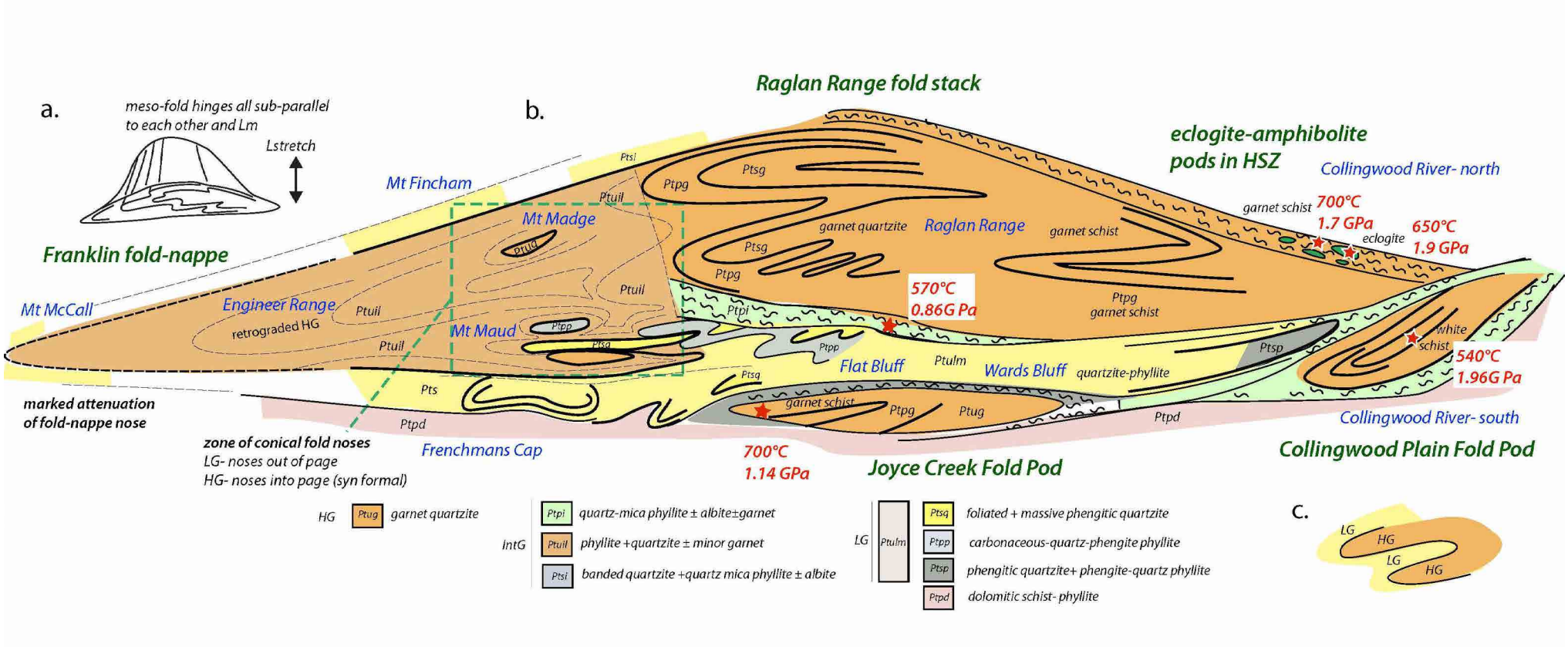

Figure16. Schematic, cartoon-like structural profile across the Central Tyennan showing the key relationships of the fold-nappe complex. The section extends from the Engineer Range in the southwest (left) to the Collingwood River in the northeast (right). The profile construction was based on the 1:25000 map pattern, down-plunge and up-plunge views and field relationships. Geographic locations are positioned with blue text. Metamorphic P-T determinations from Chmielowski (2009) are shown in red.

a) Pod-like inferred sheath form based on implied curved hinge-lines shown by fold axis trends in Figures 8 and 9. b) Cartoon-like profile. c) Simplified folded stack with high-grade sheet (orange unit) at top in-folded with low-grade sheet (yellow and grey units). This sits structurally unconformably on the low-grade Scotchfire sheet (pink) as recognised by Spry (1963a) and Duncan (1974).

Evidence of Sheath folds in the Central Tyennan

Sections through plunging sheath folds provide closed loop "eye" outcrop patterns, arcuate fold hinge traces, systematic meso-fold hinge trends relative to the transport direction (see Alsop & Holdsworth, 1999, 2004).

1. closed outcrop patterns that are not topography-related klippe or inliers:
    - disc-like or closed outcrop patterns in garnet quartzite (Ptsg) within the closure of the Collingwood Plain recumbent fold (see section 4.4.2);
    - closed loop outcrop patterns in the Mt Madge and Mt Maud area of the Franklin recumbent fold (see section 4.4.4.7).
2. curvilinear fold axis changes through interpreted hinge zones:
    - Mt Madge Ptug outcrop "wedge" pattern (see section 4.4.7.1);
    - Mt Maud region Ptsp closed loop outcrop pattern (see section 4.4.7.2).
3. suspected partial closed loop in Sm/So within Frenchmans Cap northeast face and Lions Ridge as part of the W-closing Frenchmans Cap recumbent fold (see Gray and Vicary, 2021).

4.0 DETAILED STRUCTURAL GEOLOGY OF THE NORTHERN PART CENTRAL TYENNAN REGION

4.1. Fold Axis Pattern

Limited field measurements of fold axes required fold axis determination using either the π or β method for Sm data from different parts of the major regional scale folds (Figure 17). The results are plotted as arrow vectors on the map with purple arrows indicating fold axis vectors for the early-formed recumbent isoclines, and green arrows for the younger Devonian folding.

These calculated fold axes are also plotted on a summary stereonet (Figure 18a), where the isocline fold axes appear in a simple elongated unimodal pattern. Analysing this spread by separating the fold axis data from different localities (structural positions) shows that these data can be fitted to great circles (Figure 18b). This indicates that the local fold axis variation, typical of conical or sheath-like folds with rounded hinges, lies within a plane approximating the local macro-fold axial surface.

Great circle fits to fold axis data include:

Collingwood Plain:	156°/54°W
Raglan Range:	162°/37°W
Flat Bluff:	162°/37°W
Mt Madge:	251°/61°NNW
Mt Maud:	206°/72°WNW

Changes in the inferred axial surface attitudes shown by the colour-coded great circles (Figure 18b) mostly reflect the younger Devonian folding/faulting.

4.2 Lineation Pattern

The Central Tyennan region has a consistent westnorthwest - northwest stretching lineation (Figures 19 and 20) that is clustered about a vector mean of 32°/302° and a conical fit axis of 37°/308° (cone apical angle 20°) (Figure 20b). The contoured lineation data suggest however that the population is bimodal with modes of 24°/293° and 24°/309° (Figure 20a). Colour-coding of the lineation measurements from different geographic locations and/or structural positions further shows that the overall clustering is more complex (see Figure 19b).

The bimodal pattern is related to the younger refolding, the Lm orientation change from limb to limb of the recumbent isoclinal macro-folds, and to possible folding about a steeply plunging axis. Spry and Gee (1964) had also suggested the lineation spread fitted rotation about a steep axis.

Foliation/lineation measurements from a large isoclinal fold hinge in quartzite and schist near the old Mill on the Raglan Range (Fig. 8 in Gee, 1963; and Fig.3 in Spry and Gee, 1964) show that lineations plot in a cluster around the calculated pi axis of 30°/300°. The local pattern at the Old Mill (Raglan Range stereonet, Figure 17) is different to the lineation pattern of the Raglan Range domain that contains the Mill (Raglan East stereonet, Figure 17).

4.3 Geometry

Multiple cross sections/structural profiles were constructed to establish the regional and local scale geometry. Serial sections were constructed using structural data from the 1:25000 scale map sheets (Figure 21).

Folds mapped by Gee (1963) within the Governor River Phyllite (Section A-B, Figure 21) were used as a starting point. Using fault offsets, dip changes and outcrop patterns these fold axial surface traces were projected across the late brittle faults, to define isoclinal fold closures in sections (e.g. dashed hinges in C-D and E-F, Figure 21). Hinges had not been mapped or defined by the previous workers. The result is an axial surface trace map (Figure 17).

Fold form is complex with 1) reclined macro-fold geometry, and 2) closed pod-like outcrops within both high-grade and low-grade units in the hinge zone of the Franklin fold-nappe in the Mt Madge and Mt Maud regions (sections G-H, I-J and K-L, Figure 21). The latter suggest curved conical shaped or sheath form to both upward penetrating lobes of low-grade units from the underling low-grade Fincham-Mary metamorphic sheet and synformal downward-penetrating units in the high-grade Franklin-Joyce metamorphic sheet.

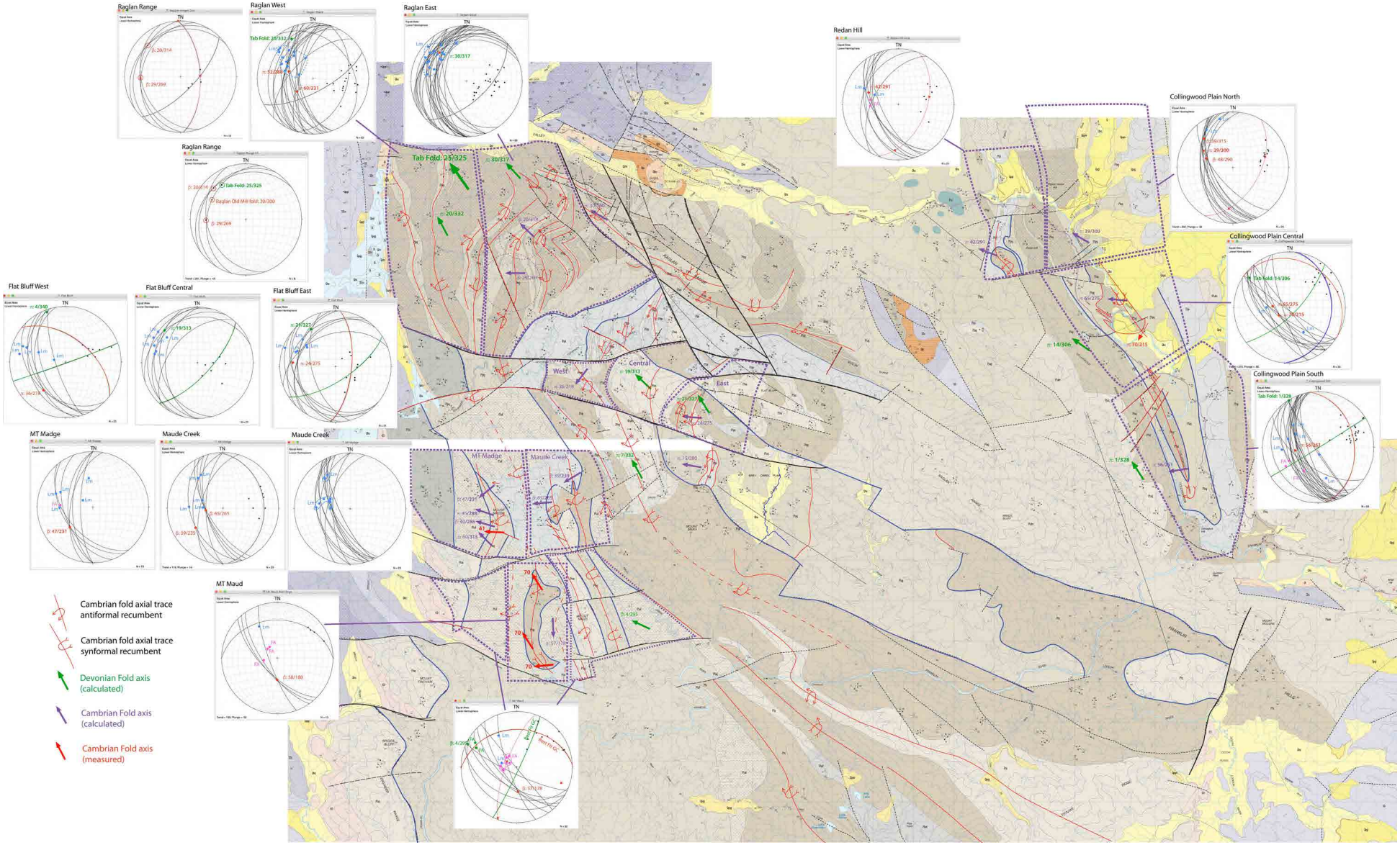

Figure 17. Stereonets of structural data from domains within the northern part of the Central Tyennan region. Map base is the 1:25000 digital geological atlas from Mineral Resources Tasmania. The closed purple dashed lines are the domain boundaries. The stereonets show So/Sm and Sm as great circle traces and poles, Cambrian isocline fold axes (FA) as pink dots and lineations Lm as blue dots. Calculated Devonian fold axis π points are shown as green dots with best fit green great circle traces. On the map the thick purple highlighted arrows show the calculated fold axis plunges for the various Cambrian recumbent isoclines. Thick green highlighted arrows show calculated fold axis plunges for the younger open Devonian folds. The red highlighted arrows are actual measured fold plunges. All readings are True North. All plotted data are from the 1:25000 map sheets.

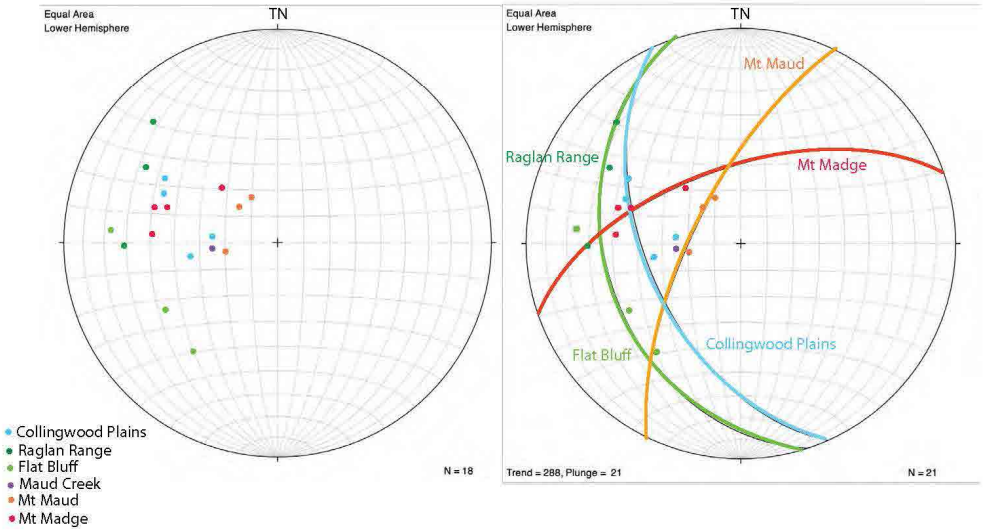

Figure 18. Stereonet showing Central Tyennan fold axis measurements including π and β determinations from Figure 17. In a) these are colour coded to highlight the fold axis spread at the different locations (structural position) and in b) the great circle fit to individual datasets.

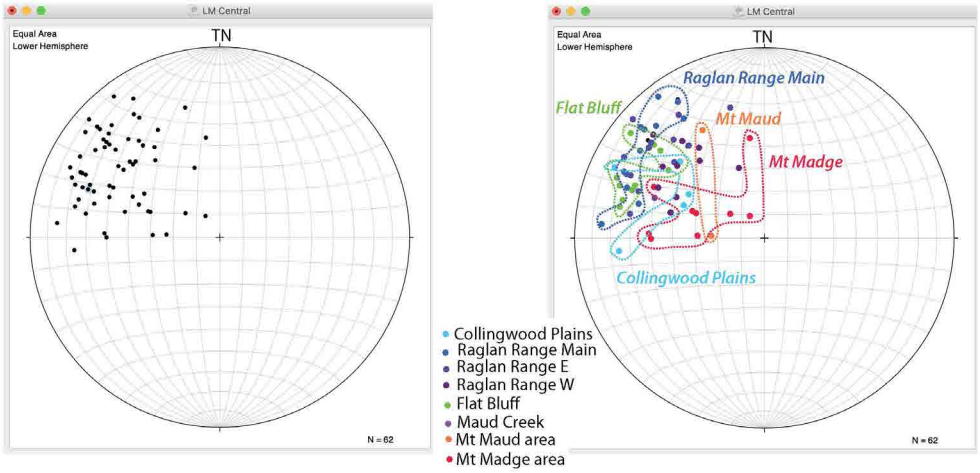

Figure 19. Stereonets of lineation Lm data for the Central Tyennan region. a) Total Lm data from 1:25,000 map sheets. Sample size n=72. b). Colour-coded Lm data for different structural positions/ geographic locations.

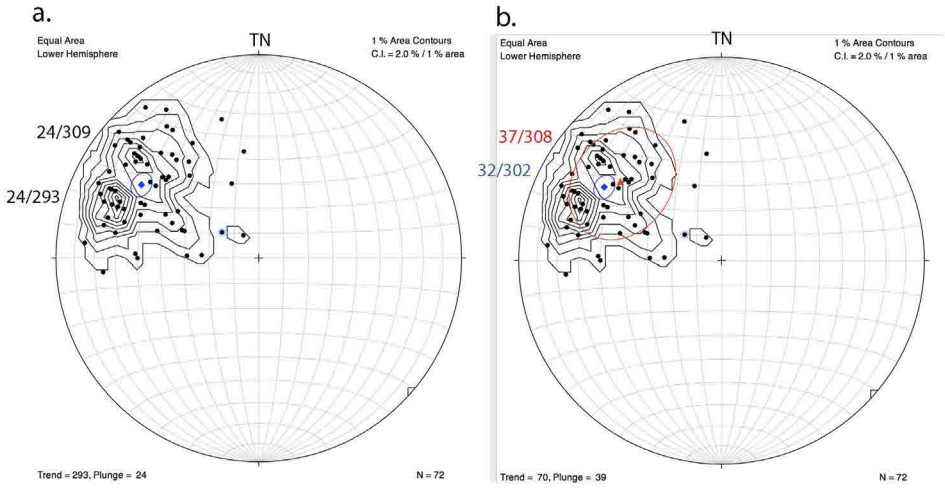

Figure 20. Contoured Lm for the Central Tyennan. a) Contouring gives bimodal pattern with mode 1 as 24°/293° and mode 2 as 24°/309°. b) Mean vector for total Lm population is 32°/302° (blue outline is 95% confidence level and conical best fit with cone axis 37°/308° with apical half angle of 22°.

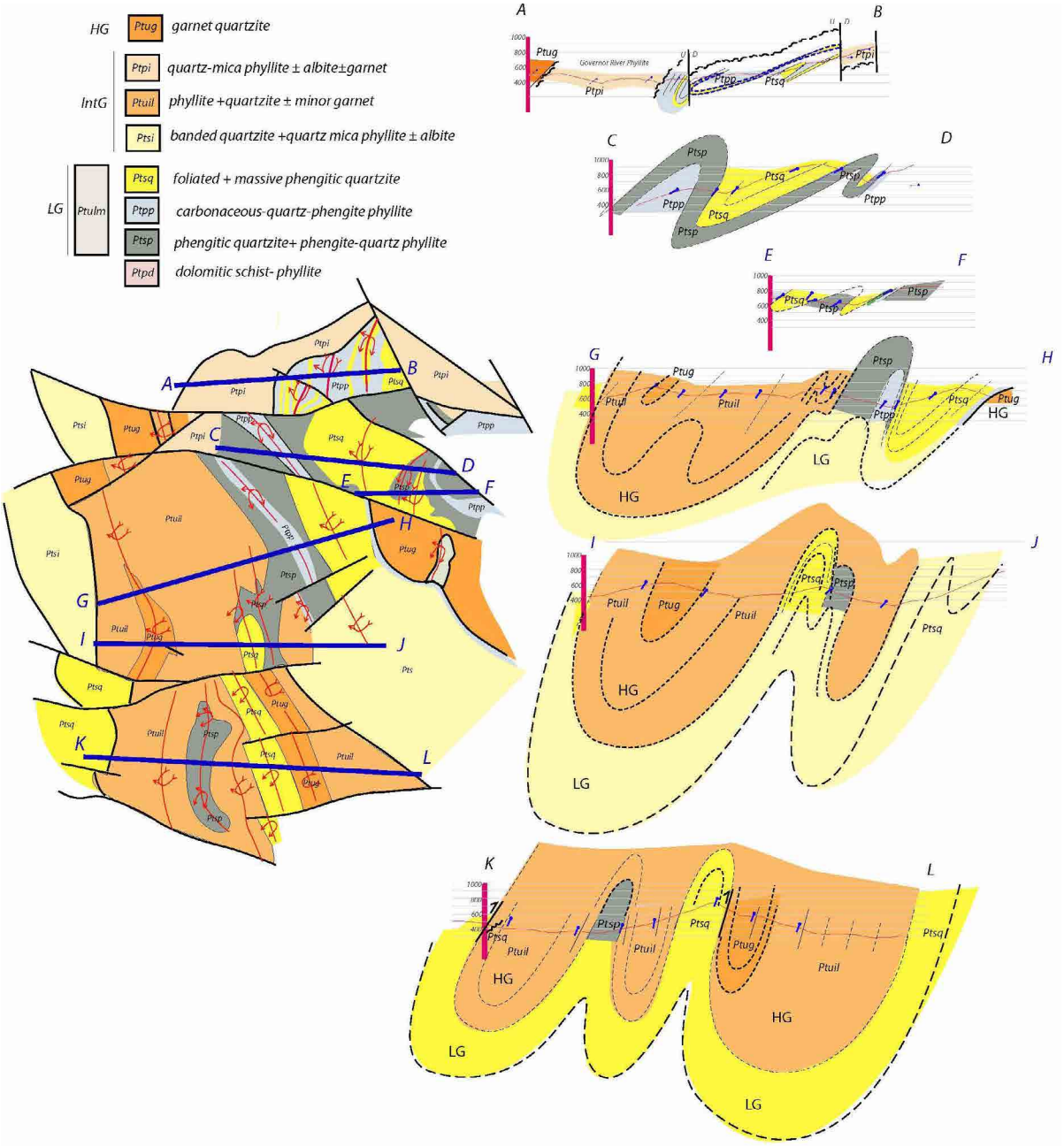

Figure 21. Cross sections through the north-south trending part of the Franklin fold-nappe. Positions of the section lines are shown by the heavy lines in the map inset (on left). Fold hinges have been inferred and are shown as dashed hinges. Fold hinges or closures were defined in part using divergence and convergence of dip control points. Axial trace positions were then transferred to the mapping base (inset map on left and Figure 17).

4.4 Lithological and Structural Elements of the Northern Central Tyennan Region

4.4.1 Collingwood River Eclogites

Eclogite boudins occur at the structurally highest part of the Central Tyennan litho-tectonic meta-sedimentary sequence (Spry, 1963c; Raheim, 1976; Kamperman, 1984; Goscombe, 1990; Chmielowski, 2009; Palmeri et al., 2009; Brown et al., 2021) (Figures 16 and 22a, b). They occur on the eastern limb of the Collingwood Syncline and are part of structurally interleaved pelitic schist, quartzite and phyllite sequence (Chmielowski, 2009; Palmeri et al., 2009). The boudins have metre to hectometre scale and are enclosed in, or wrapped by, schist with a dominant and pervasive foliation (Figure 22b). This foliation is defined by muscovite ±biotite ±garnet ±talc with some kyanite relics also present (Chmielowski, 2009; Brown et al., 2021).

4.4.2 Collingwood Plain Recumbent Fold (CPRF)

Originally mapped as a down-faulted block of Franklin Group high-grade metamorphic rocks (Spry & Zimmerman, 1959; McIntyre, 1964) the Collingwood Plain structure is now interpreted as a fault-truncated, flattened and attenuated south-closing, west-plunging recumbent isocline cored by high-grade Franklin metamorphic sheet (Figure 22a). The hinge zone is marked by a series of en echelon, disc-like outcrop patterns of garnet quartzite (Ptsg) (Figure 22a). It has an axial surface trace length of 18 km and reclined geometry with calculated fold plunges of 39°/300°, 65°/275°, and 56°/267° from north to south (Figure 22c). It is at a structurally lower level to the Franklin fold-nappe and appears to be at the same level as the fold closure in the Joyce Metamorphics (Section E-F, Figure 7).

Identifying mylonitic fabrics in schistose quartzites and

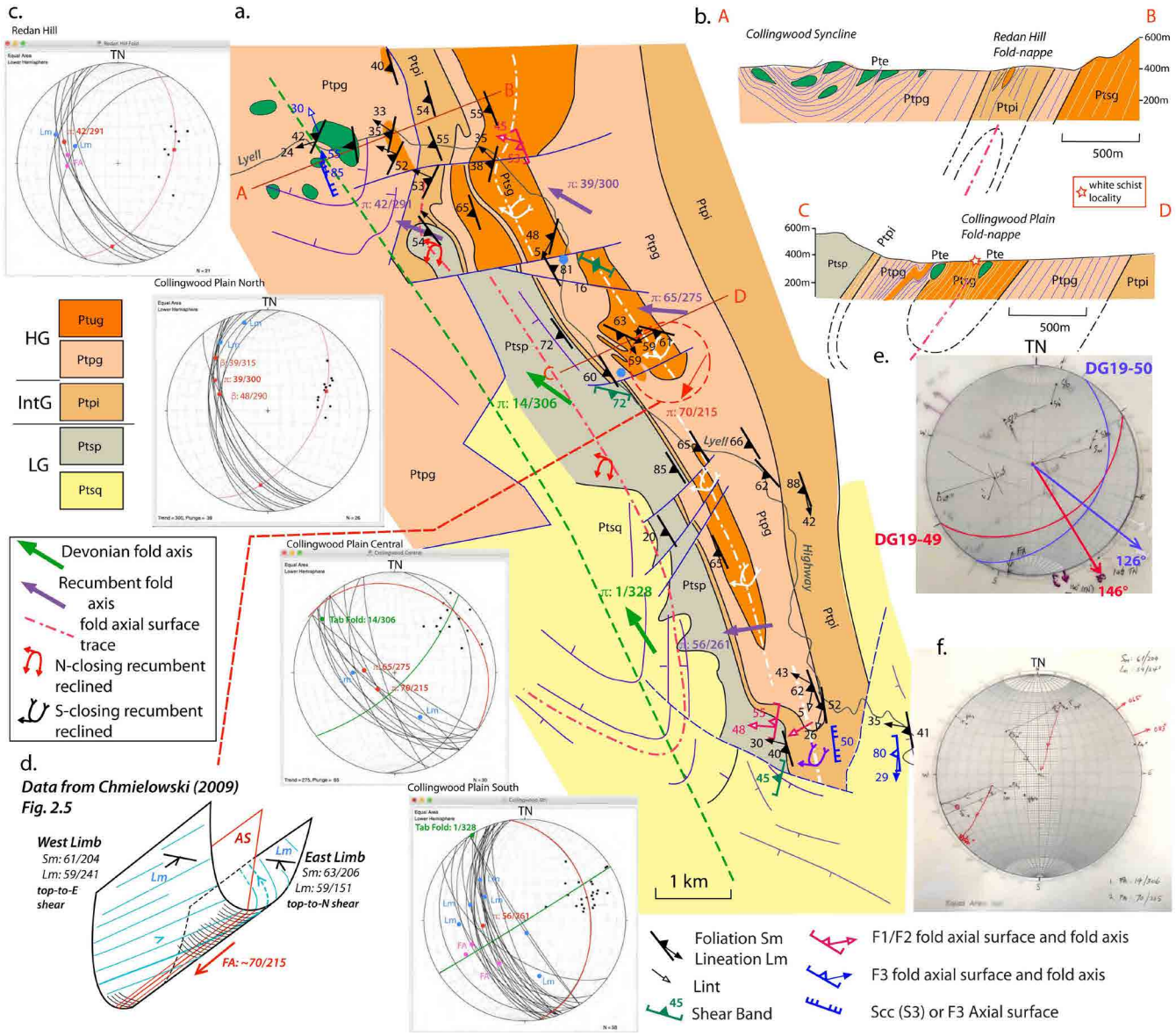

Figure 22. Structure map showing major folds in the Collingwood River area. Map base has been modified from the Collingwood 1:25000 map sheet (Vicary, 2004a) and Loddon 1:25000 map sheet (Vicary, 2004b) Mineral Resources digital atlas. The younger Collingwood Syncline (green dashed line axial surface trace), the Redan Hills recumbent fold (red dashed axial surface trace) and the Collingwood Plain recumbent fold (white dashed line axial surface trace) are shown. b) Section AB across the Redan Hill recumbent fold and section CD across the Collingwood Plain recumbent fold. The sections are from Chmielowski (2009). c) Stereonets with Sm great circles and poles, lineation Lm (blue dots) and great circle fits to pole data to generate π and β fold axes for the recumbent folds (purple arrows) and younger folds (green arrows). d) Diagrammatic representation of the Collingwood Plain recumbent fold showing reclined geometry with calculated attitude (FA: 70°/215°) to explain the foliation Sm and lineation Lm data from Chmielowski (2009, fig.2.5). The folded lineation Lm is shown by the blue line. e) Transport direction vectors determined from restoring shear bands from outcrops DG19-48 and DG19-49. f) Restoration of Chmielowski (2009, Figure 2.5) lineation data.

schists enveloping the eclogites and white schist, Chmielowski (2009) argued that these were major shear zones responsible for the ascent of the eclogites, but did not recognise subsequent recumbent folding in the form of the CPRF. Measurements and shear sense determinations by Chmielowski (2009, fig. 2-4) in the Collingwood River are at the hinge zone of the CPRF and show a reversal in transport direction that can be explained by the presence of the macro fold hinge (Figure 22d). An approximate fit of the Sm/Lm data from opposing fold limbs requires a fold axis of 70°/215° at Collingwood River south (Figure 22d).

The same folded lineation changes that Chmielowski observed along the Collingwood River can also be seen associated with small to meso-scale folds in quartzite at Donaghys Lookout (Figure 23). Flatter limbs (~20° dip) show Lm with a southwest plunge whereas steeper dipping limbs (~45° dip) show Lm with a northwest plunge (compare with Figure 22d). Lyell Highway outcrops with steeper Sm foliation dips (50°-60° dips) occur on the eastern limb of the CPRF and have definite northwest plunges (see Figure 23a: station DG19-48).

Lm and FA data from Donaghys Lookout exposures on the western limb of the CPRF show that meso-fold axes are consistently plunging more southwest of Lm requiring a clockwise rotation of the fold axis towards the lineation Lm (compare with regional data in Figure 10).

Junction Peak when viewed from Donaghys Lookout (Figure 24) shows larger scale isoclinal fold closures in

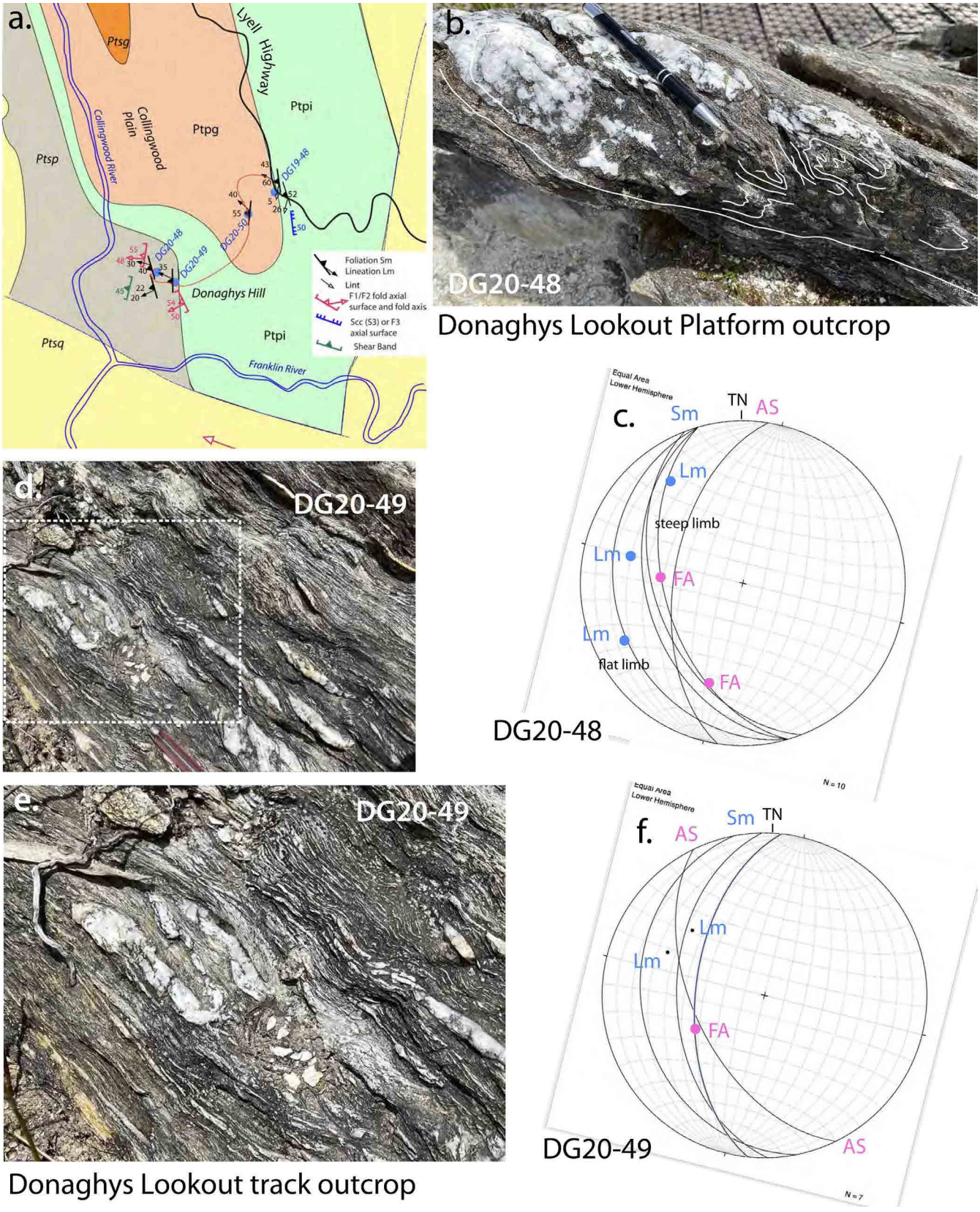

Figure 23. Structural relationships in quartzite at Donaghys Lookout and track.
a) Simplified map with structural data for Donaghys Lookout track. Map base modified from the Loddon 1:25000 Map sheet (Vicary, 2004b) Mineral Resources digital atlas.

Ptsg (orange): high-grade garnet quartzite
Ptpg (pink): high-grade garnet schist
Ptpi (green): intermediate grade quartz-mica phyllite±albite±garnet
Ptsq (yellow): low-grade phengitic quartzite
Ptsp (grey): low-grade carbonaceous quartz-phengite phyllite

b) Photograph of meso-folds in thinly bedded quartzite at Donaghys Lookout platform. c) Stereonet of foliation Sm (great circles), lineation Lm and fold axis FA data for the Lookout outcrop. d) and e) Photos of intensely foliated, platy quartzite with relict hinges in folded quartz veins from track outcrop near Donaghys Lookout. f) Stereonet of foliation Sm (great circles), lineation Lm and fold axis FA data for the track outcrop in d) and e).

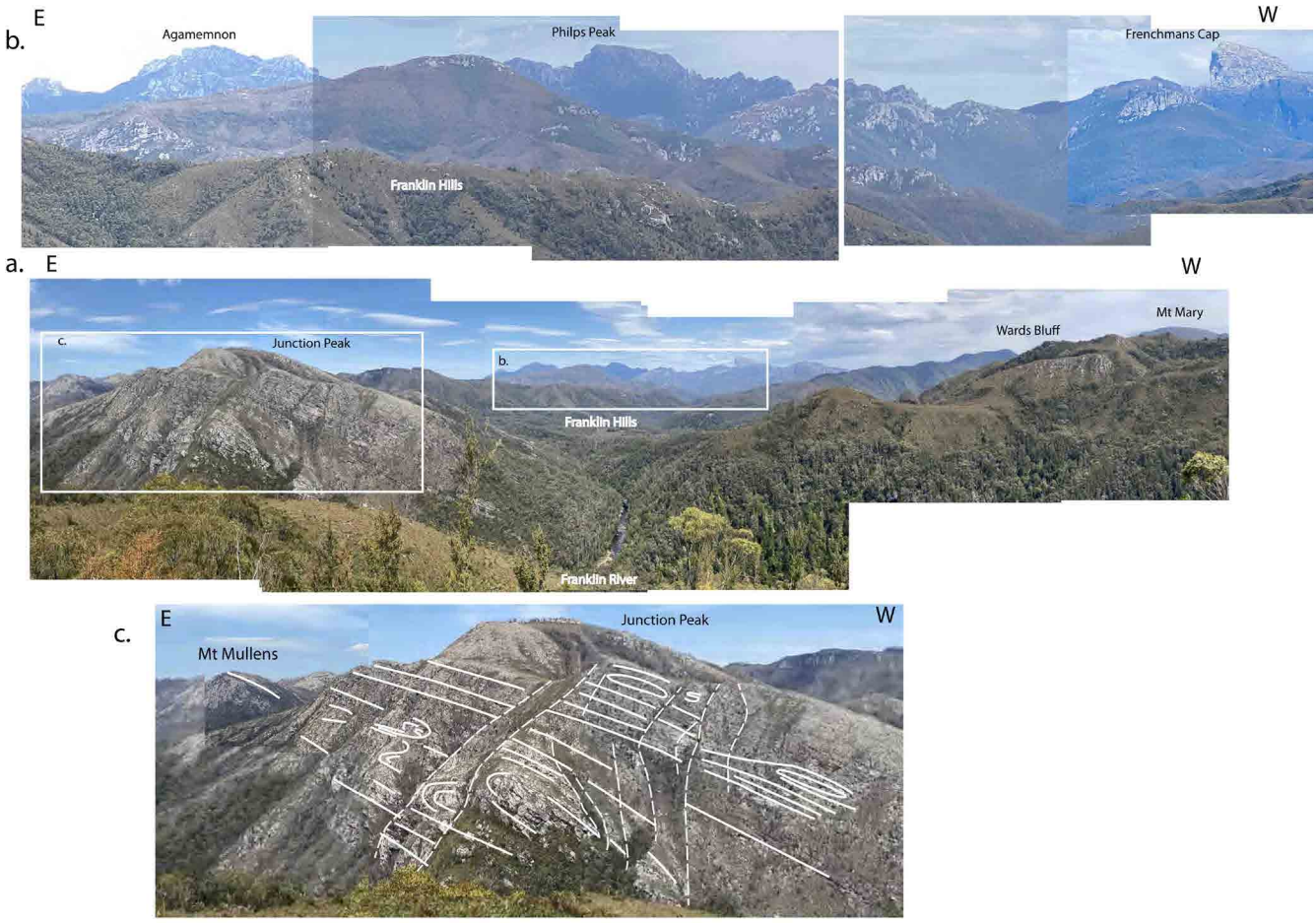

Figure 24. Views of low-grade quartzite ridges from Donaghys Lookout at the southern end of the Collingwood Plain closure.
a) Panorama view with Mt Mullens-Junction Peak (photo left) across the Franklin River valley to Wards Bluff and Mt Mary (photo right). Box outlines show the Frenchmans Cap ridgeline enlargement in b) and the enlargement of Junction Peak ridgeline in c).
b) View south towards Frenchmans Cap showing distant ridgeline with Agamemnon, Philps Peak and Frenchmans Cap held-up by quartzite of the Fincham-Mary metamorphic sheet (see Gray and Vicary, 2021). The Franklin Hills ridge in the foreground left is also quartzite of the low-grade Fincham-Mary metamorphic sheet.
c) Enlarged view of annotated Junction Creek ridgeline with white lines as traces of Sm/So and Sm. Closed loops are inferred hinges of folds whose axes are sub-parallel to the ridge.

the lower part of the ridge (Figure 24c) that must plunge in a direction sub-parallel to the ridgeline (i.e. towards 270°-290°). These match the plunges of the meso-scale isoclinal folds measured at Donaghys Lookout (compare with Figure 23a, c and f).

4.4.3 Redan Hill Recumbent Fold

The Redan Hill recumbent fold (Figure 25) is an antiformal, north-closing, isoclinal in-fold of the low-grade Fincham-Mary metamorphic sheet wedged into high-grade rocks (Ptug) of the Franklin-Joyce metamorphic sheet (Figures 2 and 3). It has reclined geometry with a measured meso-fold hinge of 48°/268° and a π determination of 47°/291° (Figure 25). It has a low-grade phengitic quartzite-phyllite (Ptsp) core wrapped by intermediate grade, retrogressive quartz-mica phyllite (Ptpi). The fold generally has a steeper east limb (~60°-70° dips) compared to a flatter west limb (30°-45° dips). Limited mapping and structural data make extrapolation of the axial surface to the south difficult (Figures 2 and 25).

4.4.4 Raglan Range Fold stack

Mapping by Gee (1963) showed the Raglan Range as an apparent fold stack of isoclinal folds within high-grade Franklin Metamorphic Complex rocks (Figure 26). Stacked sheets or slabs of garnet quartzite are in-folded with coarse-grained garnet schist. The quartzite units are thick, often discontinuous slabs sometimes as detached fold cores (Turner, 1989). The basal or lower part of the stack is retrogressed high-grade schist now as phyllite/phyllonite that overlies low-grade chlorite-quartzite-phyllite of the Mary Metamorphic sheet (Figure 26).

The Raglan Range represents the core and thickest part of the Franklin Fold-nappe where it straddles or is folded by the younger northwest-trending Mary Anticline (Figures 2 and 7). Mapping by Gee (1963) and Spry & Gee (1964) showed a consistent mineral lineation with attitude 24°/300° fitting a partial small-circle due to younger Devonian folding. The foliation Sm is folded and gives a β intersection of 24°/326° for this younger folding phase.

There is a variation in the Lm lineation pattern across the Mary anticline (Figure 27). Data from the Mary An-

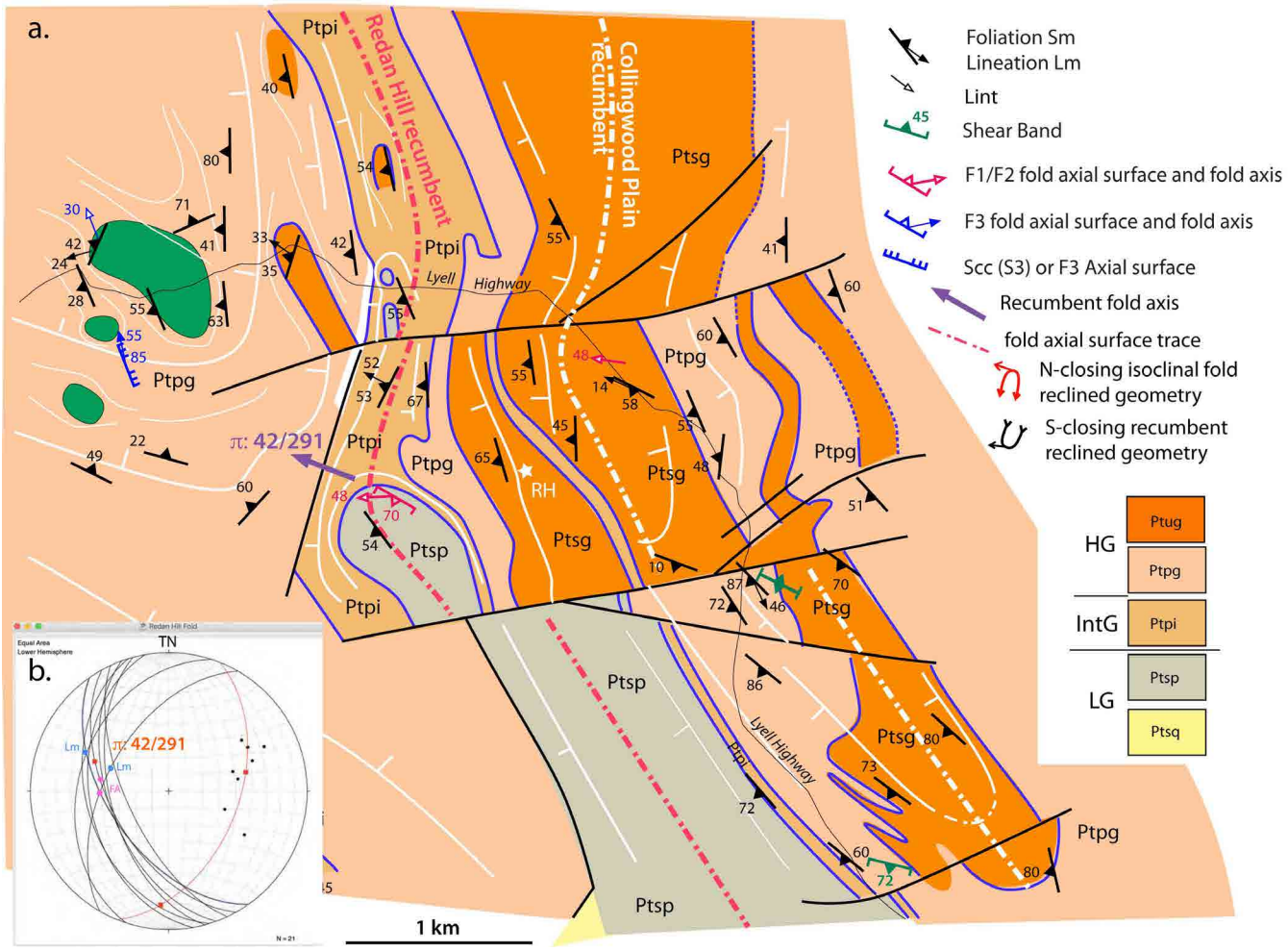

Figure 25. Structure of the Redan Hill recumbent fold closure and north end of Collingwood Plain recumbent fold. a) Map based on Collingwood 1:25000 map sheet (Vicary, 2004a) and Loddon 1:25000 map sheet (Vicary, 2004b) Mineral Resources Tasmania digital geological atlas. b) Stereonet of foliation Sm great circle traces and poles,; lineation Lm as blue dots and fold axis data FA (red dots) from around the nose of the Redan Hill closure.

Ptsg (orange): high-grade garnet quartzite
Ptpg (pink): high-grade garnet schist
Ptpi (green): intermediate grade quartz-mica phyllite±albite±garnet
Ptsq (yellow): low-grade phengitic quartzite
Ptsp (grey): low-grade carbonaceous quartz-phengite phyllite

ticline west limb (Figure 27c) show less plunge direction spread but greater plunge variation, whereas data from the Mary Anticline hinge show greater axial spread and less plunge variation (Figure 27d), whereas the Mary Anticline east limb data show the greatest range in fold trend and the least plunge variation with plunges <30° (Figure 27e).

4.4.5 Governor River Phyllite

Basal High Strain Zone or Retrograde Metamorphic Zonation overprint

The interface between the high-grade Franklin-Joyce metamorphic sheet and structurally underlying low-grade Fincham-Mary sheet chlorite-grade quartzites was defined and described by Gee (1963) as a phyllonite, the Governor River Phyllite (GRP). It represents the basal zone of the Franklin Fold-nappe (Figures 2 and 26) and has characteristics of a retrogressive shear zone. Intense S2 transposition layering with fractured and smeared out garnets, occasional broken biotites and a chlorite-muscovite assemblage superimposed on a biotite-garnet assemblage are accompanied by recrystallisation of quartz and muscovite in this zone (Gee, 1963, p.14). Gee (1963, p.13) also noted that albite porphyroblasts in the GRP were smaller (~2mm) and lozenge shaped. They contained helicitic dusty graphitic inclusion trails that represented remnants of a pre-existing folded surface preserved in the growing porphyroblast. Similar coarse albite schists occur in the upper part of the Franklin metamorphic sheet. These tend to show straight or gently curved inclusion trails.

Mapping however suggests that the phyllite is also part of a transgressive metamorphic zonation with the mineral isograds discordant to the mapped structure (Figure 26). Continuity of structure across the phyllite contact implies a metamorphic retrograde overprint with growth of post-S2 muscovite. The GRP zone has gradational and structurally conformable contacts with 1) the lower contact defined by the change from phyllite to more psammitic rock types and the appearance of bi-

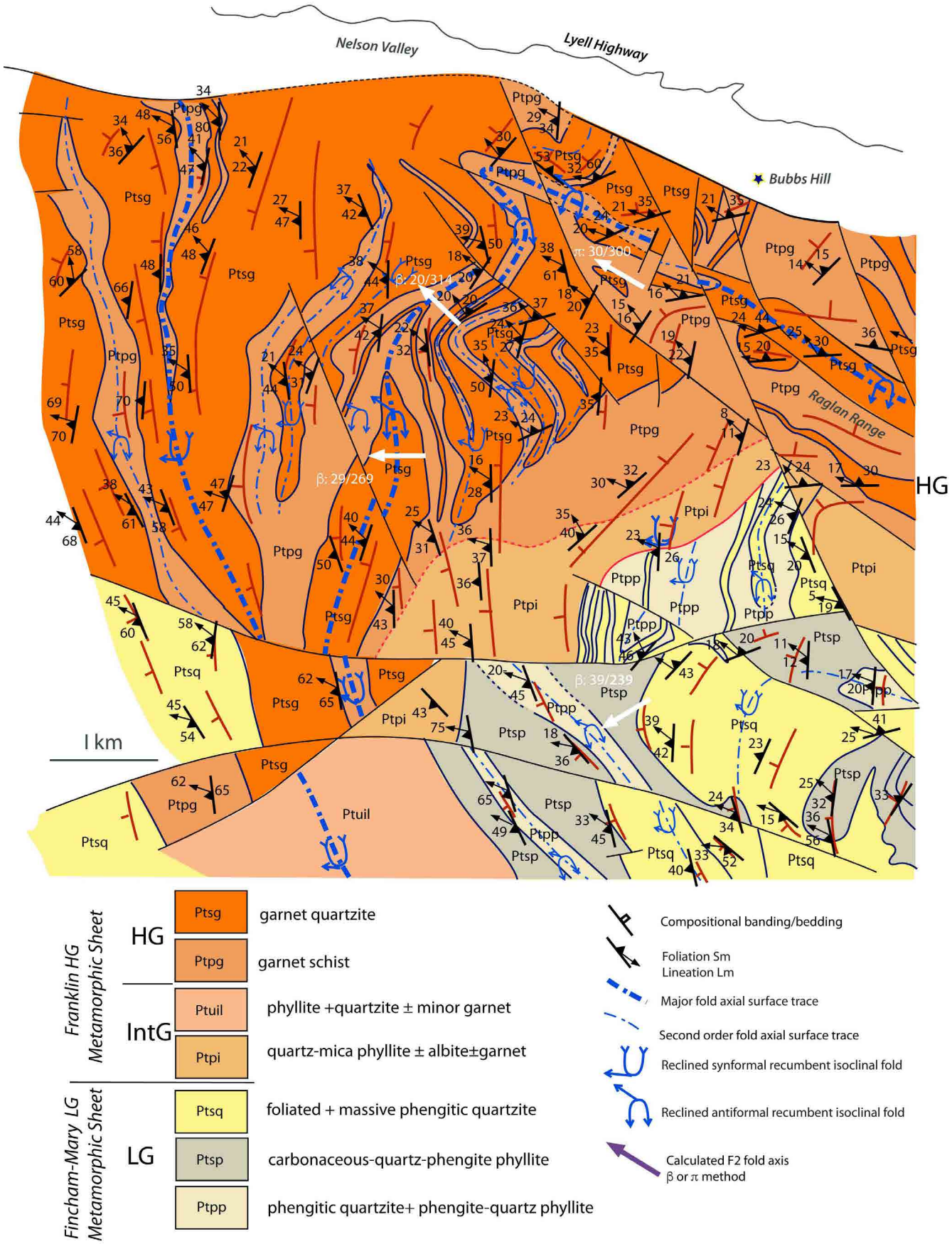

Figure 26. Raglan Range geological map after Gee (1963) showing isoclinal fold stack with apparent truncation by the Governor River Phyllite zone (designated by Ptpi and light brown colour). Note the apparent continuity of structure across the boundaries of the zone. White bold arrows are calculated early isoclinal fold axes derived from S0/Sm attitude data around apparent closures (shown as purple arrow in legend). Base map is from the Owen 1:25000 map sheet (Green and Everard, 2003) Mineral Resources Tasmania digital geological atlas.

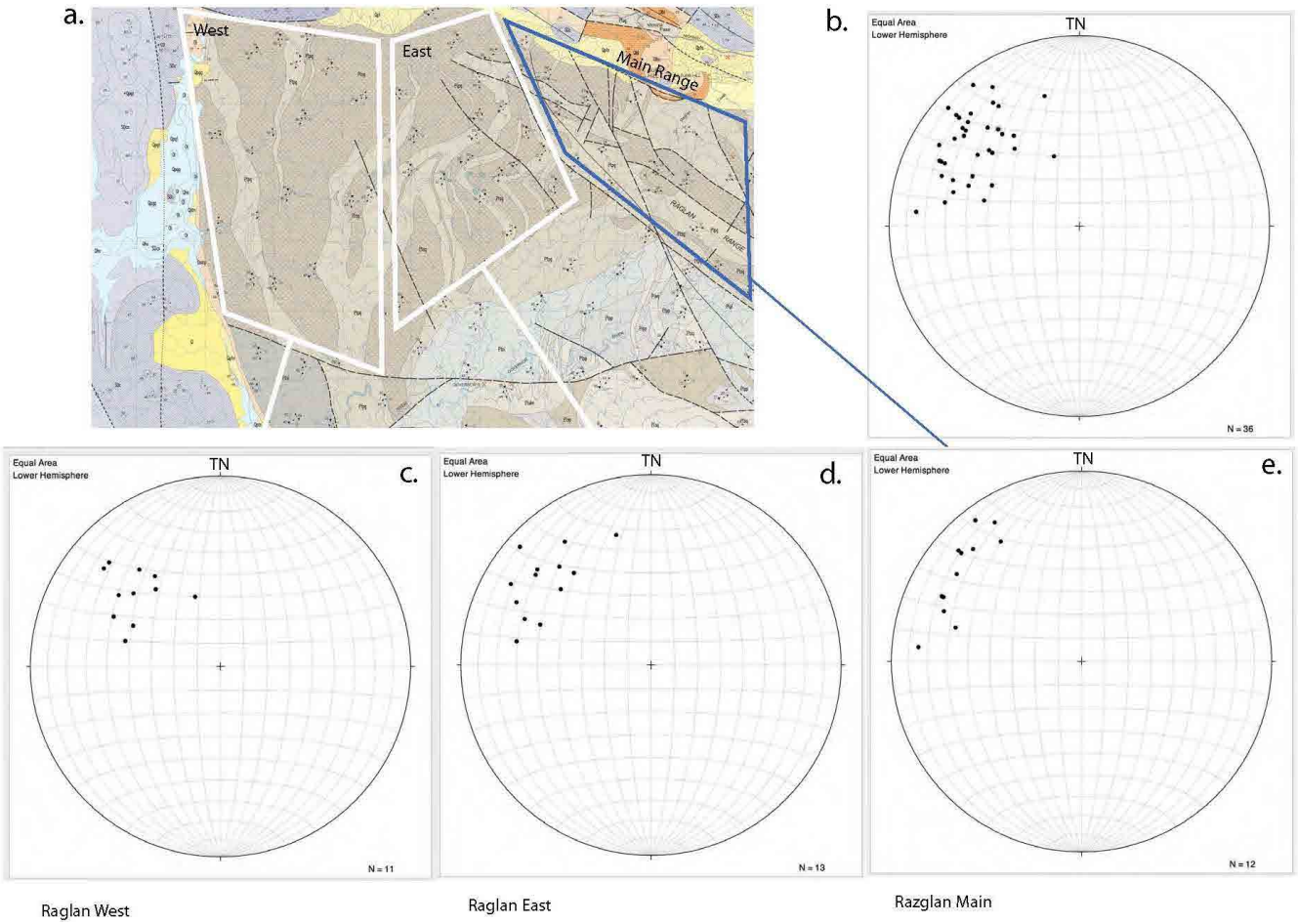

Figure 27. Lineation variability through the Raglan Range isoclinal fold stack. a) 1:25000 scale Owen map sheet (Green and Everard, 2003) showing the domains selected for segregating fold axis data. The West domain is the west limb of the Mary anticline. The Central domain is the hinge zone of the Mary anticline, and the Raglan East domain is the east limb of the Mary anticline. b) Total Lineation Lm plot for the Raglan Range (combined from the three domains). c), d) and e) are lineation plots for the West, Central and East Raglan Range domains respectively.

otite and albite, and 2) the upper contact by the change from brown schist to black phyllite, and the first appearance of mimetic post-S2 muscovite (Gee, 1963, p.14).

4.4.6 Joyce Creek Window

Originally mapped by Spry (1957) and shown as a domal culmination on the fault-bounded Mary Anticline the Joyce Creek Window exposes high-grade rocks (Franklin-Joyce metamorphic sheet) within an apparent carapace of overlying low-grade Mary metamorphic sheet (Figure 28).

The interface with the overlying Mary metamorphic sheet is a phyllite zone parallel to and defining the contact (seen along southwest contact). Other contacts are now late steeply dipping faults that parallel and bound the culmination (Spry, 1957 figs. 3 and 4). The northeastern contact is a gently north-dipping contact with conformable foliation in both the low-grade and high-grade units (Figures 28 and 29 sections A1-B1, G1-H1).

Structures in the Franklin-Joyce metamorphics within the Joyce Creek window are dominated by a large-scale, northwest-closing, reclined, recumbent isoclinal fold. This macro-fold is cored by retrogressed dark grey, carbonaceous quartz-mica phyllite (Ptpi: intermediate grade) enveloped by garnetiferous schist and quartzite. The calculated fold axis (β) plunges at 15°/300° (Figure 17).

Sections A1-B1, C1-D1 and G1-H1 (Figure 29) show the Joyce Creek window part of the Franklin-Joyce metamorphic sheet as a boudinaged, isoclinal macro-fold-pod. This fold-pod is enveloped by the low-grade Fincham-Mary metamorphic sheet quartzites and phyllites above, and the low-grade Scotchfire metamorphic sheet dolomitic schists and phyllites below (Figure 29).

This fold-pod is part of the regional scale, segmented Collingwood Plain recumbent fold (see Figures 13 and 14) juxtaposed against the underlying low-grade Scotchfire metamorphic sheet (Figures 3 and 14).

Structure within the Joyce Creek window is clearly discordant to the high strain phyllite zone and Sm foliation in the overlying sheet (west end of window in Figure 28). The macro-isoclinal folds within the Fincham -Mary metamorphic sheet are arched and folded about the Mary Anticline (sections A1-B1, C1-D1 in Figure 29).

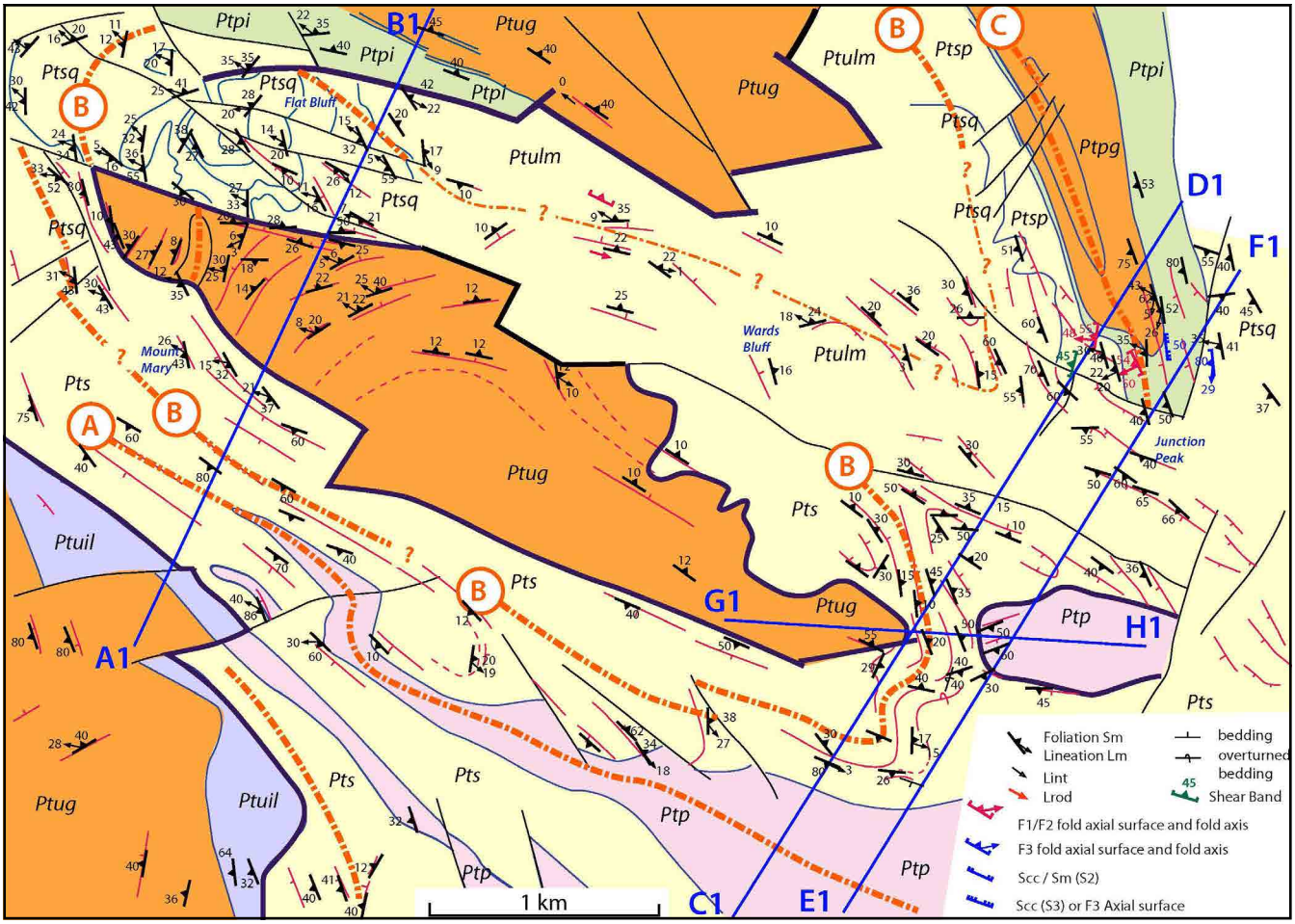

Figure 28. Map of the Joyce Creek window in high-grade Joyce Metamorphics (orange Ptug) based on the Darwin 1:25000 map sheet (Green and Everard, 1998) and Loddon 1:25000 map sheet (Vicary, 2004b). The window shows the structurally lower Franklin-Joyce Metamorphic sheet (orange: Ptug) as a wedge-shaped domain within, and therefore overlain by low-grade quartzite (yellow: Pts) of the Fincham-Mary metamorphic sheet. The window exposes an antiformal north-closing reclined, isoclinal fold-nappe in the northwest corner. Red dashed lines designated by circled A, B and C are recumbent fold axial surface traces that partially close around the window, reflecting the arching across the Mary Anticline domal culmination.

Ptug (orange): high-grade garnet quartzite
Ptpg (orange): high-grade garnet schist
Ptuil (purple): intermediate-grade phyllite-quartzite±minor garnet
Ptpi (green): intermediate grade quartz-mica phyllite±albite±garnet
Pts (yellow): undifferentiated low-grade quartzite-pelite
Ptsq (yellow): low-grade phengitic quartzite
Ptsp (yellow): low-grade carbonaceous quartz-phengite phyllite
Ptp (pink): low-grade dolomitic phyllite (Scotchfire metamorphic sheet)

The domal culmination form produces a loop-like axial surface trace in the west-closing synformal isoclinal fold directly above the Joyce high-grade fold pod (circled B axial surface trace in Figure 28).

At the outcrop scale the high-grade metamorphics in the Joyce Creek Window, the Joyce Metamorphics of Spry (1963a), show extremely flattened and attenuated tight to isoclinal folds (Figures 30 and 31), pronounced rodding (Figure 32) and a schistosity/ transposition layering due to intense crenulation cleavage development (Figure 33) (Turner, 1971).

4.4.7 Mt Madge and Mt Maud

The Mt Madge and Mt Maud area are part of an apparent narrowing of the Franklin fold-nappe where high-grade garnet quartzite pod-like bodies (Ptug) are enveloped by retrograded high-grade garnet phyllite/schist (Ptuil) and at Mt Maud in-folded with low-grade quartzite and phyllite (Figure 34). The contact between low-grade and high-grade is folded east of Mt Madge with in-folds of the low-grade Fincham-Mary metamorphic sheet.

Both the high-grade and low-grade bodies have closed loop-form in map view and have moderate to steeply plunging fold hinges (Figures 34 and 35). The low-grade schistose quartzite pod and high-grade garnet quartzite at Mt Maud are offset along east-west trending faults and have faulted terminations but show decreasing thickness, or outcrop width, towards the now truncated ends (Figure 34).

These bodies are interpreted as fold-pods and closed out fold cores (noses) with in-folded 1) low-grade Fincham-Mary metamorphic sheet (grey and yellow units), and 2) high-grade Franklin-Joyce metamorphic (orange unit: Ptug) both in retrograded high-grade Franklin Group. Fold cores here are interpreted as conical or sheath-like closures to give the pod-like outcrop patterns (Figures 21 and 34).

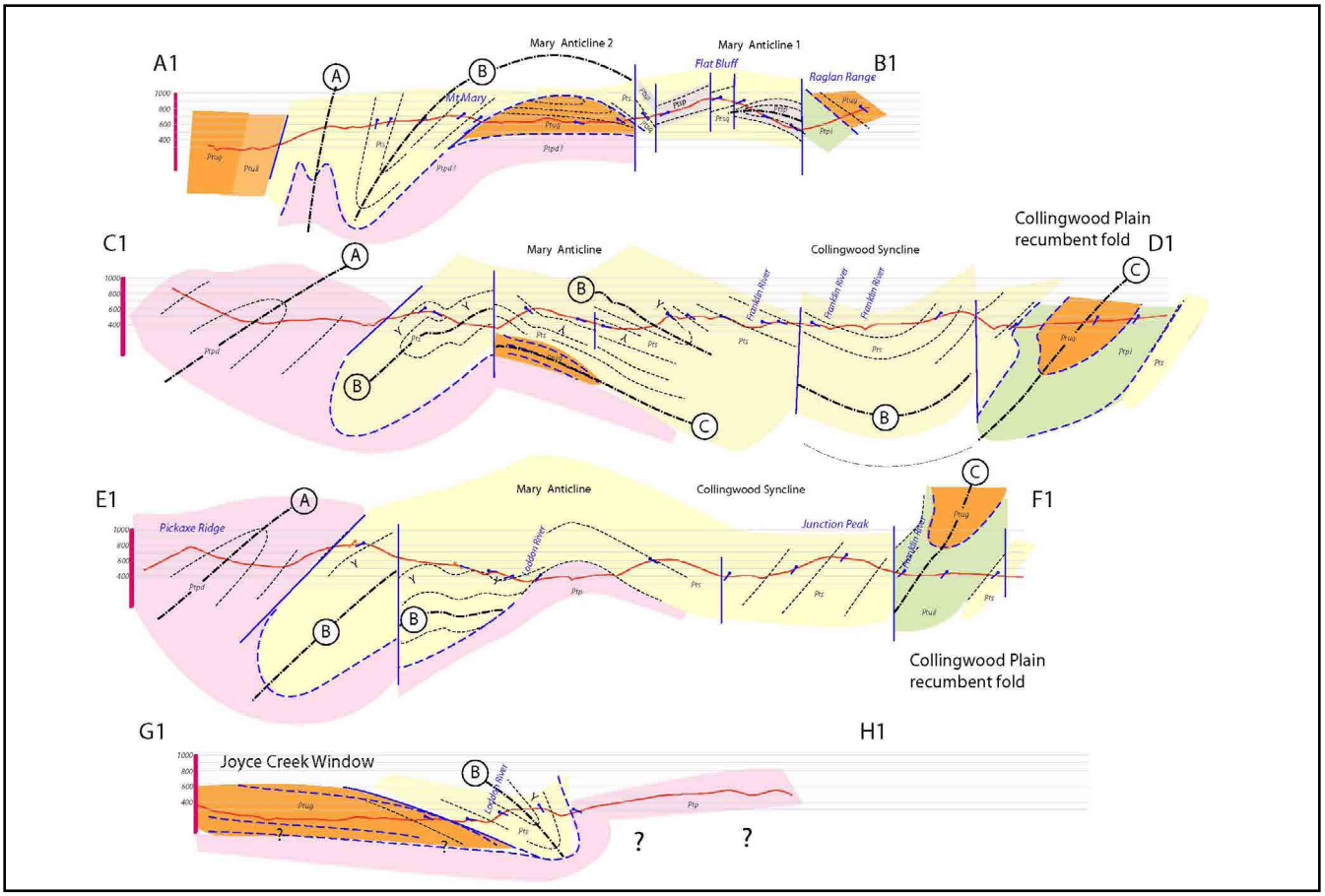

Figure 29. Sections A1-B1, C1-D1, E1-F1 and G1-H1 across the Joyce Creek Window as shown in Figure 28. Circled A, B and C dashed lines are recumbent fold axial surface traces of the stacked isoclinal folds. Legend for lithologies as in Figure 28.

Figure 30. Flattened and attenuated F2 isoclines within inter-bedded thin quartzite and micaceous schist layers. Joyce Metamorphics (photo from Turner, 1971).

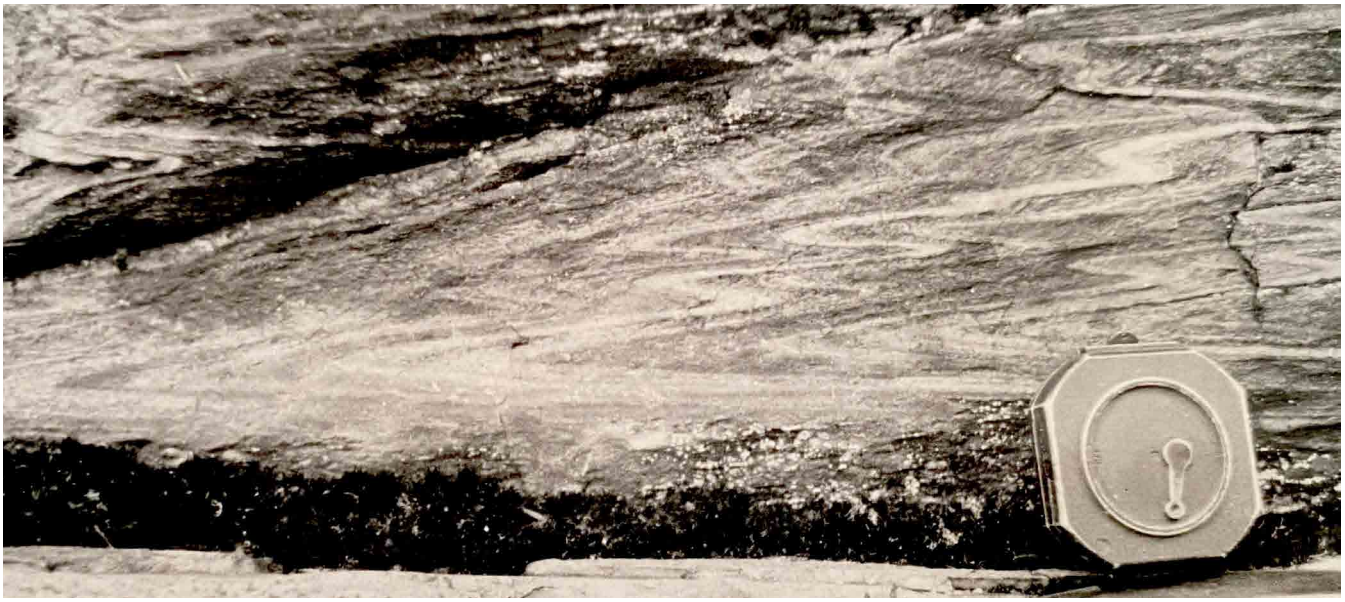

Figure 31. Tight, angular chevron folds in laminated micaceous schist. Joyce Metamorphics (photo from Turner, 1971).

Figure 32. Rodding of thin quartzite layering within micaceous schist. The rodding lineation (Lrod) is parallel to the hammer handle (photo from Turner, 1971).

Figure 33. Photomicrograph of schistosity Sm in Joyce Metamorphic schist developing from a crenulation cleavage S2 within an earlier cross-cutting S1 mica fabric visible in the crenulation hinges preserved within the S2 microlithons (upper right) (photo from Turner, 1971).

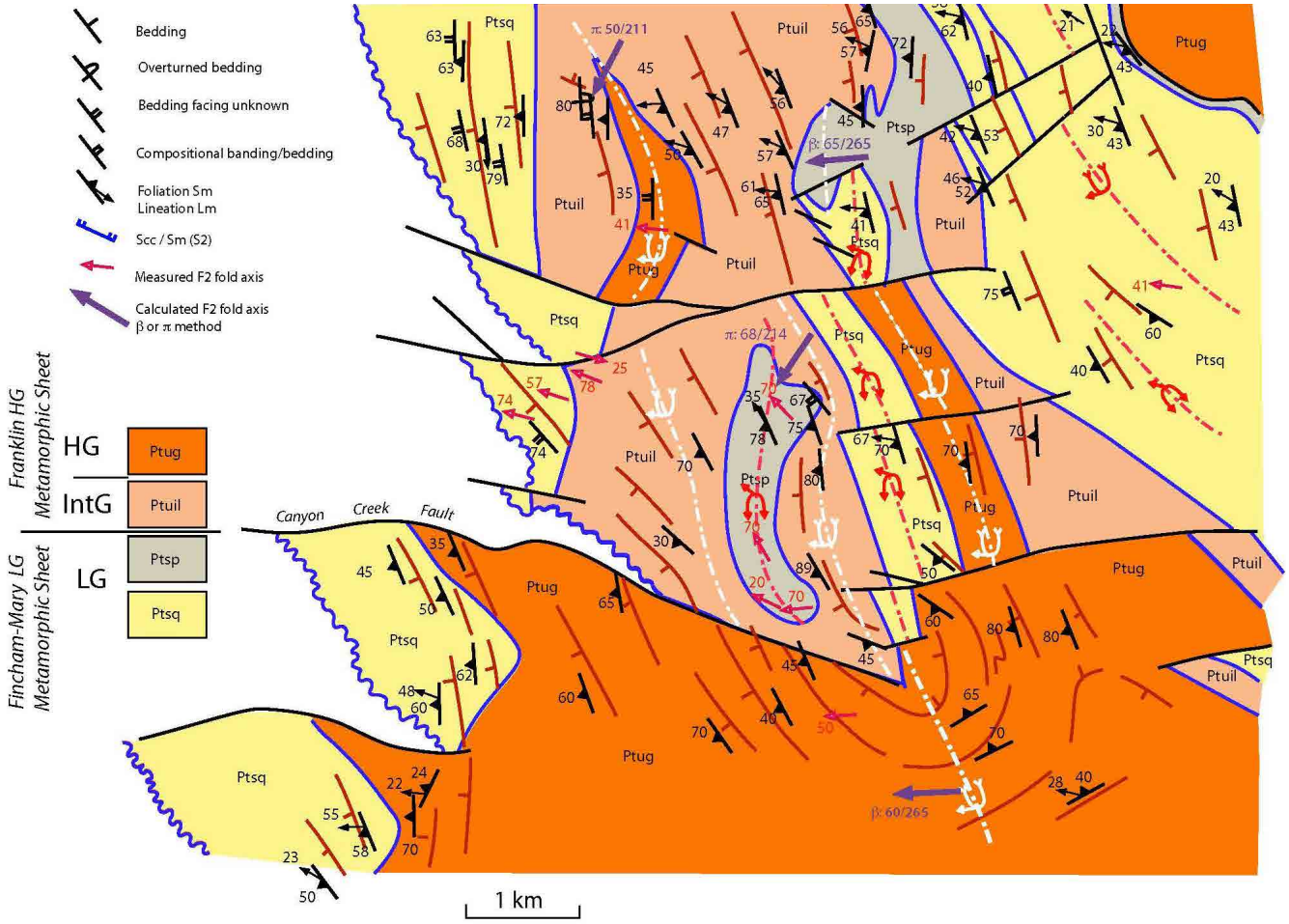

Figure: 34. Mt Madge-Mt Maud area structural map based on the Darwin 1:25000 Map sheet (Green and Everard, 1998). Red dashed lines are inferred recumbent fold axial surface traces. Orange: high-grade Franklin metamorphic sheet Ptug. Light orange is Ptuil: retrograde Franklin metamorphic sheet. Grey is Ptpp and yellow is Ptsq (low-grade Joyce- Mary metamorphic sheet).

The low-grade infolds project from the structurally lower Fincham-Mary metamorphic sheet as antiformal lobes into the structurally higher high-grade Franklin metamorphic sheet (Figure 21).

The maximum extent of Franklin metamorphic sheet retrogression, as dark grey carbonaceous phyllite with occasional porphyroblasts (Ptuil), coincides with the hinge "narrowing" in the Mt Madge and Mt Maud area (Figure 34). The narrowing is due to extreme hinge-elongation parallel to Lm with conical, sheath-like nose development. This is coincident with hinge complexity and large-scale, conical, parasitic folds in the high-grade-low-grade contact.

4.4.7.1 Mt Madge fold closure

In map view Mt Madge is a curved tapered wedge of compositionally banded, pink, micaceous quartzites (Turner, 1971) within retrograded high-grade schist and quartzite (Figure 35). Although truncated by a younger, oblique-slip cross-fault on the south, the Mt Madge slice is a relict fold-pod now preserved as a macro-scale foliation "augen" enveloped by the regional foliation. The tapered north end shows convergence of Sm with a calculated β intersection of 50°/211° (Figure 35g). The south-tapering termination has been truncated and eroded in the fault-hanging wall. This is due to inferred dextral south-side-up movement along the east-west fault. It indicates a lessening down-plunge extent towards the termination.

Attitudes of the compositional banding and S2 foliation (data from Turner (1971 fig.9) suggest a flattened and attenuated asymmetric fold pair with approximate reclined geometry (Figure 35a and b) about an axis β: 40°/286° (Figure 35 e and f). The macro-augen form, due to Sm convergence and the interpreted internal fold geometry, are shown in block diagram (Figure 35d). The original asymmetric fold-pair (Figure 35c and d) related to the western limb of the regional Franklin fold-nappe now have attenuated limbs that are sub-parallel to the regional Sm/ transposition layering. This produces a foliation "carapace" about the macro-augen containing the preserved fold pair (Figure 35b and d).

On the west the upper foliation "carapace" has steeper dips (60°-85°), a northwest trending Lm and is overturned, whereas the east limb or lower foliation "carapace" is flatter with dips 40°-50° dips and Lm more west-northwest trending (Figure 35b). Geometrically this can be produced by folding Sm/Lm about an inferred fold axis of 50°/211° (Figure 35g).

Mesoscopic fold hinges within the Mt Madge fold pod show a strong linear fabric with mullion structure parallel to the fold hinges (Turner, 1971; Turner 1986). Fold axes and lineations are sub-parallel and cluster about the calculated β axis of 40°/286° (Figures 35e and f). Fold

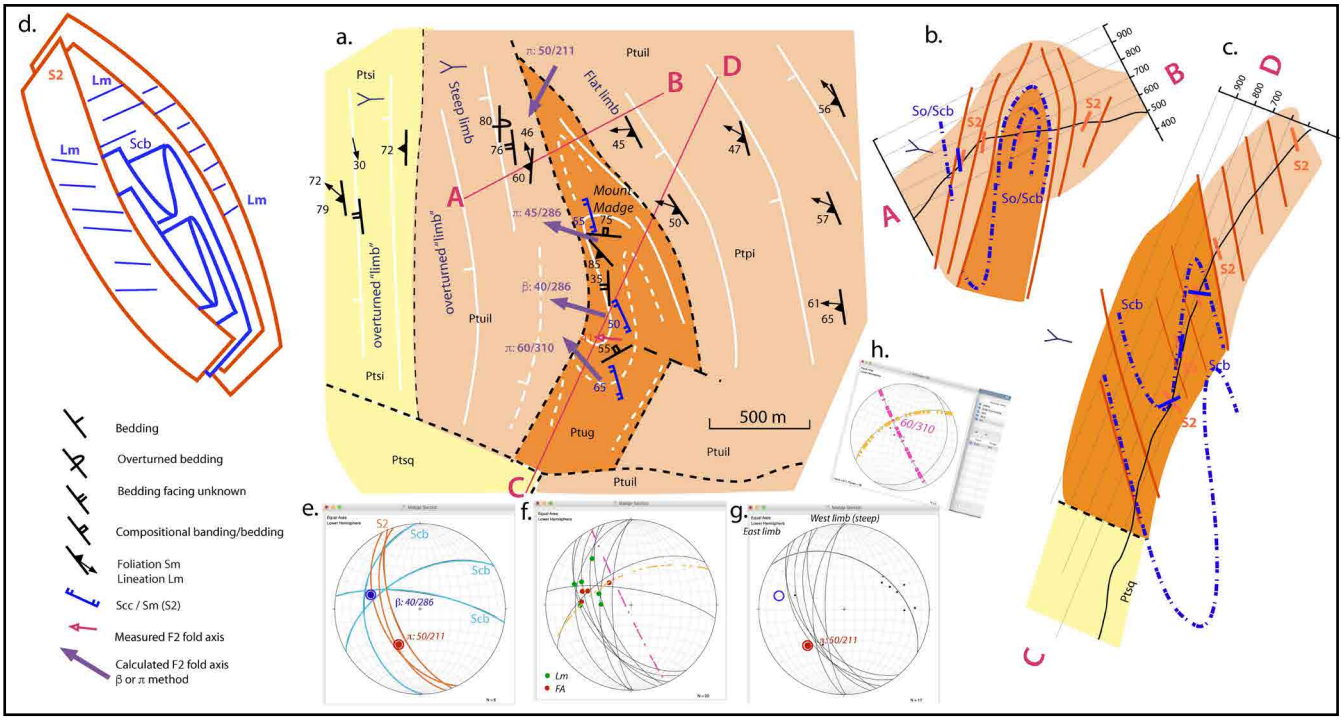

Figure 35 (Above). Mt Madge structural interpretation. a) Simplified structural map showing enveloping foliation to give tapered outcrop form. Map based on 1:25000 Darwin map sheet (Green and Everard, 1998) Mineral Resources Tasmania digital geological atlas. pink traces: Lm. blue: compositional banding. orange: Sm/S2. b) Section A-B across northern end of Mt Madge taper. c) Profile C-D along Mt Madge normal to the fold axis trend. d) 3D block form of Mt Madge structural geometry. e) Stereonet showing compositional banding great circle traces (blue) foliation S2/Sm (red). Derived major reclined fold axis of 40°/286°. f) Stereonet of all foliation great circle traces and with Lm (blue dots) and fold axes (red dots). g). Sm great circle traces showing east limb versus west limb groupings. Red dot is pi at 50°/211° for intersection of bounding foliations at northern termination. h) Stereonet showing β determination of 60°/310° for south-closing synformal hinge within Mt Madge pod.

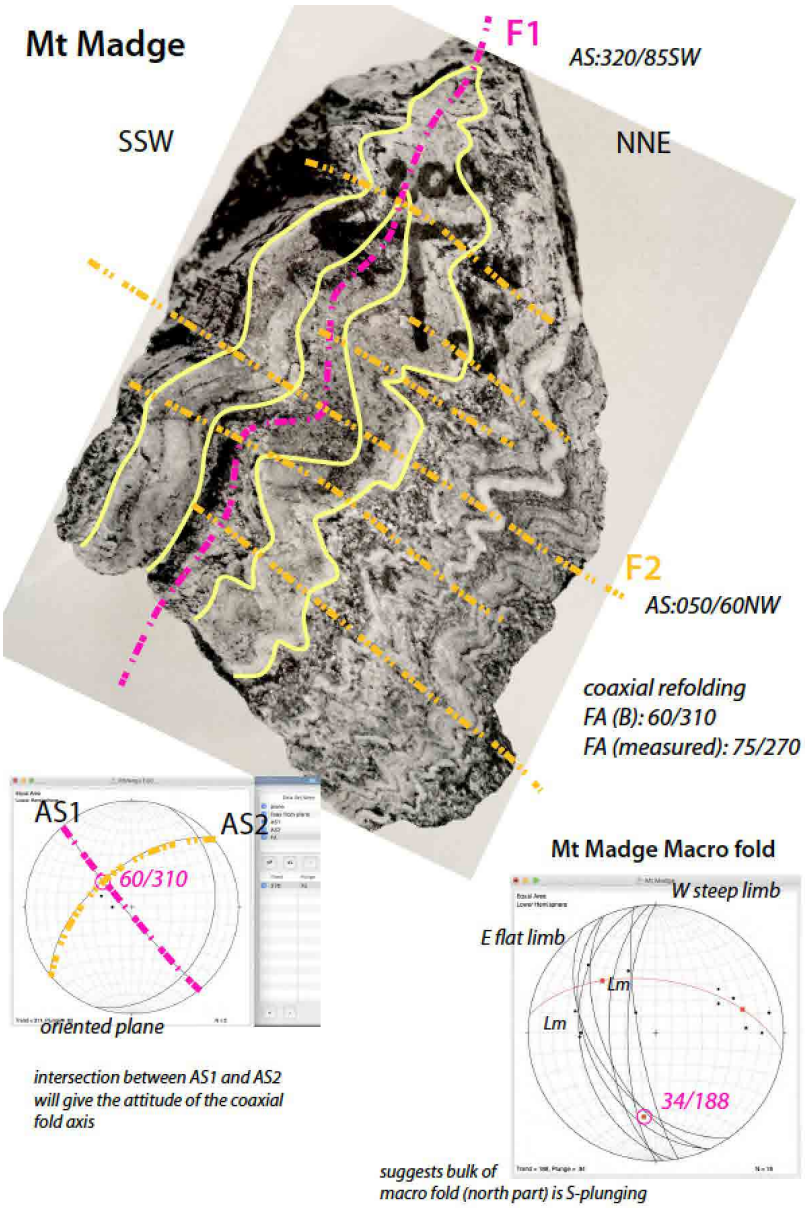

Figure 36 (Left). Coaxially refolded F1 isoclinal fold in compositionally banded quartzite from the hinge zone of the Mt Madge syn-formal infold (photo from Turner, 1971). F1 axial surface trace (pink) and F2 axial surface traces (orange).

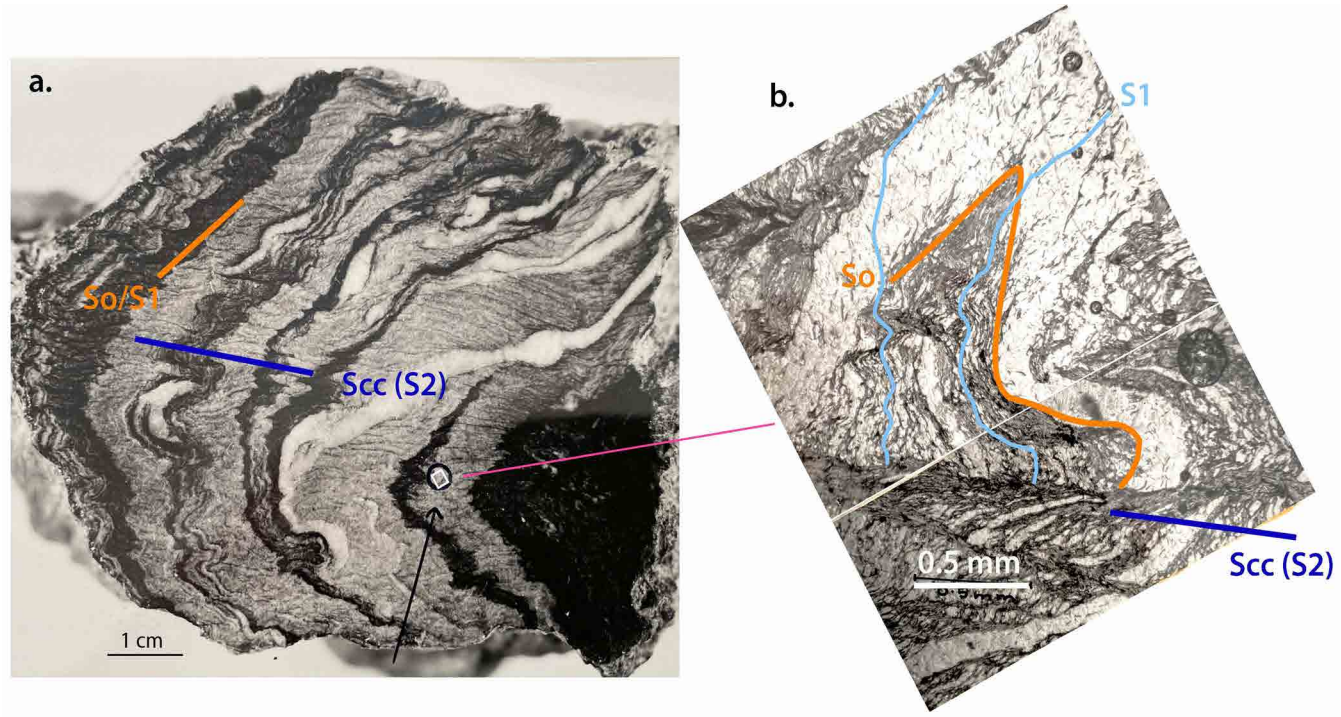

Figure 37. F2 fold hinge east of Mt Madge in retrograded schist and quartzite (Ptpi) showing spaced crenulation morphology of the axial surface foliation (photos from Turner, 1971 and Turner 1989, Figure, 2.14). b) Thin section photomicrograph enlargement of part of a) showing F1 closure in quartz vein (sub-parallel to So) with cross-cutting S1 mica trains as F1 axial surface fabric. These are both crenulated by a strong crenulation cleavage fabric (Scc/S2) showing marked pressure dissolution. This crenulation cleavage morphology is typical of the axial surface fabric of the Franklin Fold-nappe.

axis measurements and β determinations reflect a gradual change in plunge direction from 211° to 286° to 310° (Figure 35a). Hinge migration lies within surface 251°/61°NW (a best fit great circle to the fold axes: see Figure 18b) with a generalised 41°/275° fold axis.

Meso-folds and axial surface fabrics all show F2 character with folding of the compositional banding (transposed So/Sm) and S1 (Figures 36 and 37).

4.4.7.2 Mt Maud Fold closures

In the Mt Maud area the regional Franklin fold-nappe hinge zone contains a series of low-grade and high-grade "layers" within retrograded garnet phyllite and schist (Figures 34 and 38). There is 1) a lobate-shaped closure in low-grade, interbanded phengitic-quartzite and quartz-mica phyllite (Ptsp), 2) a tapering, fault-truncated and offset low-grade quartzite layer (Ptsq), juxtaposed against 3) a linear belt of high-grade garnet quartzite (Ptug) bounded to the east by west-dipping retrograded garnet phyllite and schist (Ptuil). Dips in the Mt Maud quartzites are ~70° W but there are limited structural data available (Figure 38a).

Mesoscopic fold hinges within the lobate Ptsp "closure" suggest a curving macro-fold hinge line (Figures 38 and 39). Hinge migration lies within surface 206°/70°W (a best fit great circle to the fold axes: see Figure 18b) with a generalised 70°/320° fold axis. The overall Franklin fold-nappe geometry (Figures 15 and 38b) requires this closure to be antiformal, as an in-fold into the overlying high-grade Franklin metamorphic sheet (Figure 38b). The Mt Maud quartzite layer (Ptsq) must also have antiformal geometry about a 67°/275° fold axis. South of the southernmost Canyon Creek cross-fault Sm foliation measurements suggest a simple large-scale fold closure with reclined geometry about an axis 50°-60°/272° (Figure 38a). This is in contrast to the more complex hinge zone with parasitic folds between Mt Maud and Mt Madge (Figure 40).

4.4.8 Fincham-Mary Metamorphic sheet

The low-grade Fincham-Mary metamorphic sheet shows folded domains bounded or enveloped by higher strain domains of transposition layering, intense crenulation cleavage and complexly deformed phyllite. Folds in quartzite layers have flattened and attenuated, tight to isoclinal form (Figures 41, 42 and 43). They commonly have reclined recumbent geometry and are somewhat pod-like in three dimensions, with hinge-parallel elongation and alignment with the regional lineation Lm (Turner, 1971). Limb segments display boudinage (Figure 44). Similar relationships were described by Gee (1963) for the fold structure in the high-grade Franklin-Joyce Metamorphic sheet of the Raglan Range.

Zones of complexly deformed phyllite with rootless isoclinal folds (Figure 45) coupled with transposition layering and intense crenulation cleavage (Scc) development (Figure 46) occur at the interface with the

underlying Joyce Metamorphics (Franklin-Joyce metamorphic sheet) as well as zones enveloping fold zones (macro-pods) with the Fincham-Mary low-grade sheet.

4.4.9 Scotchfire Metamorphics

The Scotchfire metamorphic sheet includes brown dolomitic phyllite and schist intercalated with thin dolomite layers. The lower part contains thicker dolomite layers (dark olive green in Figure 47). It is the structurally lowest unit in the Central Tyennan region litho-tectonic stratigraphy. It is overlain by, and in contact with, Fincham-Mary metamorphic sheet quartzites at Frenchmans Cap, Clytemnestra and Agamemnon, and also at southern end of the Joyce Creek "window" (Figures 7 and 28).

The map pattern and mapped structural relationships suggest regional scale isoclinal folding of the Scotchfire-Mary metamorphic sheet contact west of the "win-

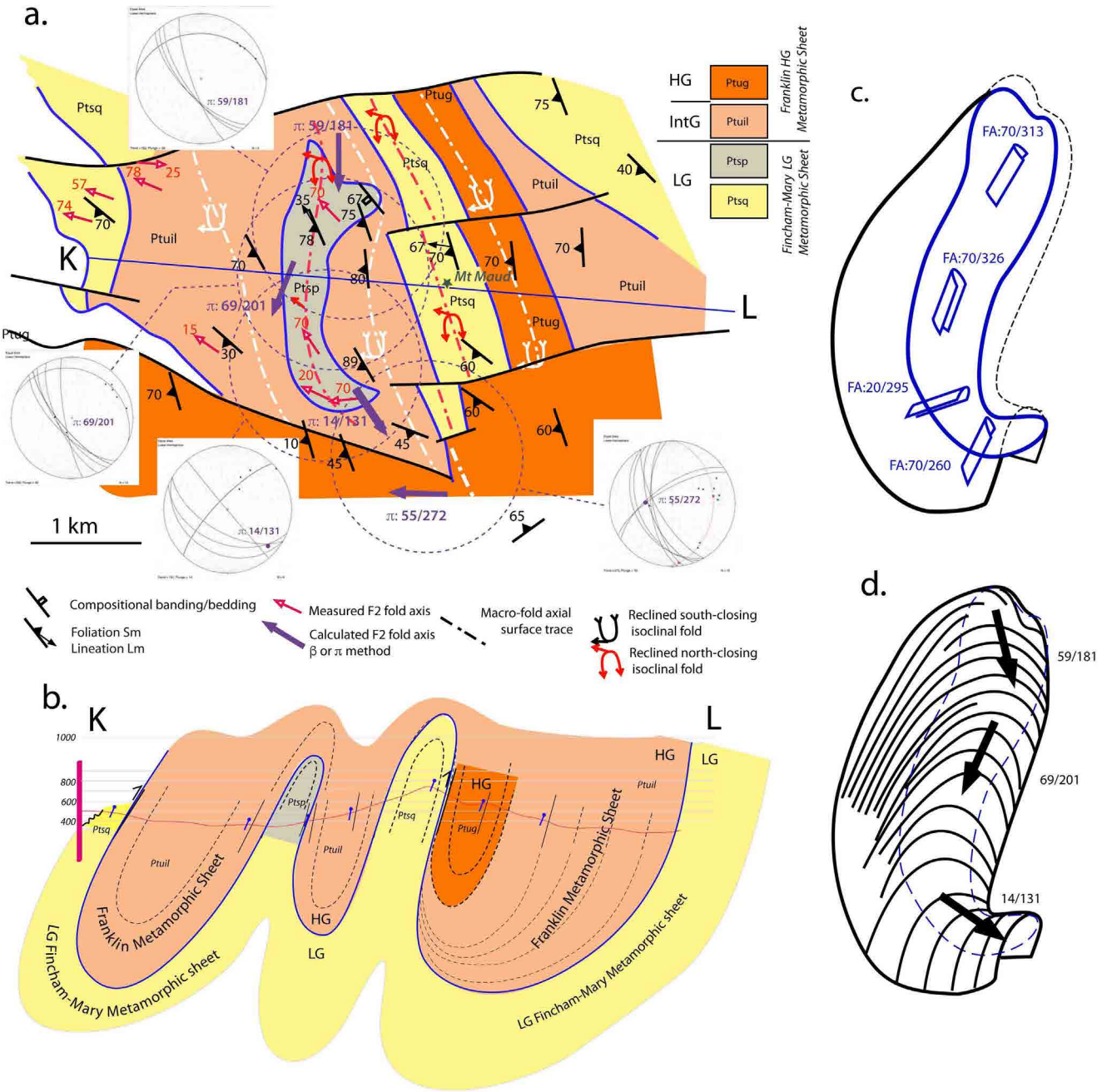

Figure 38. Structure of the Mt Maud domain area. a) Map modified from 1:25000 Darwin map sheet (Green and Everard, 1998) showing outcrop pattern, structural attitude data and axial surface traces. Stereonet insets show plunge geometry of the northern, central and southern ends of the lobate Ptsp closed loop (grey area) and the high-grade area (orange) to the south. b) Structural profile K-L showing the inferred complex geometry of the Maud domain. c) Mesoscopic fold geometry inside the lobate Ptsp closed loop. d) 3D geometry of the antiformal conical to sheath-like form of the lobate Ptsp closed loop. Black arrows indicate the plunge variation along the curvilinear hinge based on the π determinations from the stereonet insets in a).

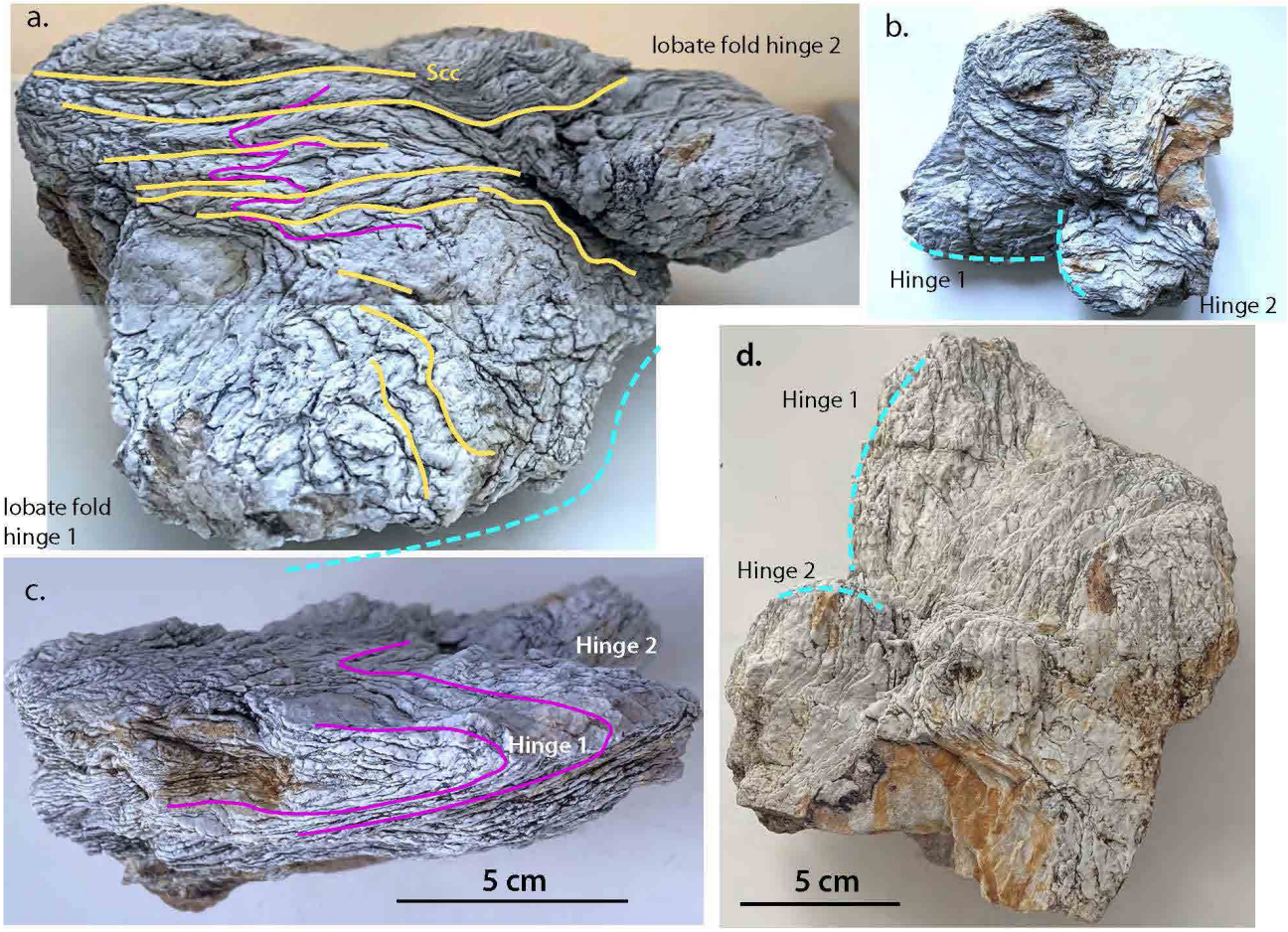

Figure 39. Small-scale, lobate fold geometry in crenulated quartzite from the Southern Tyennan region. These lobate folds encapsulate aspects of the Franklin fold-nappe macro-fold geometry (see Figure 40). Width of sample is 15cm. Folds 1 and 2 have oppositely closing hinges that are at 90° to each other. a) View of the upper limb of lobate fold 1 transitional with crenulation cleavage traces (yellow) and an earlier layering Sm (pink lines). Blue dashed line is parallel to the curved hinge-line of lobate-fold 1. b) View along lobate fold 2. Hinge lines of lobate folds 1 and 2 are shown by the blue dashed curved lines. c) Side view of the chevron-like folds within Sm (pink lines) that define lobate fold 1 showing transition into the crenulation cleavage seen in (a). d) under side of lobate fold pair showing the curved nature of the hinge lines (blue dashed lines).

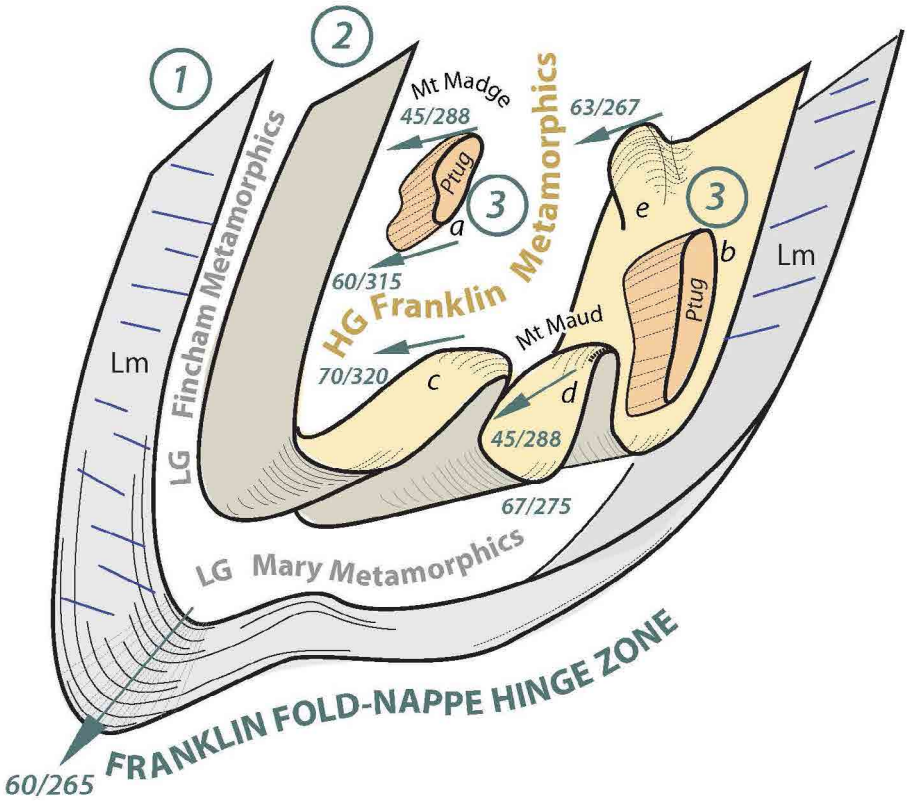

Figure 40 (Left). Schematic 3D form of the reclined Franklin fold-nappe hinge in the Mt Madge-Mt Maud area. Core of the fold is retrograded Franklin metamorphics (orange) with relict noses of 1) synformal sheath-fold pods in high-grade garnetiferous schist (Ptug) (dark orange) enveloped by intense S2 foliation, and 2) antiformal sheath-fold pods from the underlying low-grade Fincham-Mary metamorphic sheet (grey layer). Fold noses are steeply to moderately plunging to the west and northwest (into the page). Measured and calculated fold plunges are shown. Circled 1 is the outermost and lower surface of the low-grade Fincham-Mary metamorphic sheet. Circled 2 is the interface or contact between the high-grade Franklin-Joyce Metamorphic sheet and the low-grade Fincham-Mary sheet. Circled 3 are the synformal fold noses of high-grade Franklin metamorphics (Ptug) of the Franklin-Joyce metamorphic sheet.

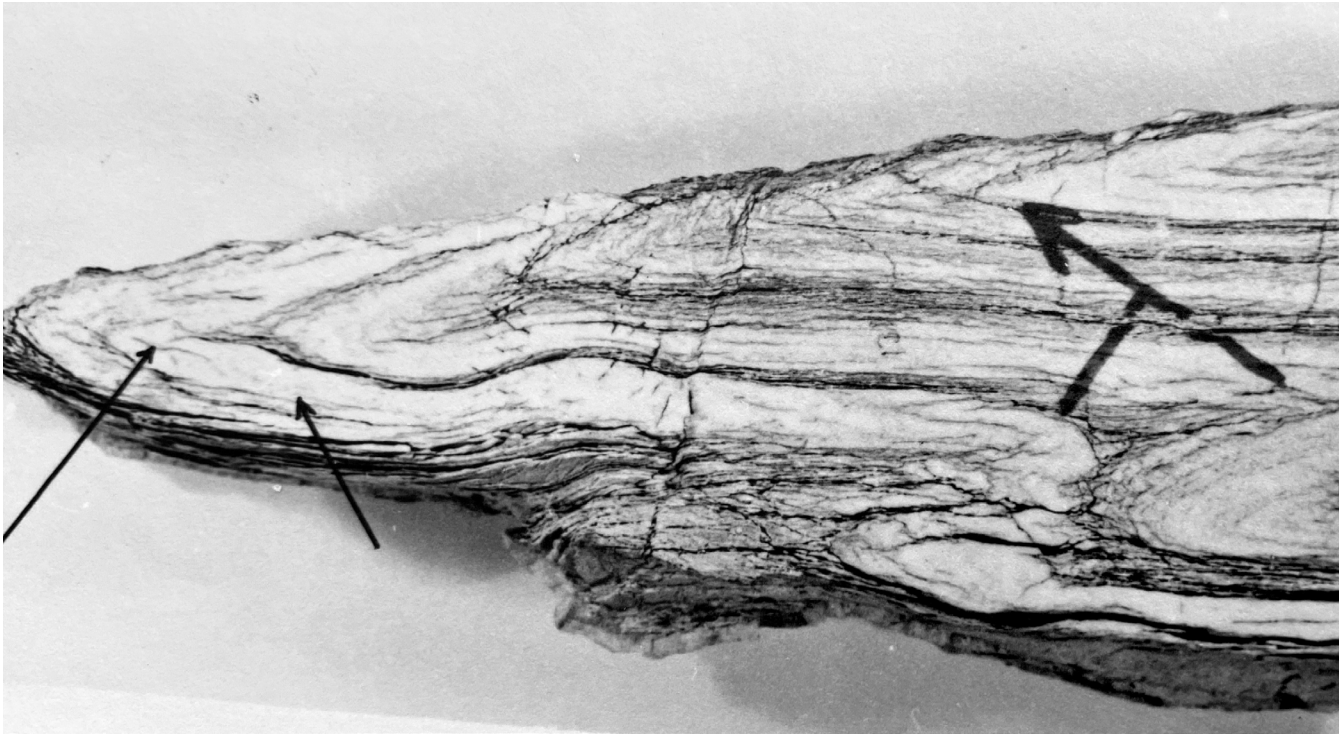

Figure 41. Isoclinal fold in Mary sheet quartzite showing spaced crenulation cleavage in hinges of micaceous layers (photo from Turner, 1971).

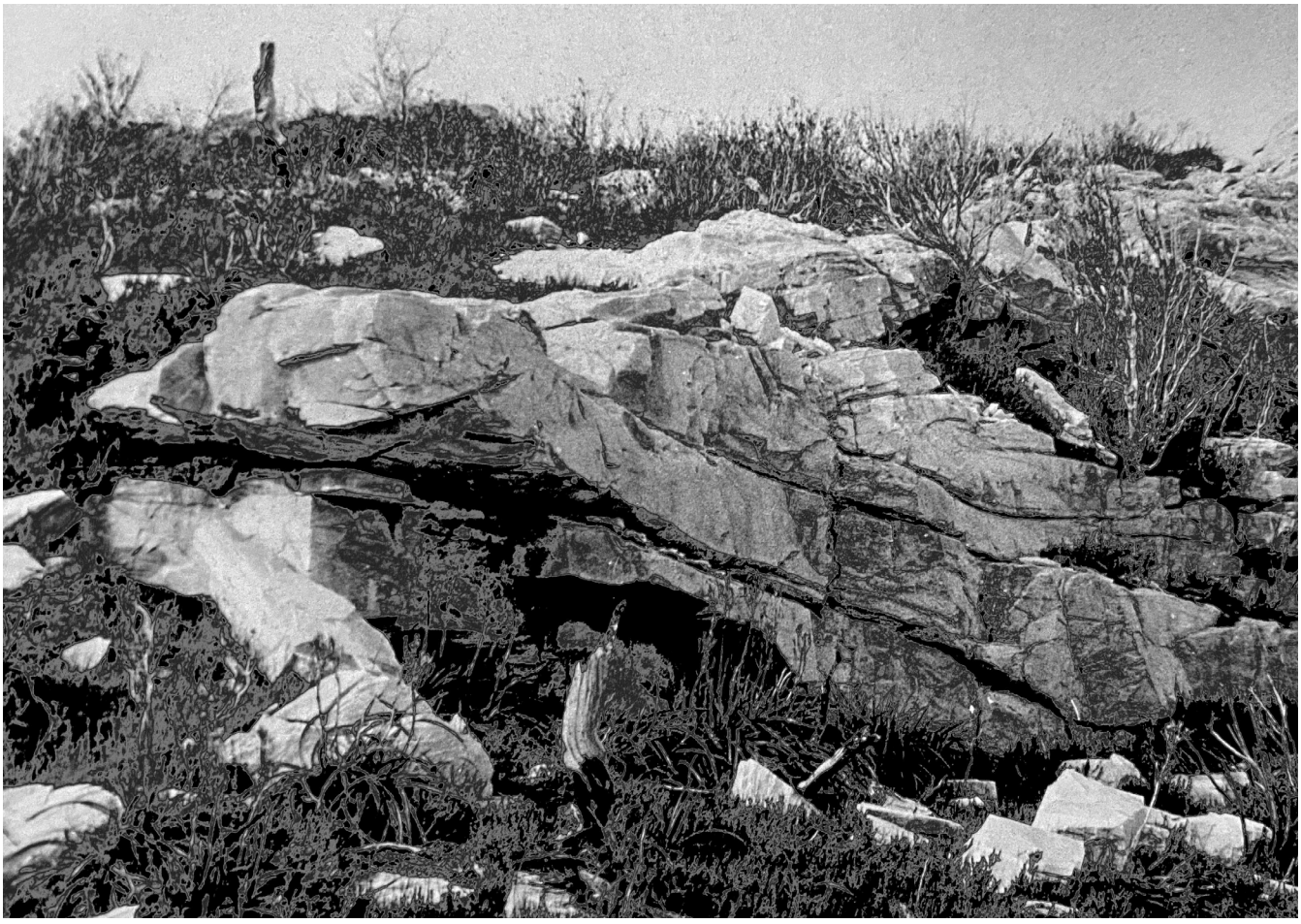

Figure 42. Isoclinal recumbent fold hinge in Mary sheet quartzite (photo from Turner, 1971).

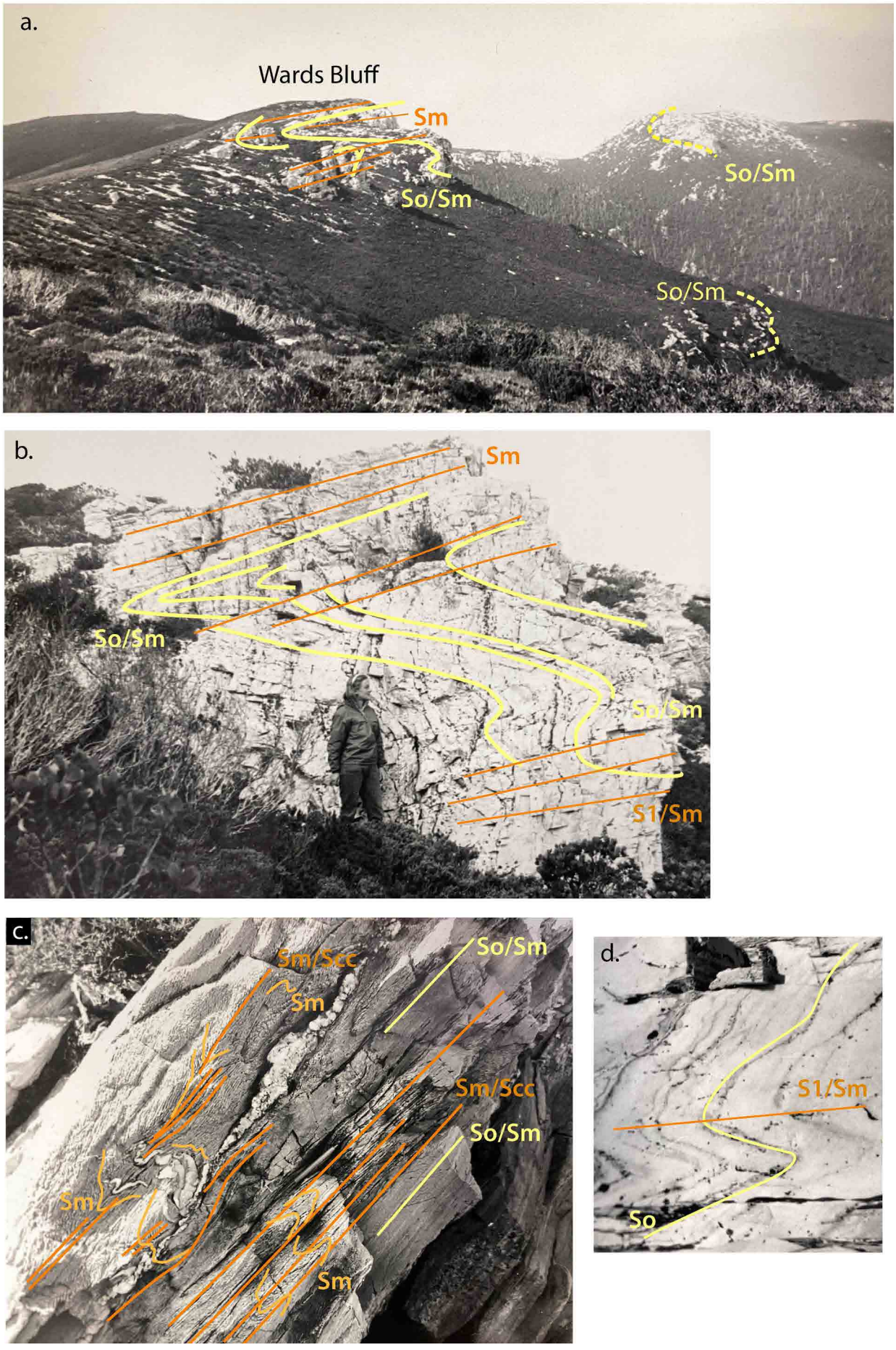

Figure 43. Photographs of structure in the low-grade Fincham-Mary metamorphic sheet quartzites of Wards Bluff (photos from Duncan, 2021). a) Inferred isoclinal hinges in the ridges of Wards Bluff. b) Tight to isoclinal recumbent folds in quartzites. c) Zones of higher strain characterised by more intense Sm and multiple foliations in the less deformed parts. d) Character of the bedding and cleavage of the outcrop shown in b).

Figure 44. Internal boudin within quartzite of the Mary sheet representing layer flattening and elongation (photo from Turner, 1971).

Figure 45. Mary sheet phyllite with rootless fold hinges in folded - boudinaged quartz veins. Flattened and attenuated limbs have tad-pole-like tails (photo from Turner, 1971).

Figure 46. Intense transposition layering developing from ropy-style crenulation cleavage in the low-grade Fincham-Mary metamorphic sheet (photo from Turner, 1971).

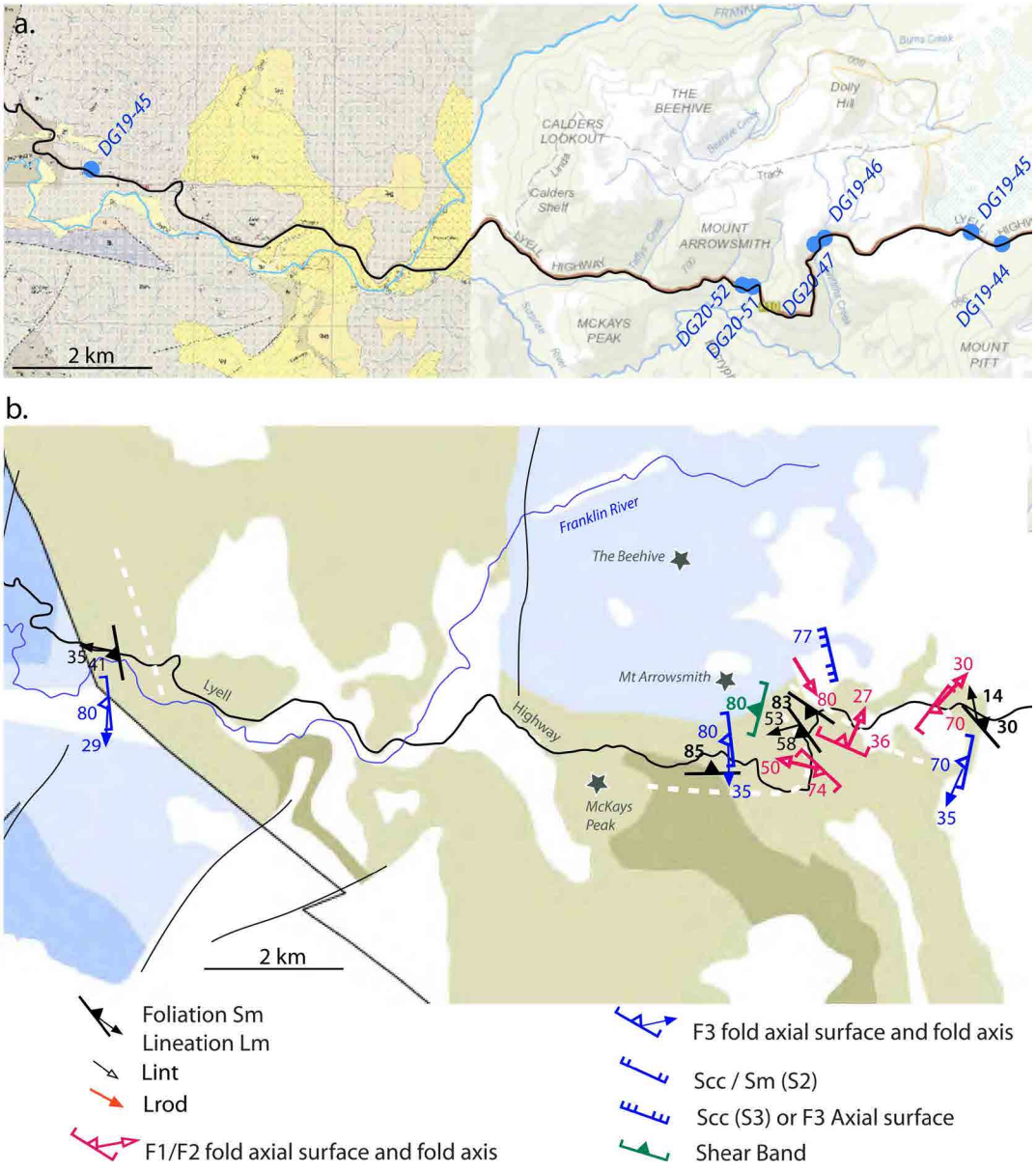

Figure 47. Maps of part of the Lyell Highway showing distribution and structural data for the Scotchfire metamorphic sheet (olive green) with dark olive green: dolomite). a) LISTmap topographic map showing the outcrop stations where structural data was collected. b) Map modified from the 1:25000 digital atlas maps with plotted structural orientation data collected at the stations shown in a). White dashed are formlines in So/Sm.

khaki colour: Scotchfire dolomitic phyllite; olive green: Scotchfire dolomite; light blue: undifferentiated Proterozoic rocks; dark blue: low-grade Fincham-Mary metamorphic sheet quartzite

dow" into Joyce Metamorphics of the Franklin-Joyce metamorphic sheet (Figures 28 and 29).

The contact and upper part of the Scotchfire metamorphic sheet at Frenchmans Cap show marked transposition layering due to intense crenulation cleavage development and internal boudinage (see Gray and Vicary, 2021).

The northern part of the Scotchfire metamorphic sheet, as seen along the Lyell Highway (Figure 47) show the schist/phyllite with isoclinal folds (Figure 48a), intense transposition layering (Figure 48b) and associated crenulation cleavage in less deformed zones (Figures 49, 50 and 51). The outcrops are dominated by upright, north-south trending younger Devonian folds with an axial surface S3 crenulation cleavage (see blue dip/strike symbols on Figure 47b). These folds plunge moderately to steeply south. The outcrops are cut by steeply to moderately dipping reverse faults (Figure 49a).

The dominant foliation in outcrop is a composite fabric with visible relicts of a folded S1 foliation (Figures 50 and 51). Lenses and lozenges with So/Sm layering and the S1 foliation are preserved within dolomite pods as relict-fold hinges bounded by intense fabric along limb zones (Figure 50b). This can be seen at centimetre to metre scale (compare Figures 50 and 51). It is suggested that the intensity of this crenulation cleavage fabric is not related to the younger Devonian deformation but is an early, intense second foliation fabric that has been folded by the younger upright folds.

The early small-scale isoclinal folds and the early dominant foliation are clearly folded at the outcrop scale (Figure 50b, c) and at the map scale by the variability in Sm and F1/F2 axial surface attitudes (see Figure 47b).

Figure 48. Scotchfire Metamorphics along the Lyell Highway (station DG19-46) showing a) complex isoclinal recumbent folds cut by high angle reverse faults, and b) Intense schistosity (Sm) as transposition layering, with relict isoclinal hinges and boudinaged veins sub-parallel to Sm. Lithology is thicker bedded dolomite and carbonaceous pelite in a) and carbonaceous phyllite in b). Note the moss and lichen covered nature of the outcrop in a). This is typical of the road outcrops through the Scotchfire metamorphic sheet.

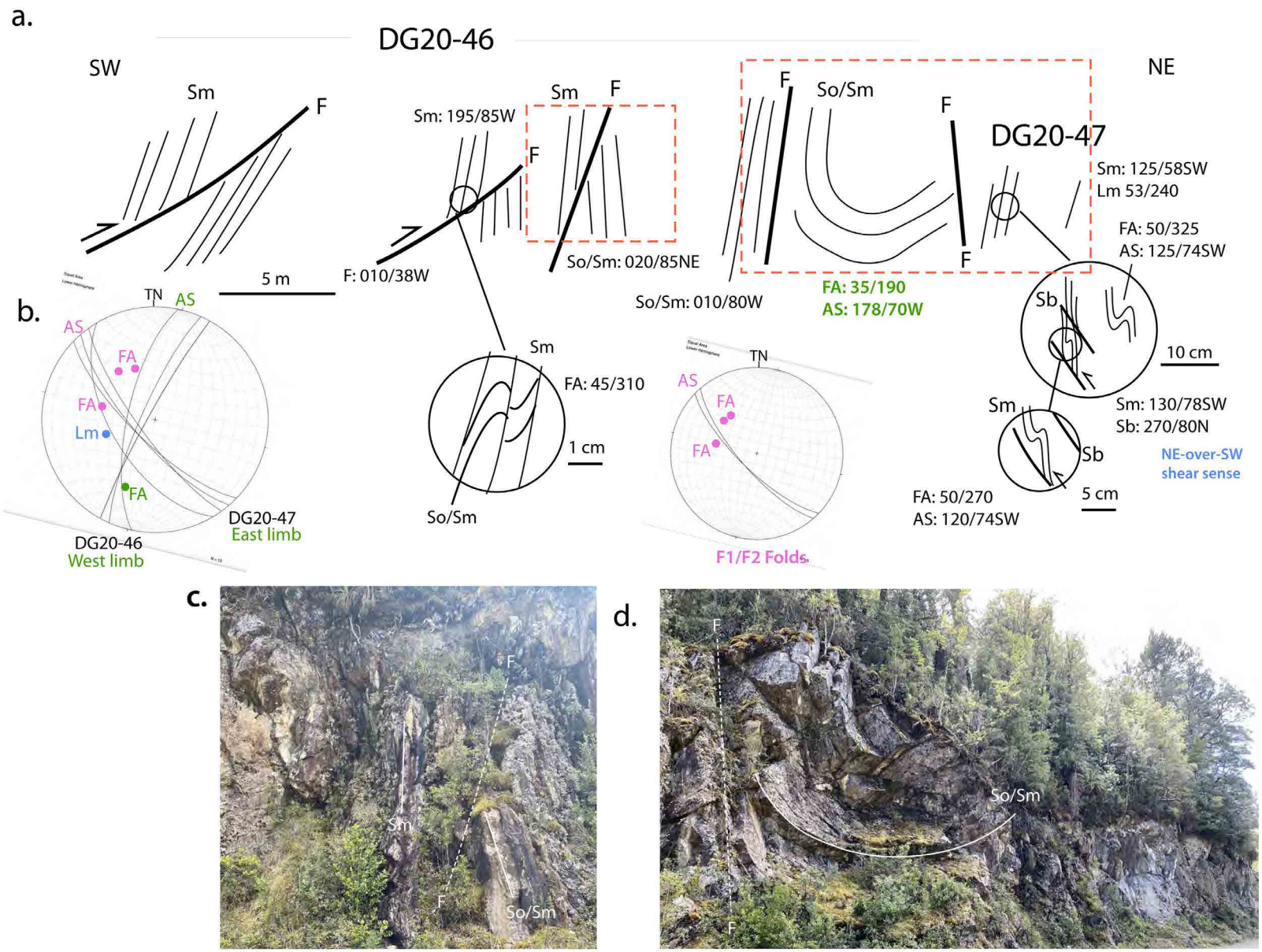

Figure 49. Lyell Highway structural profile at Stations DG20-46 and DG20-47 (see Figure 47a for location). a) Sketch profile dominated by open, plunging synform truncated and offset by several moderate to high angle reverse faults. b) Stereonet showing Sm great circle traces, fold axes FA (pink dots) and lineation Lm (blue dots). c) Photograph of steeply dipping Sm and So/Sm cut by high angle reverse fault. d) Photograph of plunging Devonian synformal hinge bounded by late brittle faults.

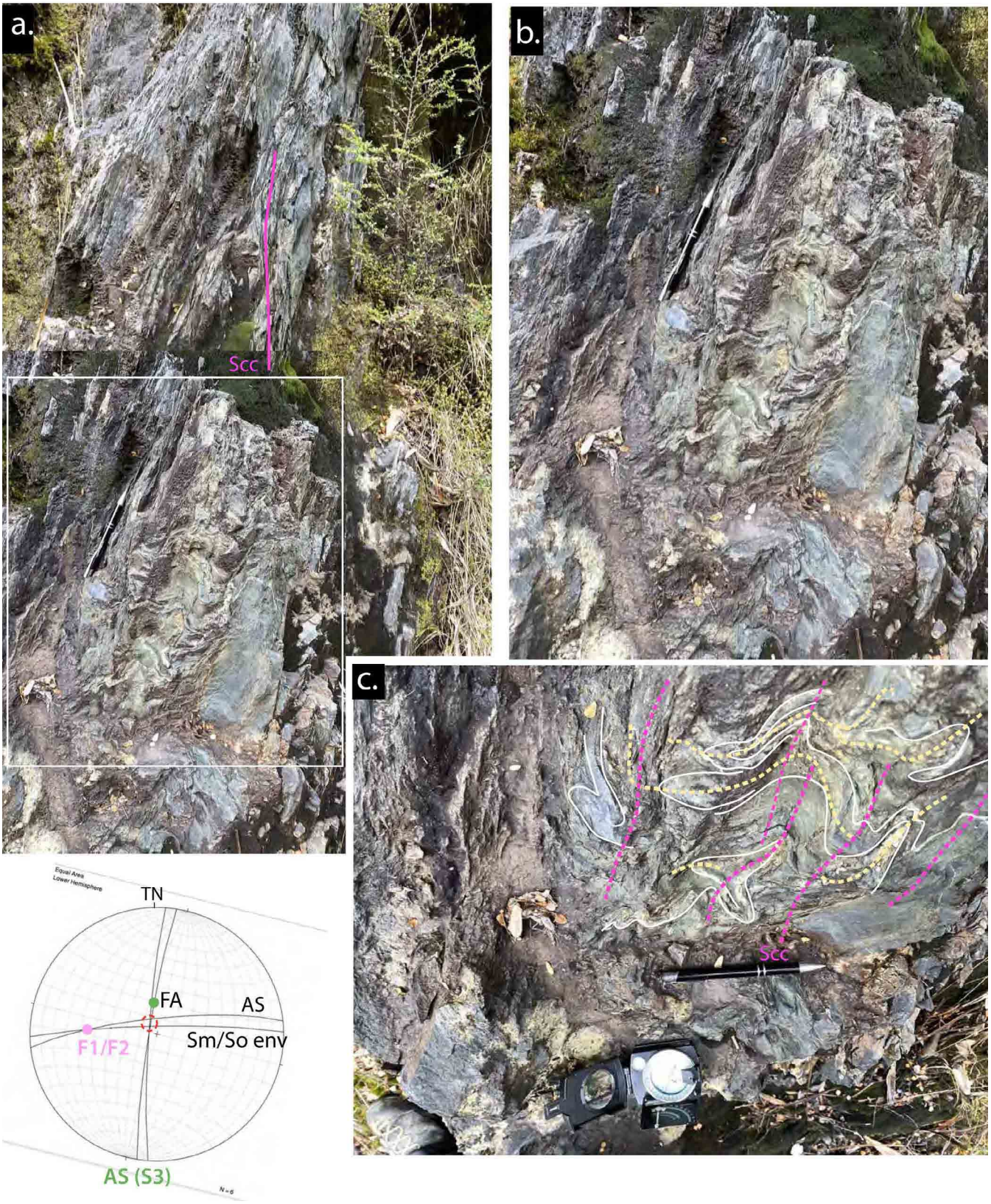

Figure 50. Outcrop at station DG20-52 (see Figure 47a for location) showing intense Sm enveloping relict hinge-zone "pods" with coaxially refolded Sm/So. The apparent intense Sm fabric is a steeply dipping crenulation cleavage. Two sets of folds are present in the "pod": an early series of isoclinal folds (yellow dashed axial surface traces) refolded by the upright fold set (purple axial surface traces). The early F1/F2 folds have a steeply north-dipping axial surface (084°/80°N) and moderate west-plunge (44°/264°). The late folds have a steep N-plunge (70°/356°) and a sub-vertical north-south axial surface (184°/85°W). The β intersection (red dashed circle) is 81°/320°.

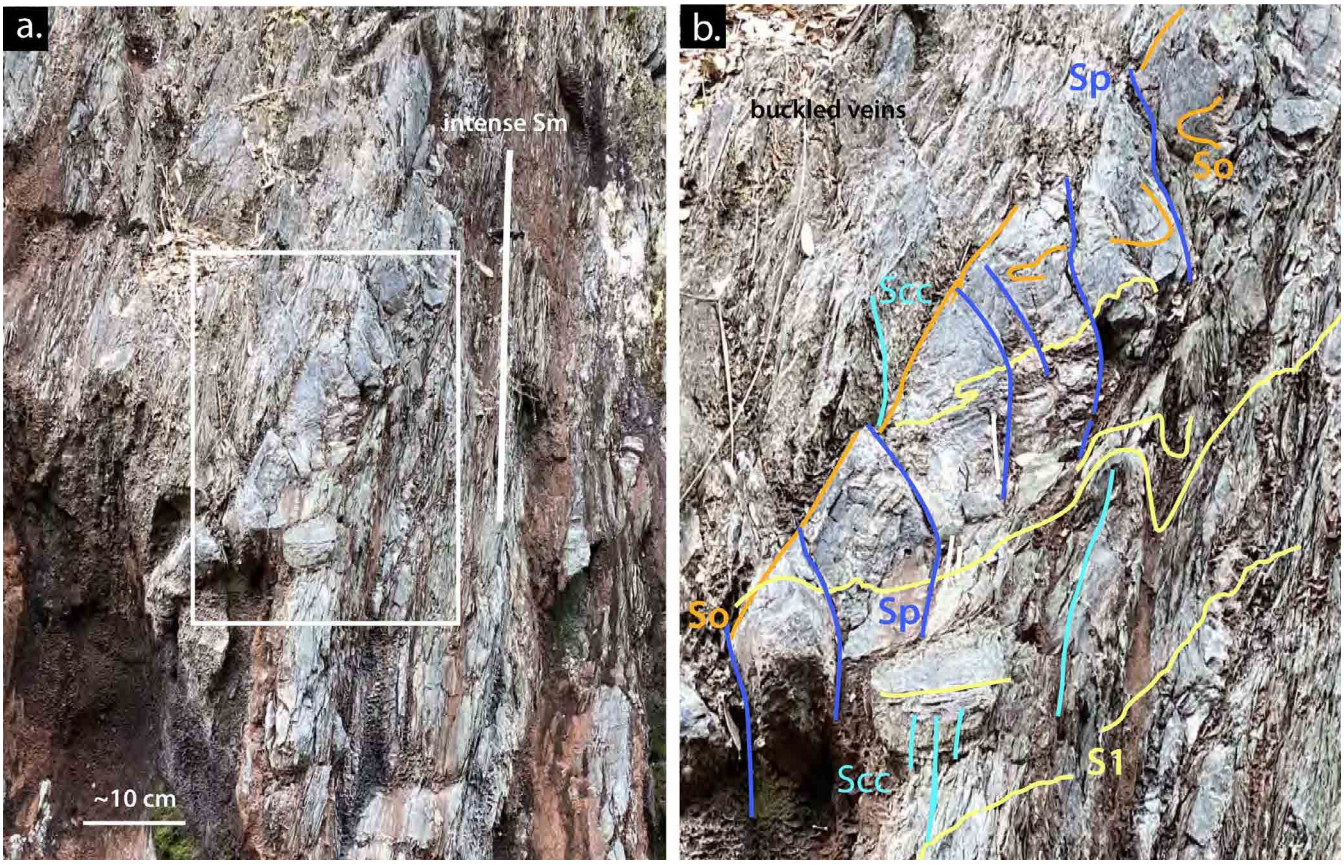

Figure 51. Road outcrop in Scotchfire metamorphics on the Lyell Highway at station DG20-52 (see Figure 47a for location). a) Disrupted dolomitic layer cut by an intense Sm fabric. b) Close up of dolomite layer showing complex multiple fabrics with bedding (orange: So), an early slaty "type" cleavage (yellow: S1), both overprinted by an intense crenulation cleavage fabric (light blue: Scc). The Scc fabric becomes a spaced, discrete, dissolution-style (stylolitic) cleavage Sp in the dolomite layer (dark blue line traces). The buckled veins (top left) were folded during the development of the S1 cleavage and have been flattened during the crenulation cleavage-forming event.

There is a strong overprint by the younger Devonian deformation with brittle reverse faults and open plunging folds. The intense Sm fabric is considered part of the early deformation.

The low-grade nature of the fabrics is reflected by the fine grainsize and slaty character of the first cleavage (see Figure 52a, b). The dissolution character and stylolitic form of the spaced discrete crenulation cleavages are shown in Figure 52c.

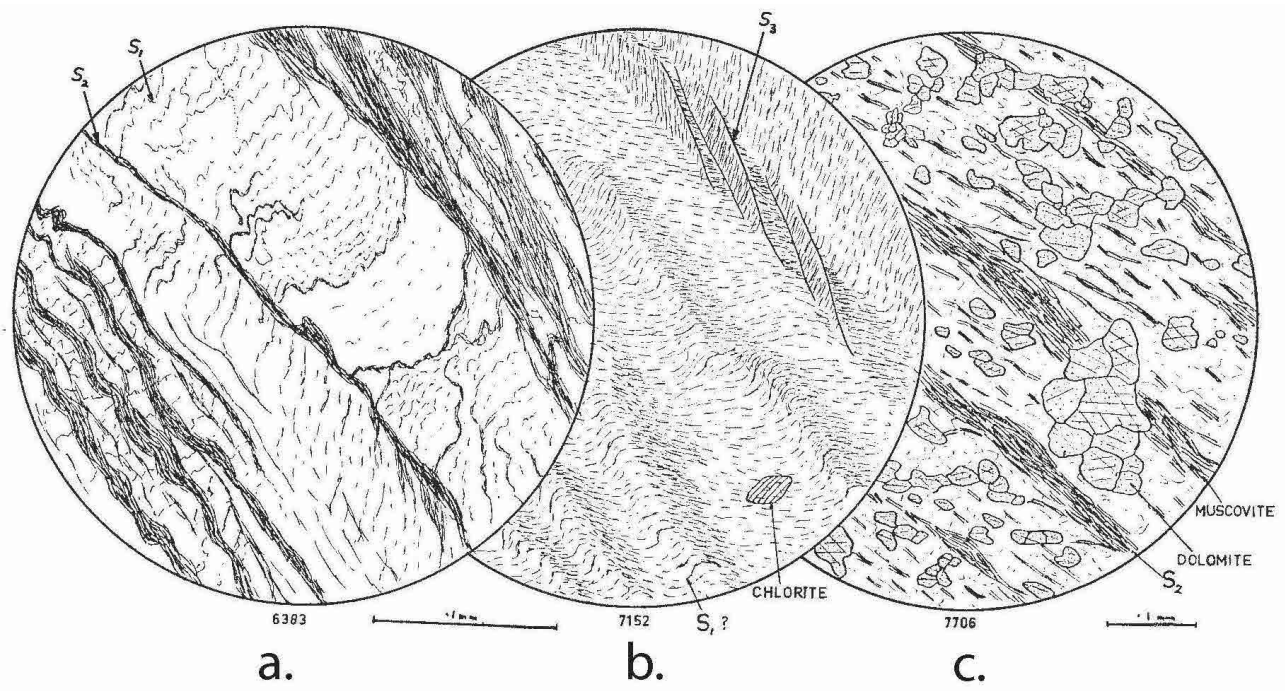

Figure 52. Scotchfire metamorphic sheet phyllite and schist fabrics in camera Lucida sketches from Spry (1963a, fig.3). a) S2/Scc spaced, discrete crenulation cleavage fabric with folded S1/Sm foliation in the microlithons. b) Crenulated S1/Sm fabric with S3/Scc crenulation cleavage on limb zone of F2 crenulations. c) Calc-schist fabric with spaced Sm fabric and post-tectonic dolomite porphyroblasts.

5.0 STRUCTURAL GEOLOGY OF MT MCCALL

Mt McCall (Figures 2 and 53) provides the southernmost continuation of the Franklin fold-nappe cored by the retrograded high-grade schists of the Franklin-Joyce Metamorphic sheet and bounded by quartzites of the low-grade Fincham-Mary sheet (Figure 2).

The Mt McCall area was mapped by Williams (1971), as part of a University of Tasmania Honours Thesis, with emphasis on structural petrology, microfabrics and metamorphic petrology.

The Mt McCall road traverse (Figures 53 and 54) provides 1) a section across the Devonian Mt McCall Anticline, 2) a section across the high-grade Franklin metamorphic sheet incorporating the Franklin Fold-nappe, and 3) shows contacts with the overlying Fincham quartzite (low-grade Fincham-Mary metamorphic sheet), and underlying series of quartzites, quartz-mica schists and mica schists (low-grade Fincham-Mary metamorphic sheet) (Figure 53).

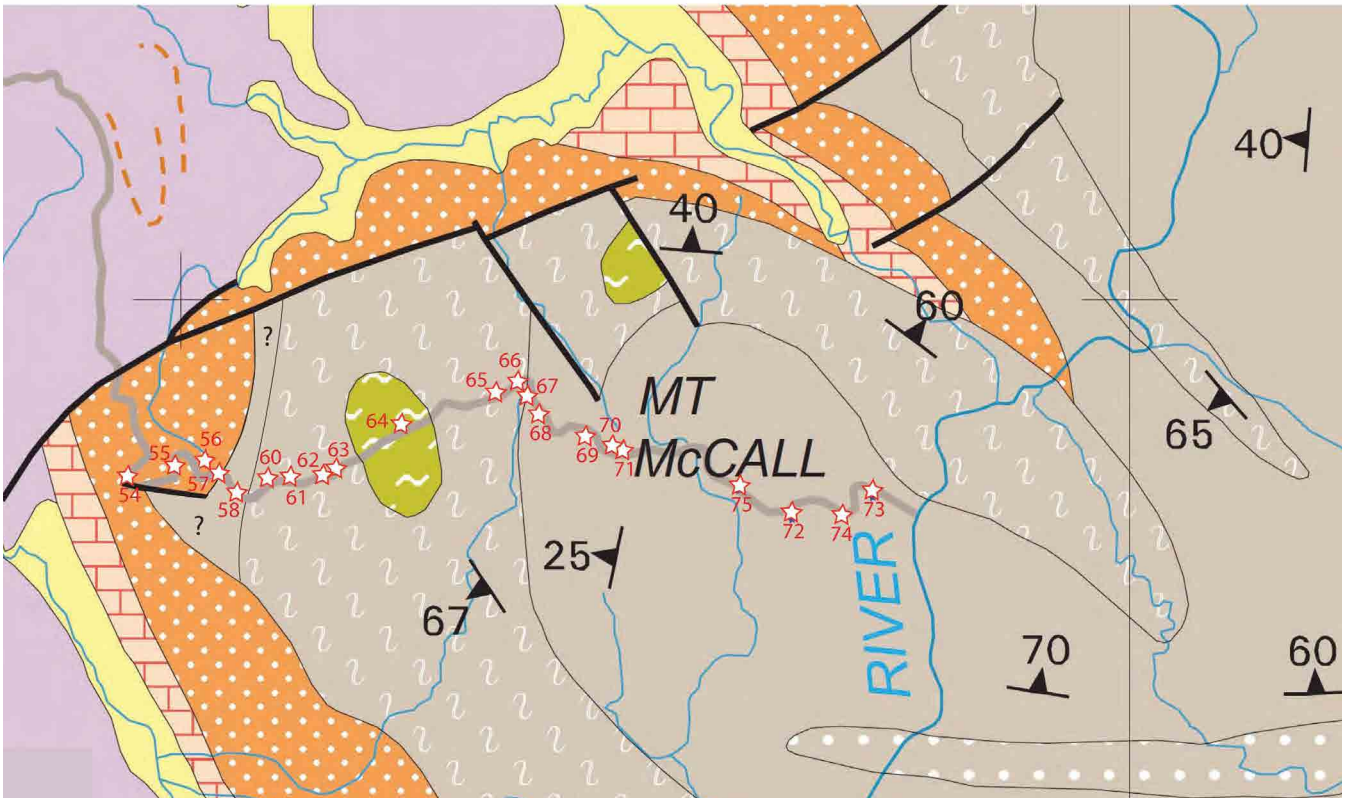

Figure 53. Simplified geological map of the Mt McCall region with foliation Sm strike and dip data defining the northwest-trending Devonian Mt McCall anticline. Map base from the Mineral Resources Tasmania 1:250000 digital geological atlas. The Mt McCall access road is shown by the thick grey line trace. Measurement stations along the Mt McCall road are shown by the red-outlined white stars with red DG19 station numbers.

grey: low-grade quartzite sequence (Fincham-Mary metamorphic sheet); grey with white stipple: low-grade pelitic sequence (Fincham-ary metamorphic sheet); grey with white squiggle: high-grade schist/carbonaceous phyllite (Franklin-Joyce metamorphic sheet); olive green: amphibolite; orange with white stipple: Late Cambrian-Ordovician sandstone/conglomerate; pale orange with orange; hatch: Late Cambrian-Ordovician carbonates; mauve: Siluro-Devonian shale-sandstones

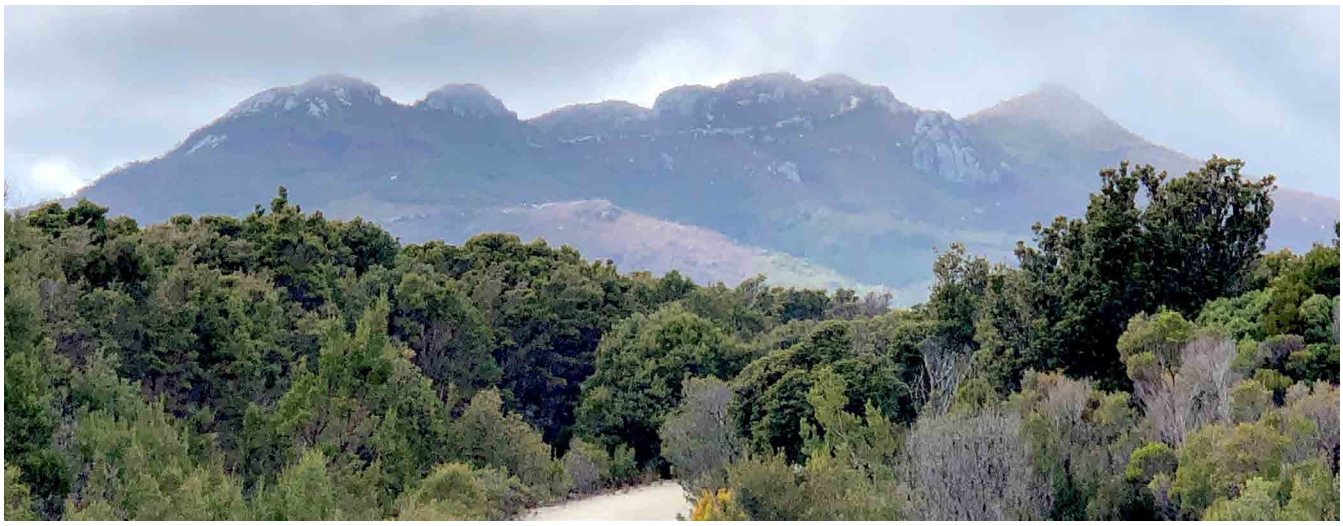

Figure 54. View of Mt McCall (top right) and quartzite ridgeline that forms the core of the Devonian Mt McCall anticline. Foreground is the poorly out cropping high-grade Franklin-Joyce Metamorphic sheet rocks.

5.1 Lithology, Metamorphism and Structural Petrology

The high-grade rocks are a series of intercalated dark coloured, chlorite-mica-phyllitic schists, pyritic carbonaceous mica schists, biotite-muscovite quartz schists, albite schists, garnet-albite schists (Figure 55) and minor garnet amphibolites as pods within the garnet-albite schists (Williams, 1971). Metamorphism is biotite-grade greenschist facies (Williams, 1971), above the garnet isograd but still within greenschist facies based on the widespread presence of albite (Berry, pers. com. 2021).

High strain zones (HSZ) bounding the high-grade rocks consist of intensely foliated zones made up of 1) black quartz-chlorite-mica schists and phyllites containing folded and boudinaged quartz veins in high-grade rocks, and 2) platy quartzites and quartz-mica schist/phyllite in the contact zone of the low-grade rocks.

The low-grade rocks of the Mt McCall Quartzite (Fincham-Mary metamorphic sheet) are a series of quartzites, phyllite, quartz-mica schists and micaceous quartz -schists, where metamorphism is low greenschist facies (Williams, 1971).

Williams (1971), using criteria established by Spry (1969), argued that:

1. garnet and albite growth is pre-S2
2. small garnets are post S2
3. some albites have sigmoidal, some straight inclusion trails
4. no albite growth syn- or post- S2
5. Garnet either pre-S2 and post-S1 and also syn- to post-S2.

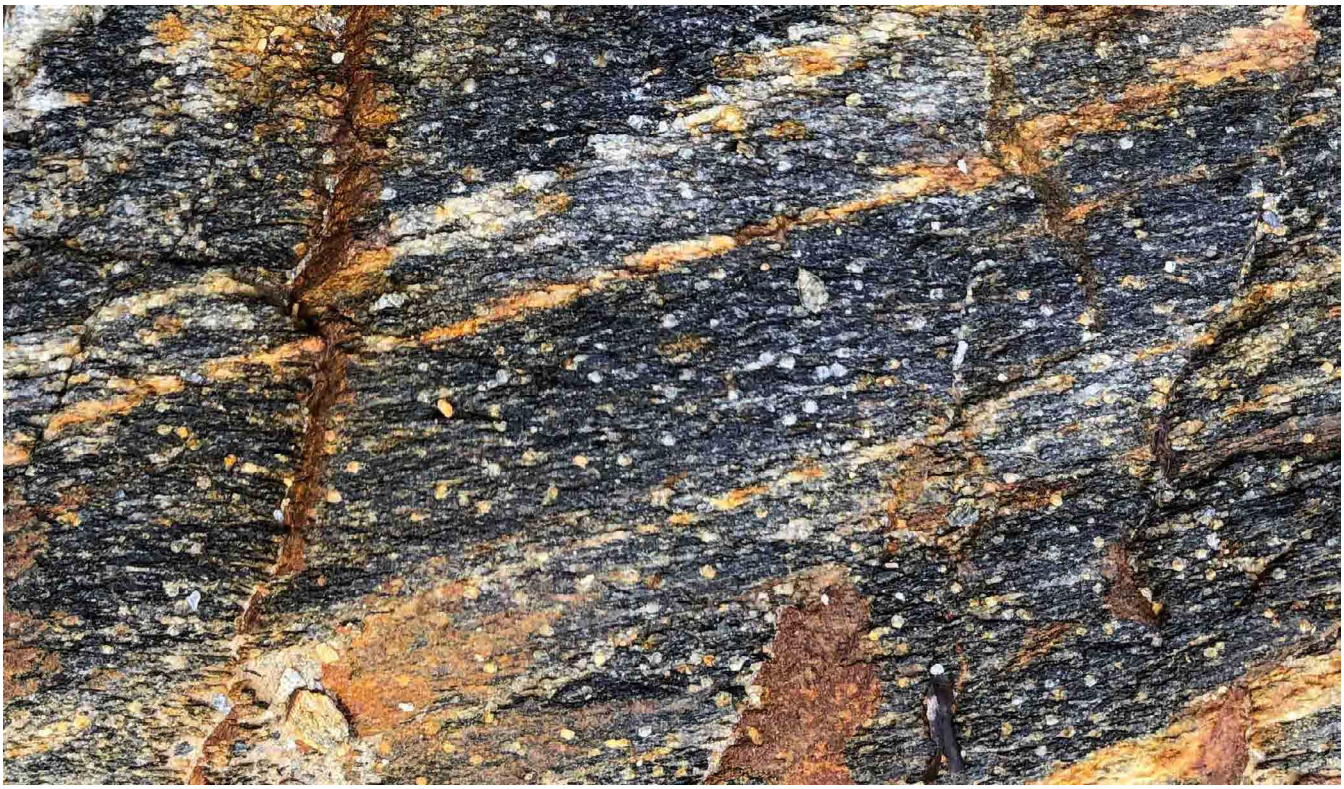

Figure 55. Laminated porphyroblastic albite-garnet schist typical of the high-grade Franklin metamorphic schists along the Mt McCall road (DG 19-62, Mt McCall road).

5.2 Mt McCall Regional Structure

The Mt McCall region appears as a stacked sequence of intensely deformed, platy quarzite overlying high-grade schist with mesoscopic folds, overlying a low-grade quartzite-quartz schist sequence with meso- and macro-folds (Figures 56, 57, and 58).

This apparent low-grade quartzite-high-grade schist-low-grade quartzite stack (Figure 58) is folded at regional scale by the Devonian northwest-trending fold sets (F3) into a broad anticline (Williams, 1971). Mesoscopic F3 open folds and steeply dipping, northwest-trending crenulation cleavage (Figures 56 and 57) are part of the Mt McCall anticline. F3 and Lcren plunge to the north-northwest on the western limb of the Mt McCall anticline but to the south-southwest on the eastern limb of the anticline (blue arrows, Figure 56) as shown and defined in the structural profile of Figure 58.

The high-grade schists appear as a homoclinal, northwest-dipping wedge between a thin zone of foliated quartzite on the western and upper contact (Figures 57 and 58). The limited preservation of this quartzite (Fincham Quartzite) is affected by late-stage faulting

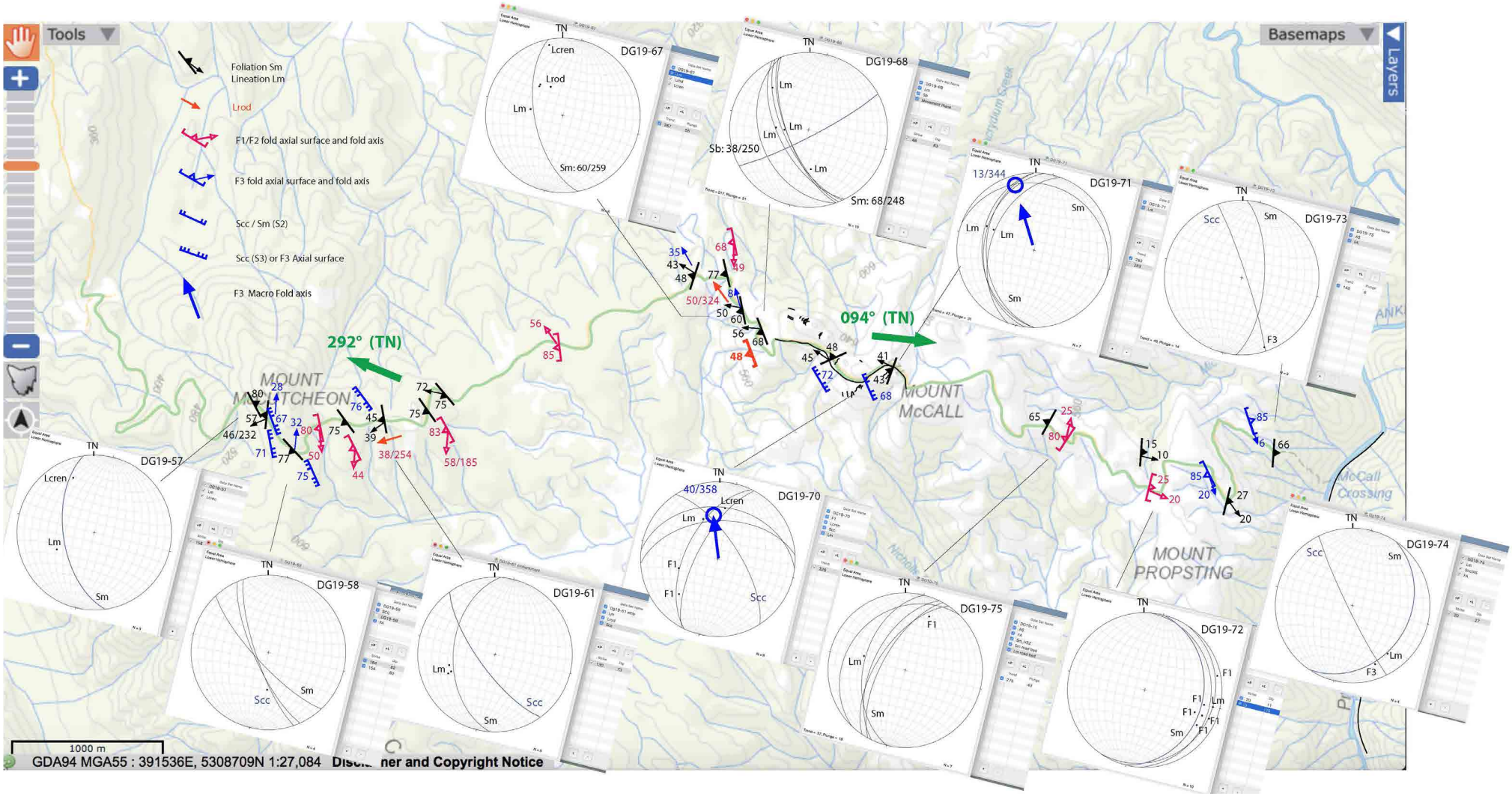

Figure 56. Structure map of the Mt McCall region with stereonet insets of the structural element attitudes. Map base is the Tasmanian ListMap topographic map.

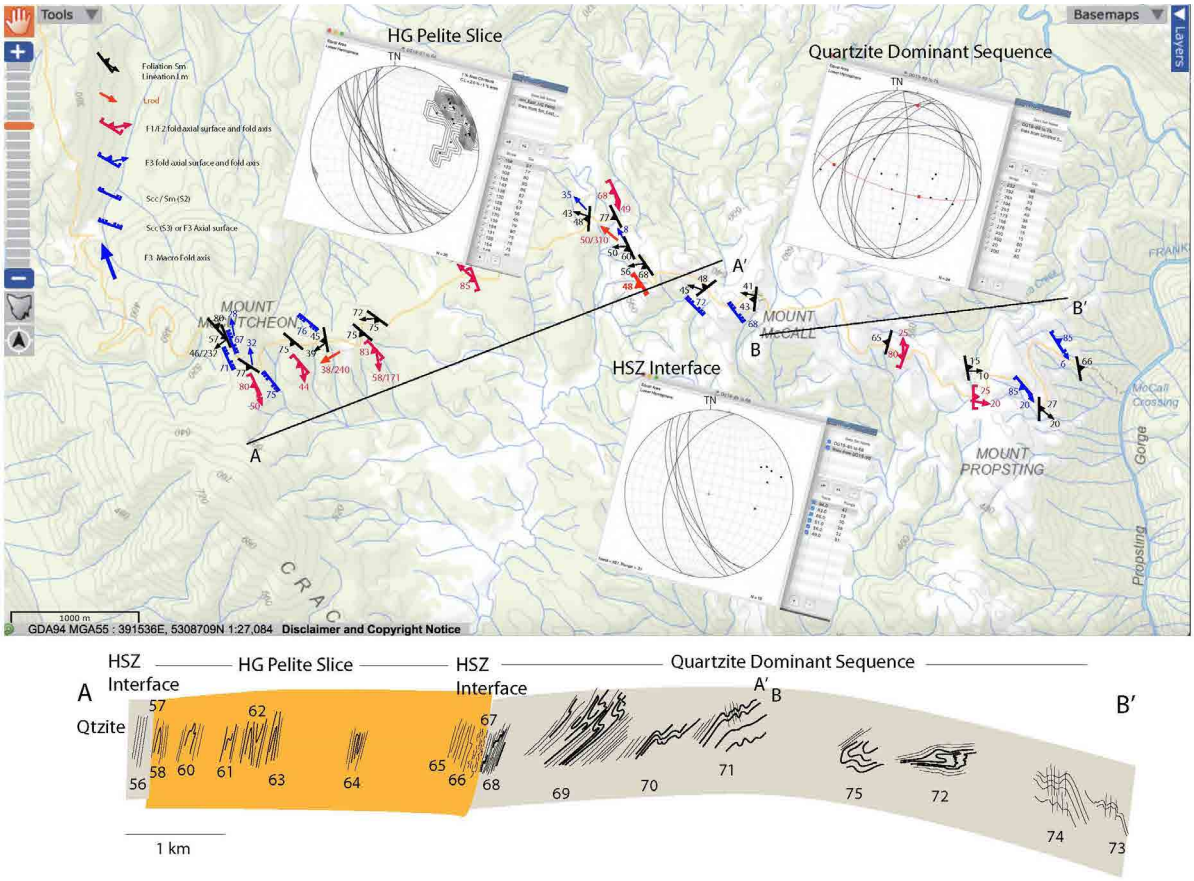

Figure 57. Mt McCall structure map showing a) stereonets of the foliation Sm attitudes in the high-grade slice, the high strain zone (HSZ) interface between the high-grade and the structurally underlying quartzite sequence. b) Sketch profile constructed from outcrop sketches across Mt McCall showing the relative juxtaposition of the high-grade slice and the quartzite sequence. Positions of section line A-A' and B-B' are shown. The Mt McCall anticline is defined by the arched form of the So/Sm traces within the quartzite dominant sequence on the right side of the profile A-B' (see also Figure 58).

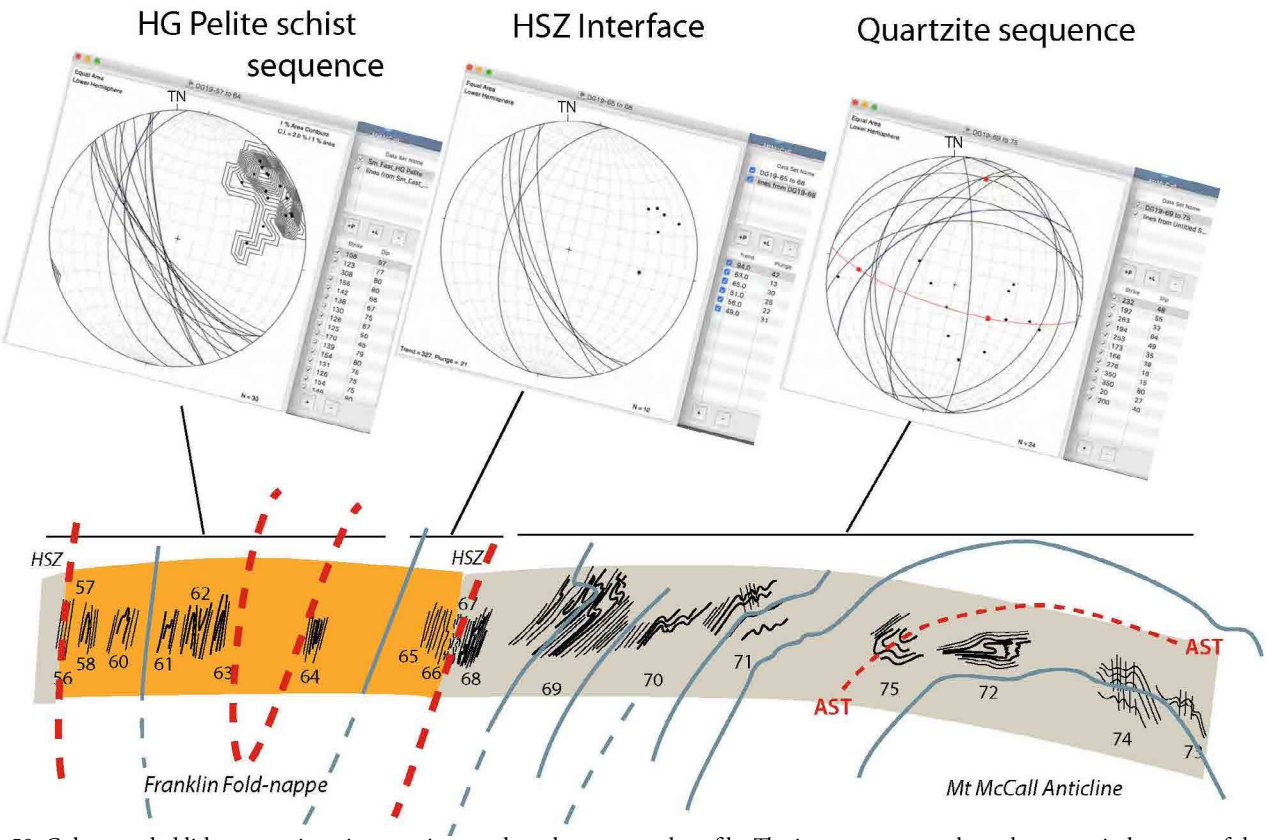

Figure 58. Colour-coded litho-tectonic units superimposed on the structural profile. The inset stereonets show the great circle traces of the dominant foliation Sm for the high-grade schists, the low-grade quartzites and the high strain zone interface (HSZ). The red-dashed line approximates the inferred hinge of the Franklin fold-nappe. Orange: high-grade Franklin-Joyce metamorphic sheet schists; grey: low-grade quartzite of the Fincham-Mary metamorphic sheet.

and the unconformably overlying Cambro-Ordovician conglomerate (Figure 53). The quartzite sequence (Mary Quartzite) is broadly arched about the Mt McCall anticline. Calculated Mt McCall anticline plunges are 40°/358° and 13°/344° (see stereonet insets of DG19-70 and DG19-71 as well as Lcren in DG19-57 and DG19-67, Figure 56). The axial surface trace position on the section is between DG19-71 and DG19-75 (Figures 57 and 58). The high-grade schists occupy the western limb of the anticline (Figure 58).

5.3 Structure of the High Grade unit

The high-grade unit (Franklin-Joyce metamorphic sheet) exposed along the traverse is made up of homoclinally dipping, intensely- to moderately-foliated, dark schistose lithologies (Figure 59). Mesoscopic isoclines are present in quartzite bands and the thin layering, but there are no apparent macro-fold(s) (but see Section 5.5). The isoclines are small scale, metre- to sub-metre-scale, with tight to isoclinal form approaching reclined geometry. They have "similar" style and occur within the laminated schist (Figures 59, 60 and 61).

The mesoscopic folds show changes in the degree of isocline flattening based on fold interlimb angles (ILA) across the exposed road section in the high-grade schist (Figures 61 and 62). These changes provide a qualitative measure of bulk-rock strain and show a clear increase in strain at the top and base of the slice/slab indicated by extreme fold flattening (i.e. marked hinge thickening compared to fold limbs) and low ILA (Figure 63). These zones of higher strain are in the order 10's of metres wide.

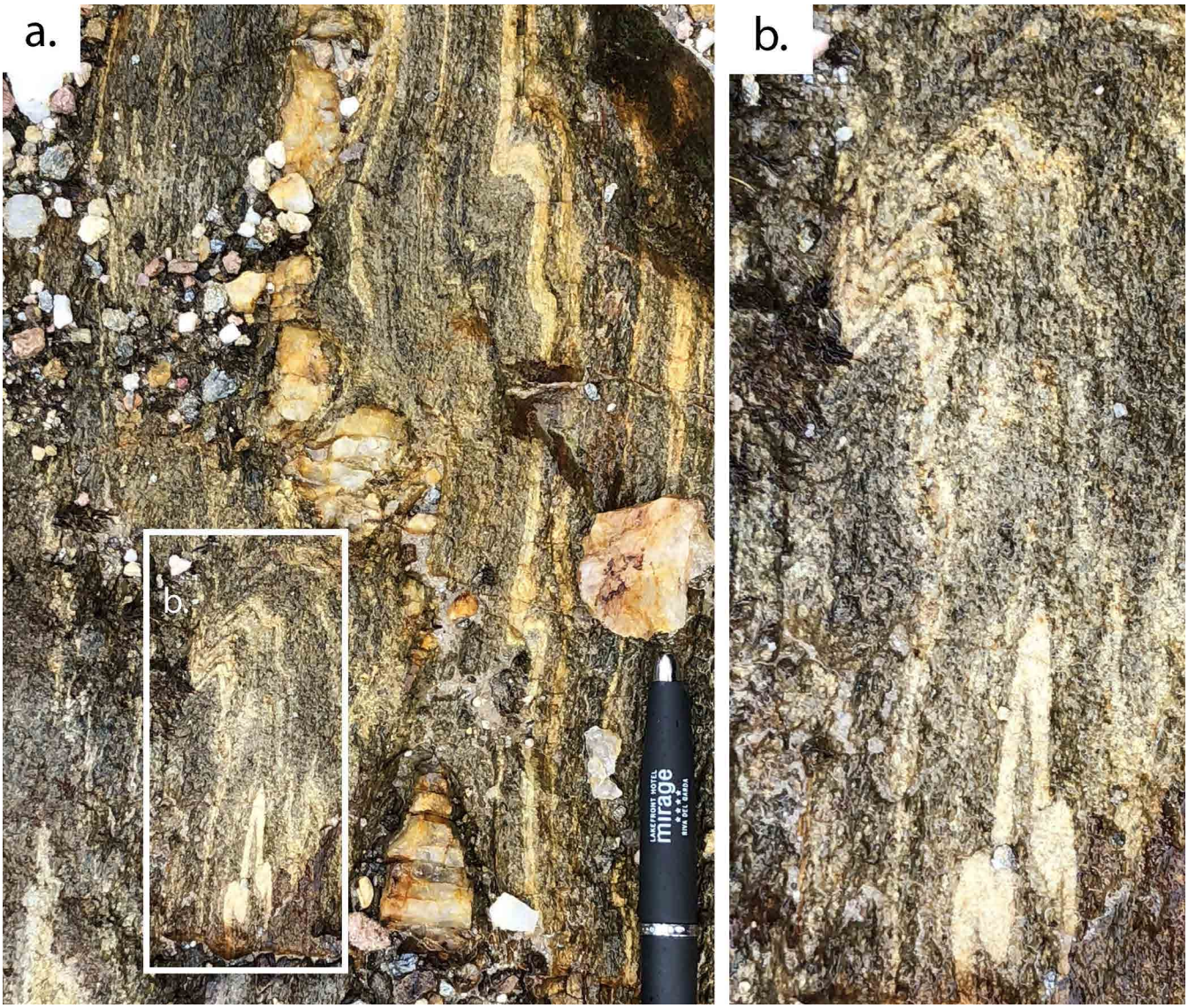

Figure 59 a). Steeply plunging, refolded isoclinal folds in laminated high-grade porphyroblastic schist. Outcrop station DG19-58, Mt McCall road. Refolding is by northwest-trending F3 folds associated with the Mt McCall anticline. b) Enlargement of yellow boxed area in a).

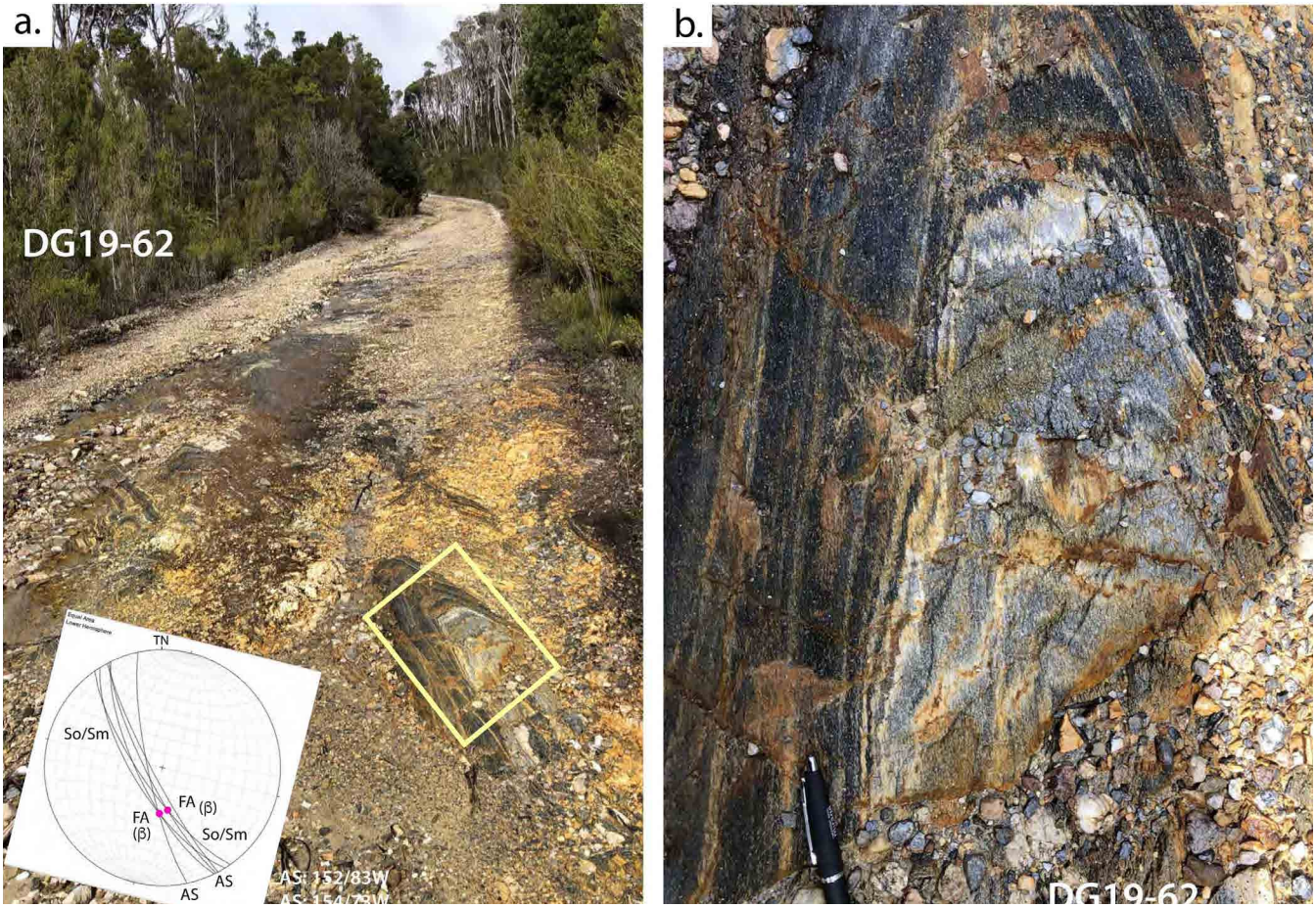

Figure 60 a). Tight to isoclinal, approximately reclined folds in laminated, porphyroblastic, albite-schist and dark carbonaceous albite-schist. Outcrop station DG19-62, Mt McCall Road. b) shows enlargement of similar-style fold in a).

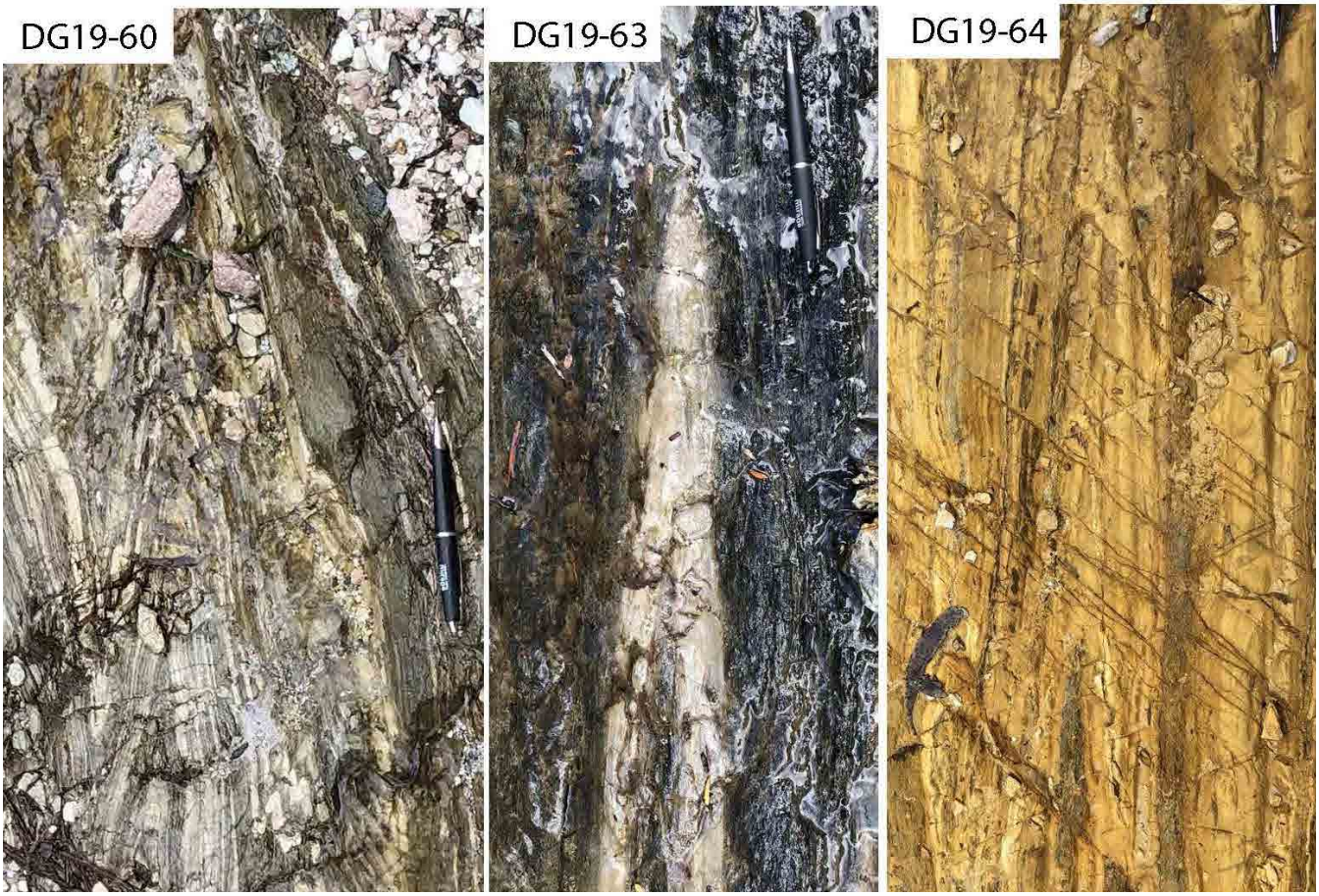

Figure 61. Profile view photographs of steeply plunging tight to isoclinal folds in high-grade schists/carbonaceous phyllite of the Franklin-Joyce metamorphic sheet.

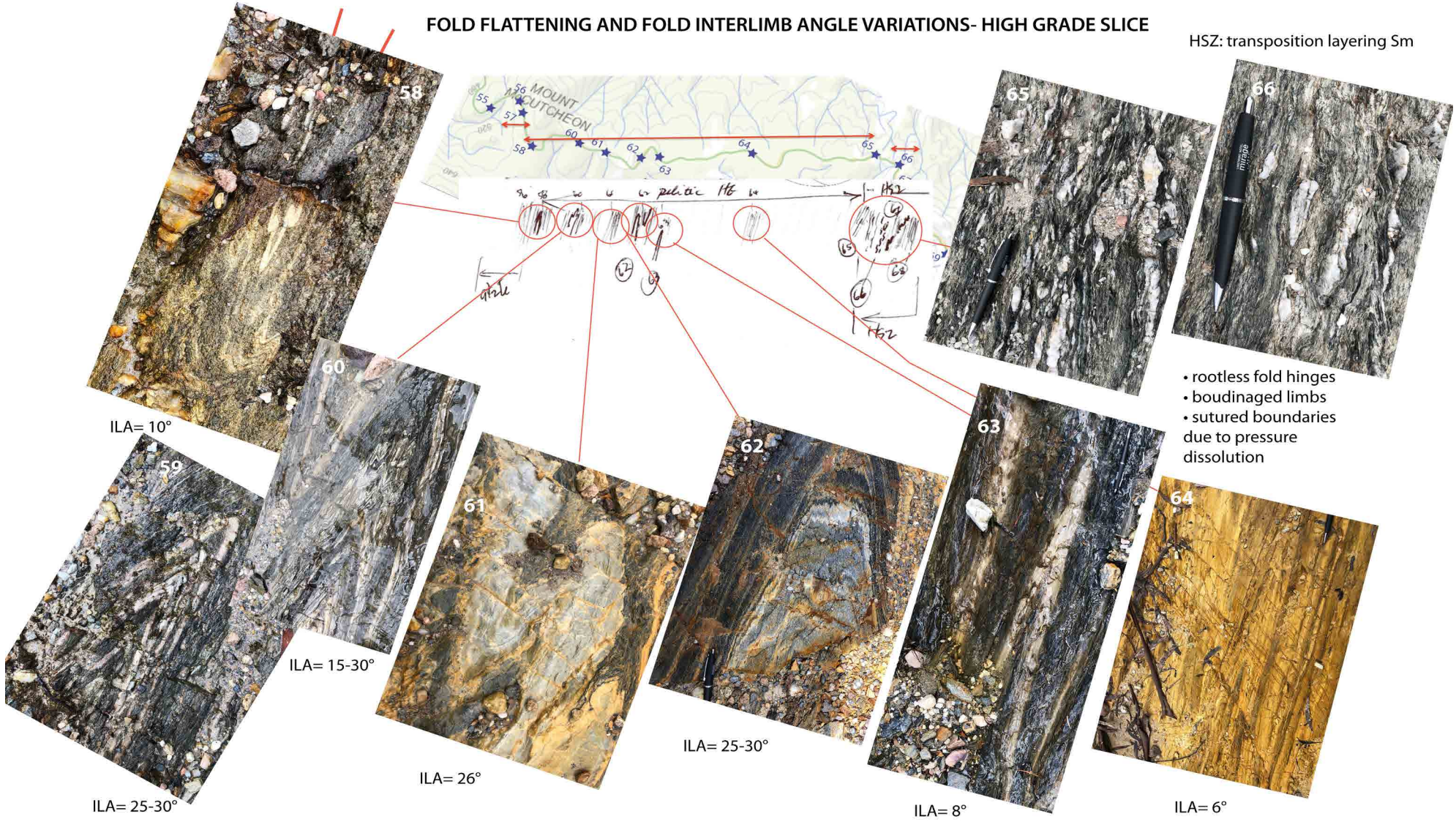

Figure 62. Fold profile photographs taken in the Mt McCall road pavements showing changes in the degree of flattening of isoclines and changes in fold interlimb angles (ILA).

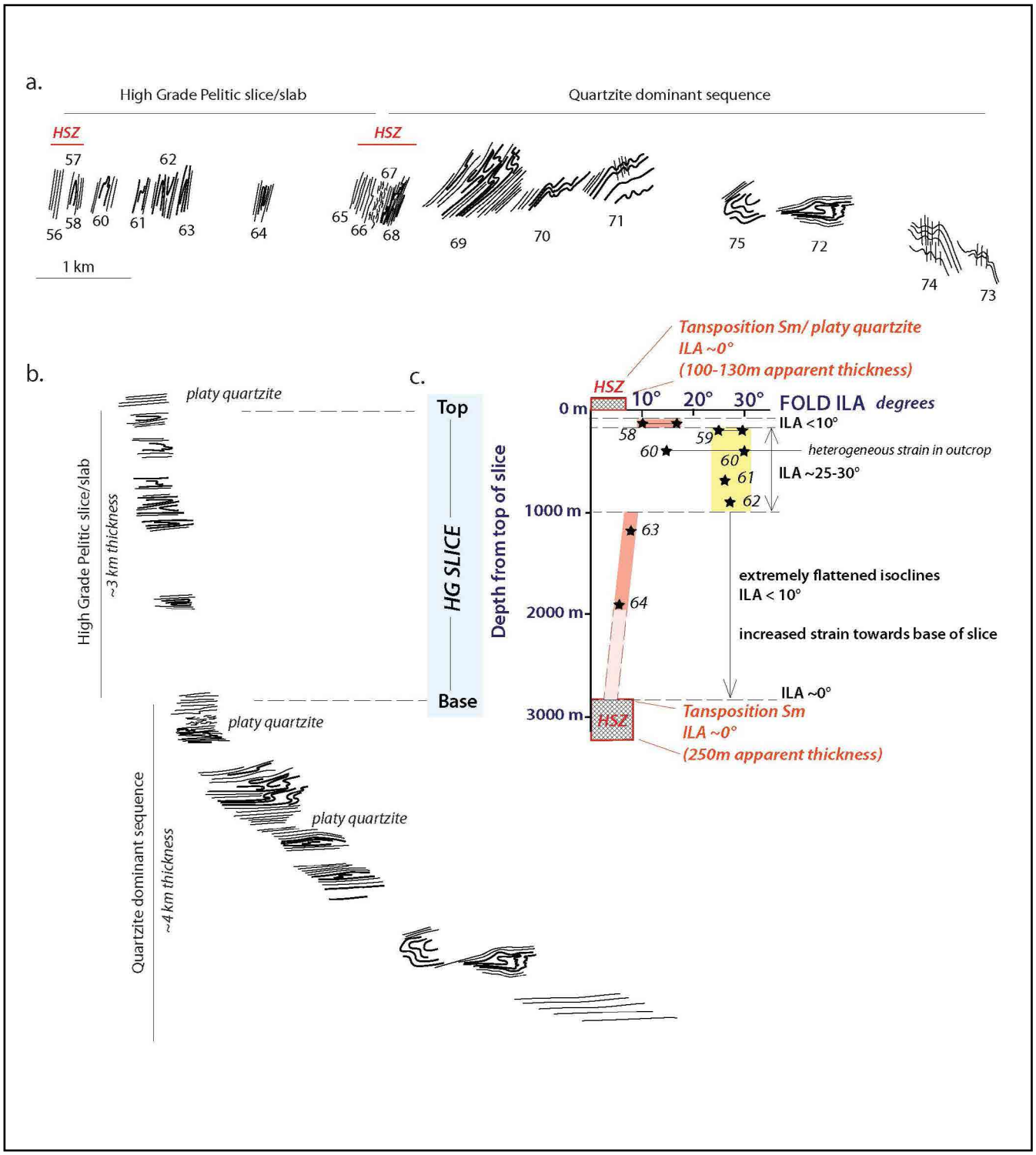

Figure 63. Fold interlimb angle (ILA) versus level (depth) in the high-grade slice after removal of the younger Devonian Mt McCall anticline folding. The folds analysed are shown in Figure 62 above.

5.3.1 High Strain Zone contacts in the high-grade Schist

Both the upper (western) and lower (eastern) parts of the high-grade schist, at the contacts with the overlying and underlying mylonitic low-grade platy quartzite sequences, show intense transposition layering/foliation development (Figures 64, 65 and 66). They are high strain zones (HSZ) at the top and basal interfaces of the high-grade slice (Figure 58).

The original layering is now completely transposed with relict generally cm-scale fold hinges in quartz veins, as well as boudinaged veins elongated within the transposition layering (Figures 64 and 65). Occasional larger scale hinges occur (Figure 66).

Figure 64. Discontinuous transposed layering in formerly interlaminated dark carbonaceous phyllite and mica schist. Basal HSZ of the high-grade schist unit. The layering is now segmented as pods or lense-like slivers. Note the rootless isocline hinge at bottom right (DG19-65, Mt McCall Road).

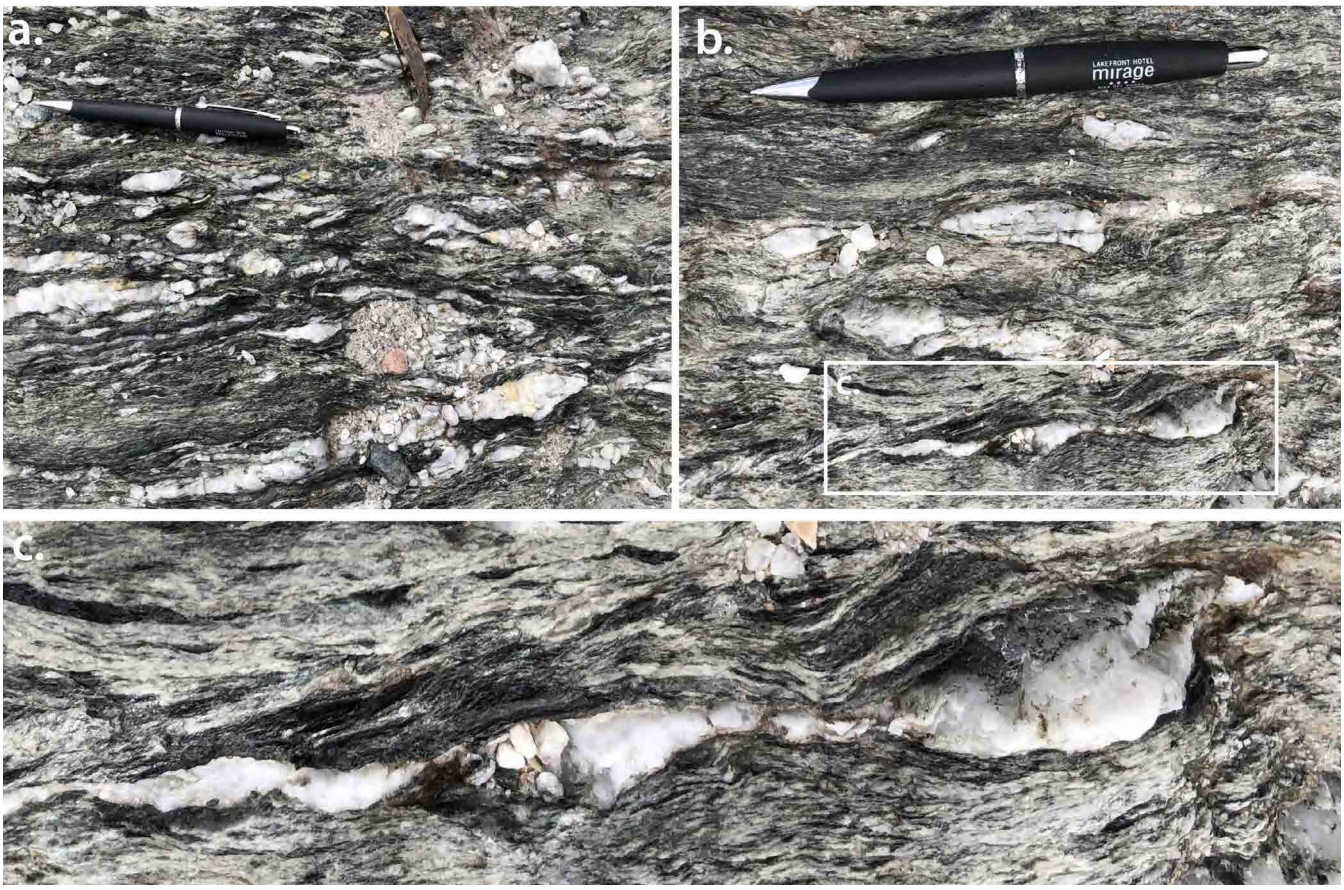

Figure 65. High strain zone transposition layering with "strung out", boudinaged quartz veins with sutured boundaries, relict centime-tre-scale isoclinal hinges within quartz-mica schist matrix. Basal HSZ of the high-grade unit (DG19-66, Mt McCall Road).

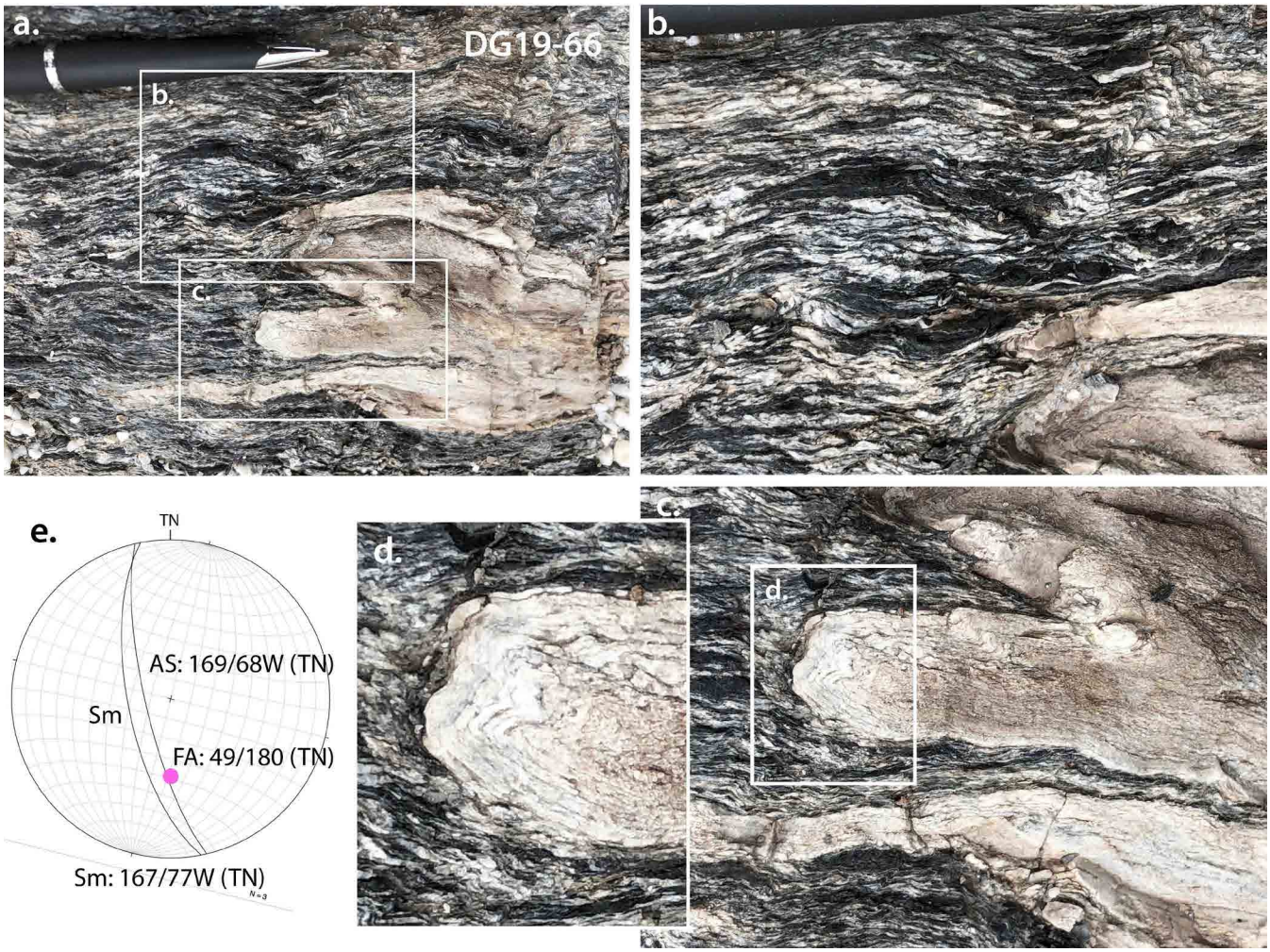

Figure 66. Rootless isoclinal fold in quartzite Interdigitating with transposed quartz-mica schist at station DG19-66. This represents the basal HSZ of the lower part of the high-grade Franklin schists (Franklin-Joyce metamorphic sheet) in contact with the underlying low-grade quartzite (Fincham-Mary metamorphic sheet). b) Intense transposition foliation Sm showing centimetre-scale rootless fold hinges in thin white quartz layers. c) Noses of the in-folded quartzite layer. d) Close-up of the rounded fold nose highlighted in (c) showing folding of a So-parallel spaced cleavage. e) Stereonet showing structural data from the outcrop with foliation Sm and fold axial surface (AS) great circle traces and the fold axis (pink dot).

5.4 Structure in the low-grade Quartzite sequence

Folds within the low-grade quartzite sequence (Fincham-Mary metamorphic sheet) occur in 10m-scale fold-pods, or shear lozenges, enveloped by the high strain foliation Sm. Many of these are now preserved as quartzite knolls on the ridgeline west of Mt McCall. The folds have tight to isoclinal form at metre scale (Figures 67 and 68). Some show conical or sheath-like form with curved fold hingelines (upper folds in Figure 67a).

Most appear as asymmetric vergence folds either grouped (Figure 69) or as isolated fold pairs (Figure 70). They provide classic examples of shear lozenge development at different scales in the quartzite (see in particular Figure 70). In grouped fold pairs, they tend to climb in ladder-like form through the outcrop-knoll (or fold-stack). Within these fold-stacks individual asymmetric fold pairs are bounded by small, mylonitic, high-strain zones in the quartzite (Figure 69).

Isolated individual asymmetric fold pairs (Figure 70) develop pod-like form where the folded Sm within the pod becomes enveloped by the "external Sm" as it intensifies. This high strain mylonitic Sm essentially wraps the fold pair to form the macro-pod or shear lozenge. In Figure 70c, the banana-shaped closed loops below the dominant asymmetric fold pair (central part of the photo) indicate curved hinge-lines where the folds must have conical or sheath-like form.

Figure 67. Flattened and attenuated F1/F2 isoclines near Mt McCall. a). Fold stack with conical to sheath-like oppositely closing hinges (uppermost folds) and attenuated flattened isoclinal hinge (lower fold) in zone bounded by intense mylonitic Sm. b) steeply plunging reclined flattened and attenuated isocline (photos from Williams, 1971).

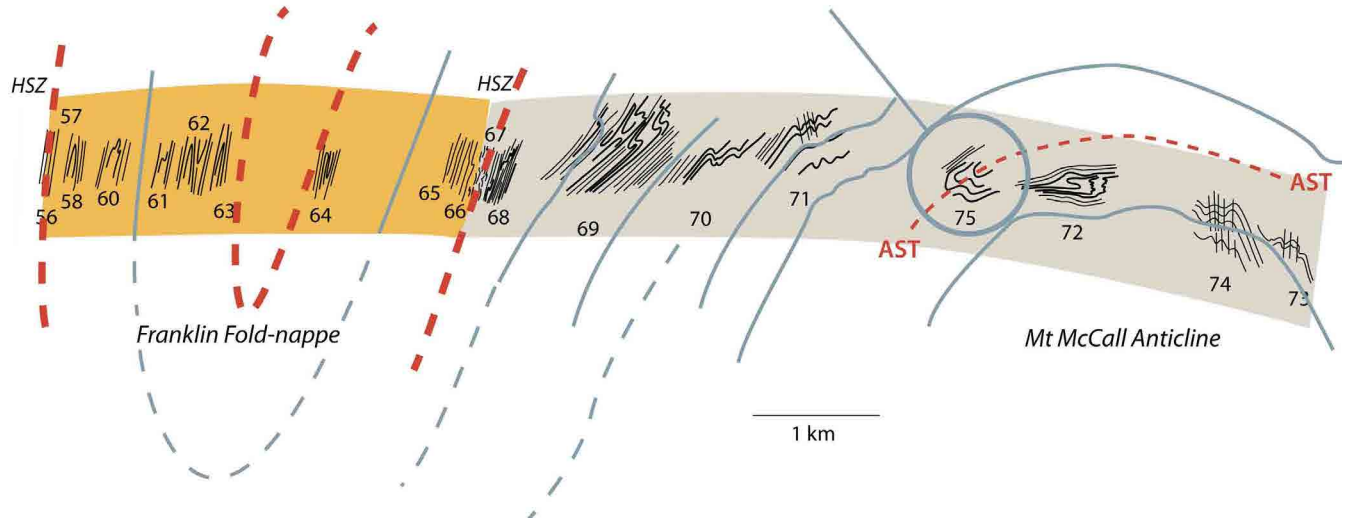

Figure 68. Rounded, metre-scale recumbent isoclinal closure in thick-bedded quartzite at outcrop DG19-75 on the Mt McCall road. b) Mt McCall structural profile showing the structural position of the outcrop. It is interpreted as a second order hinge within low-grade quartzite on the lower limb of the Franklin fold-nappe.

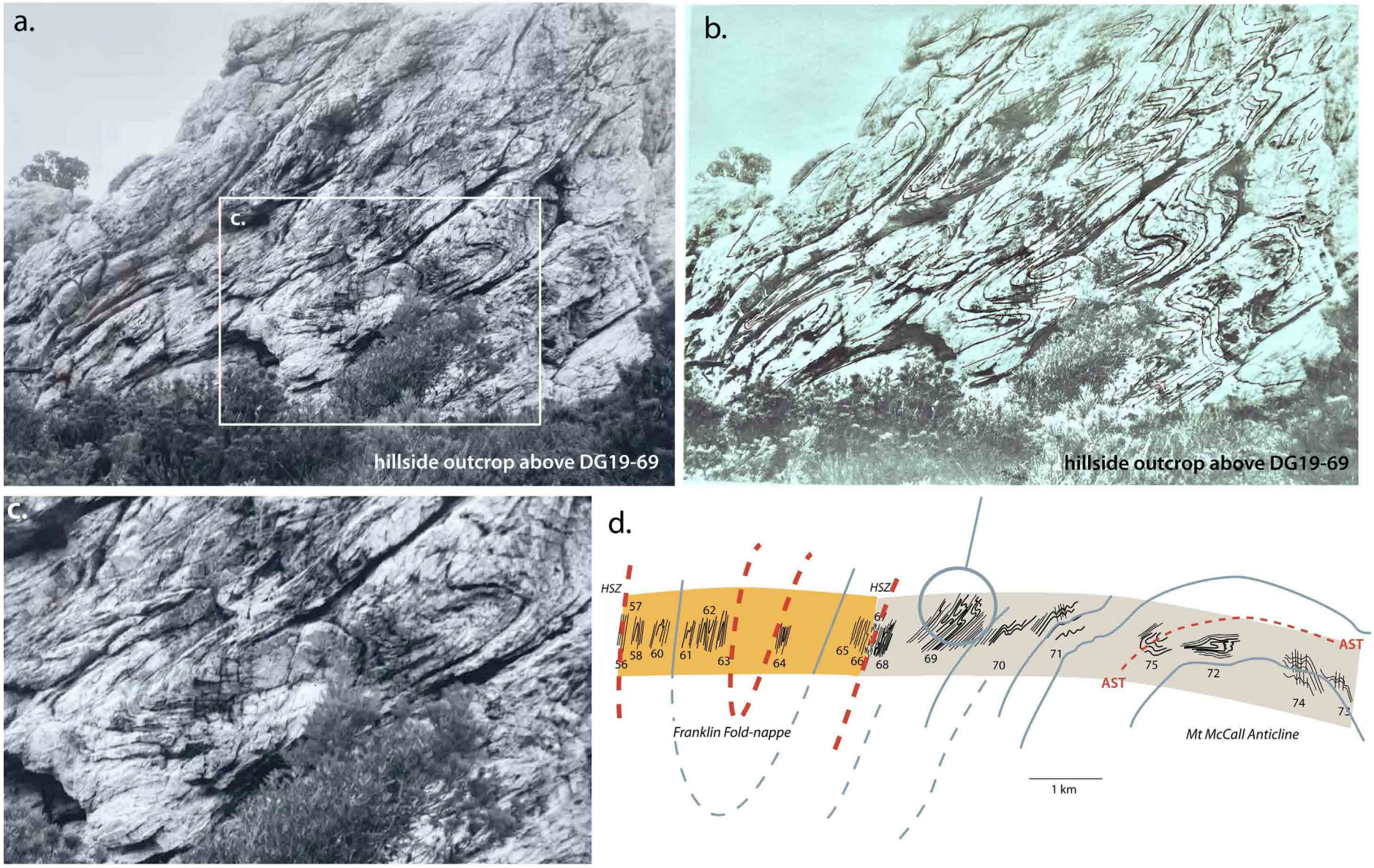

Figure 69. Flattened, sheath-like asymmetric folds within tapered, macro-fold lozenge bounded and enveloped by high strain foliation Sm (photo from Williams, 1971). a) Fold pod knoll above DG19-69. b) Enlargement of the asymmetric fold pair highlighted by the white rectangle in (a). c) and d) Formline interpretation of the Sm layering. e) Mt McCall structural profile showing the position (grey circle) of this asymmetrically-folded quartzite on the lower limb of the Franklin fold-nappe.

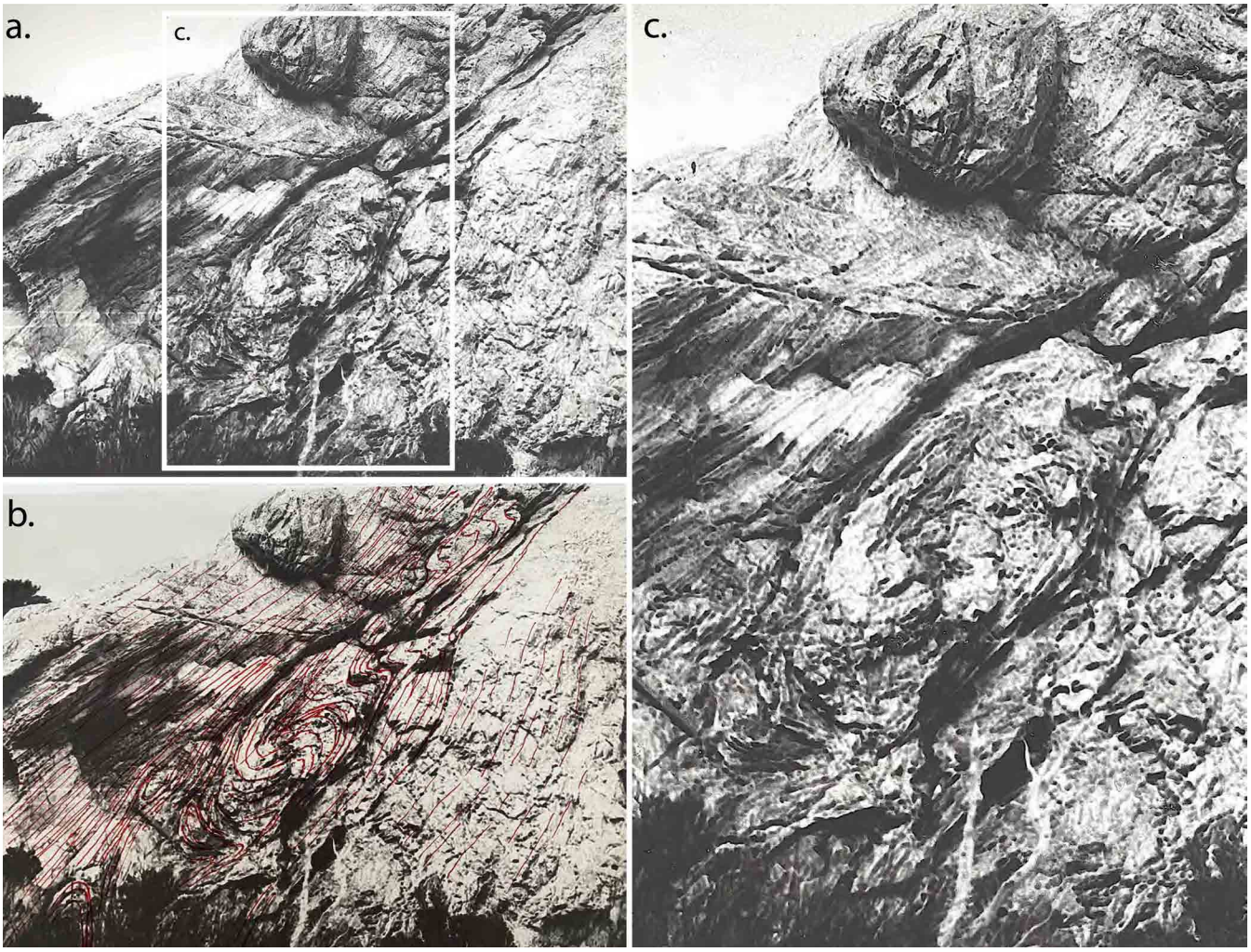

Figure 70. Flattened sheath-like asymmetric folds within macro-pod bounded and enveloped by high strain mylonitic foliation Sm (photo from Williams, 1971). This is a smaller-scale example of the foliation Sm-fold relationships shown in Figure 69. In the bottom left of photo (c) note the closed loop pattern in So/Sm below the asymmetric fold-pair. This indicates curvilinear changes in fold hinge-lines typical of sheath folding.

Away from the asymmetric fold pairs and fold-stacks, the layering has undergone extreme flattening and layer-parallel elongation, now preserved as internal boudins within the dominant foliation Sm (Figure 71).

5.4.1 HSZ Quartzite Contacts

The high strain zones that define boundaries of the low-grade quartzite sequence (Fincham-Mary metamorphic sheet) are characterised by platy quartzite and intense transposition layering (Figures 72 and 73). Both fabric types contain relict pods or augens of small-scale asymmetric fold pairs. These are small-scale examples of the process involved in development of the fold-pairs in Figure 70.

The platy quartzite tends to have a strong quartz elongation lineation where the pods (or augen) of relict rootless fold hinges plunge around the stretching/mineral lineation (Figure 73).

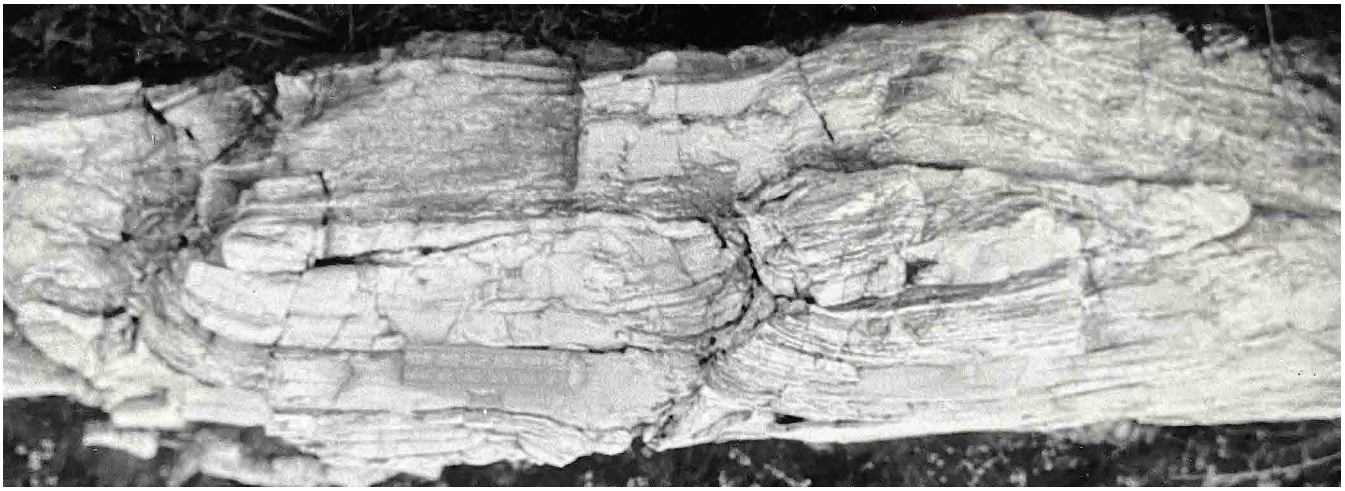

Figure 71. Intense foliation Sm in quartzite with relict isoclinal hinge (right centre) and internal boudinage reflecting extreme layer flattening and elongation (photo from Williams, 1971).

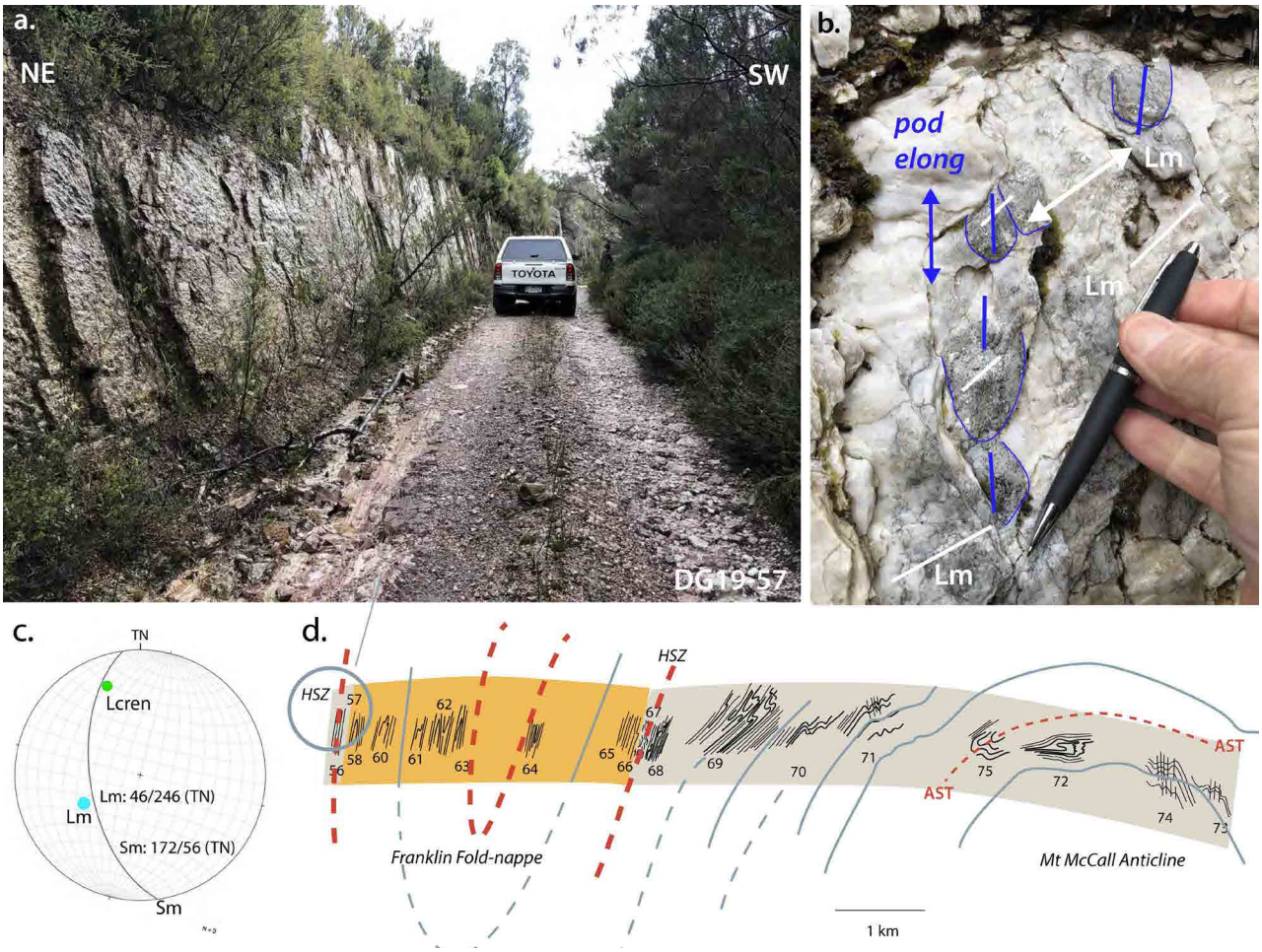

Figure 72. Platy quartzite-mylonite marking the high-strain zone (HSZ) on the western margin of the high-grade metamorphic schists/phyllite of the Franklin-Joyce metamorphic sheet at DG19-57 (highlighted by the grey circle). a) Photo of road section that is sub-parallel to the platy quartzite foliation Sm. b) Photo of the dominant foliation surface (Sm) showing boudinaged and segmented fold hinges as rodded and elongated quartz vein pods (darker grey). Note the obliquity of the pod elongation (blue arrows) with respect to the mineral stretching lineation (Lm: white arrows). c) Stereonet of the foliation attitude (172/56N), the mineral stretching lineation Lm (blue dot), and the younger crenulation (green dot). d) Position of DG19-57, shown by the grey circle, at the quartzite (grey)-high-grade schist (orange) contact on the inferred upper limb of the Franklin fold-nappe. Note the similarity of the quartzite deformation with that at the lower contact (Figure 73).

Quartzite on the margins of these high strain zones show varying lineation attitudes within the local Sm (Figure 74). This reflects fabric reworking by small-scale isoclinal folding within the Sm. These isocline hinges have curvilinear form to give a swing in Lm from Sm surface to Sm surface through the foliation "stack".

5.5 Franklin Fold-nappe

The inferred presence of the Franklin Fold-nappe at Mt McCall (red-dashed formline, Figure 58) is suggested by the presence of the quartzite (Fincham quartzite unit) west of the high-grade Franklin schist unit, as well as the underlying quartzite sequence (Mary quartzite unit). This litho-tectonic stacking matches that through the Mt Madge to Mt Fincham region where the Franklin fold-nappe has been defined (see Figures 2 and 7).

Variation in fold axis (FA) orientation relative to the mineral (stretching) lineation (Lm) (see Figure 10 and Section 3.2) supports the continuation of the Franklin fold-nappe across the Andrew River Fault to Mt McCall (Figures 2, 7 and 58). Like the northern part of the fold-nappe, there is a change from clockwise rotation of meso-fold hinges (FA) towards Lm on the structurally higher west limb to an anti-clockwise rotation of FA to Lm on the structurally lower east limb of the macro-fold. The westernmost exposure in the Mt McCall Quartzite of the Fincham-Mary metamorphic sheet (DG19-72) shows a change back to a clockwise rotation of FA to Lm. This, along with fold geometry changes, suggests the presence of a second- or third-order recumbent fold within the quartzite (Figure 58). Possible hinge is at DG19-75 (see Figure 68) with transition to flattened and attenuated asymmetric folds on the lower limb at DG19-72.

The angular variations between fold axes and the lineation (FA^Lm) also provide a qualitative measure of the strain through the structural pile (Figure 75). The FA and Lm are sub-parallel at very high strains, whereas at low strain they are at high angles to each other. Overall the high-grade and low-grade units at Mt McCall are typified by heterogeneous strain reflected by variations

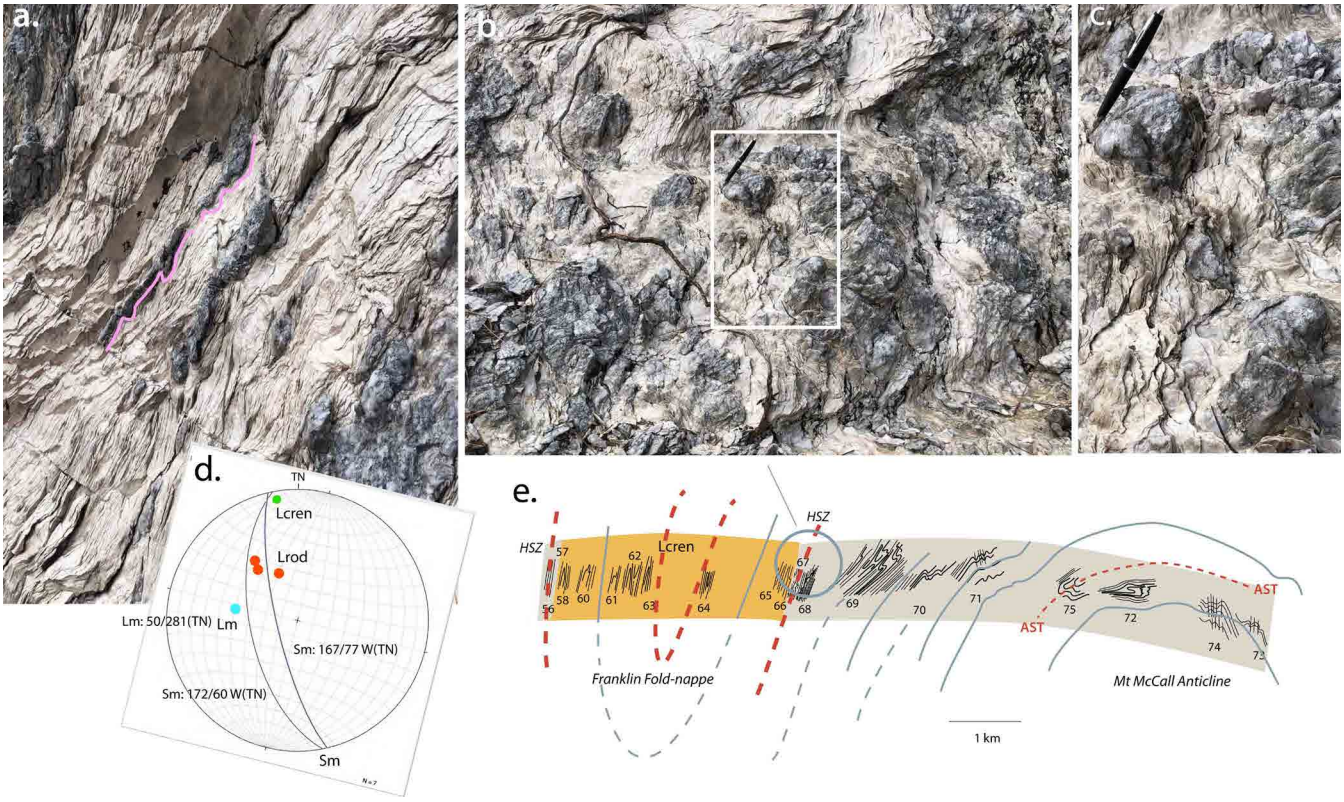

Figure 73. Platy quartzite-mylonite along the eastern margin of the high-grade pelite (DG19-67) with rootless asymmetrically folded grey quartz veins in Sm. a) Profile view of folded veins denoted by the pink line traces. b) View onto foliation Sm showing isolated fold-hinges of asymmetric fold-pairs in the grey quartz veins, now preserved as plunging, elongated pods (augen) marking the rodding lineation Lrod. c) Enlargement of pods within the highlighted white rectangle in (b). d) Stereonet showing the relationships between the mineral stretching lineation Lm (blue dot), the rodding lineation Lrod (red dot) and the younger crenulation Lcren (green dot). e) Mt McCall structural profile showing the position of the platy quartz-mylonite at the eastern contact of the high-grade pelite (orange) with the underlying quartzite (grey).

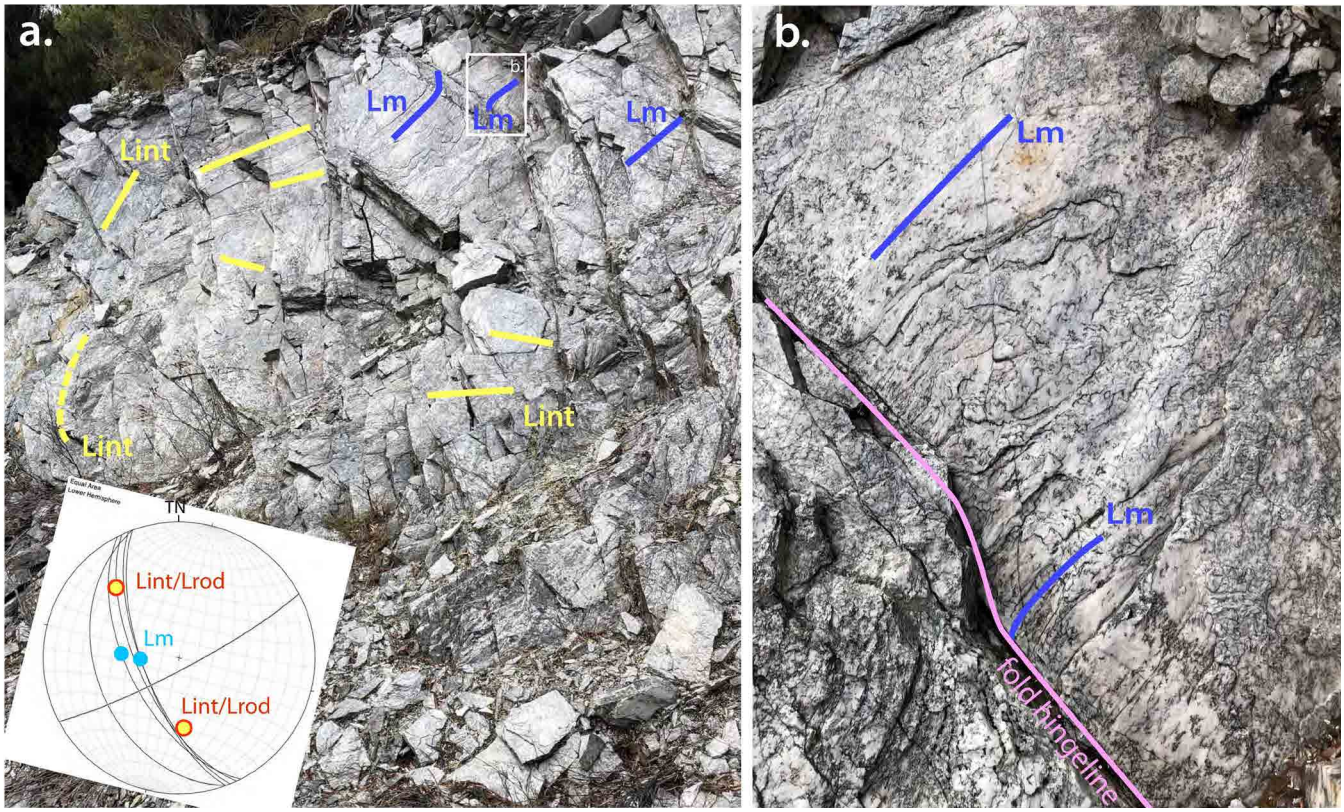

Figure 74. Varying rodding/intersection lineation (Lint: yellow line traces) in quartzite layering immediately adjacent to the high-strain zone marking the eastern contact of quartzite with the high-grade pelites (HSZ shown in Figure 73). The inset stereonet (bottom left) shows the significant variation in the rodding lineation Lint/Lrod attitude within the foliation Sm. There is a range in pitch of this lineation within Sm of ~90° (i.e. plunge changes from towards 170° to towards 320°). b) Enlargement of fold hinge highlighted by the white rectangle in (a) showing folding of the mineral stretching lineation (Lm: blue line traces). The pink line trace is the fold hingeline (DG19-68, Mt McCall Road).

in the intensity of foliation, fold flattening and fold axis variation (Figure 75).

There is also the conundrum that most asymmetric minor folds have S-vergence at all levels through the quartzite, suggesting east-over-west shear sense (Figures 76). Shear band data on the other hand, require west-over-east shear sense with a transport vector towards 110° (see Section 3.3). The opposed transport direction vectors (green arrows, Figure 76) is related to the presence of both synthetic and antithetic shear bands at Mt McCall. The restored shear band angles between Sb and Sm of 50° at DG19-61 and 25° at DG19-68 suggest that the shear bands at DG19-61 areantithetic, with sense opposite to the main shear direction. It is also important to note that the shear bands at DG19-61 occur in high-grade schist between two closely spaced east-west trending brittle faults (Figure 77).

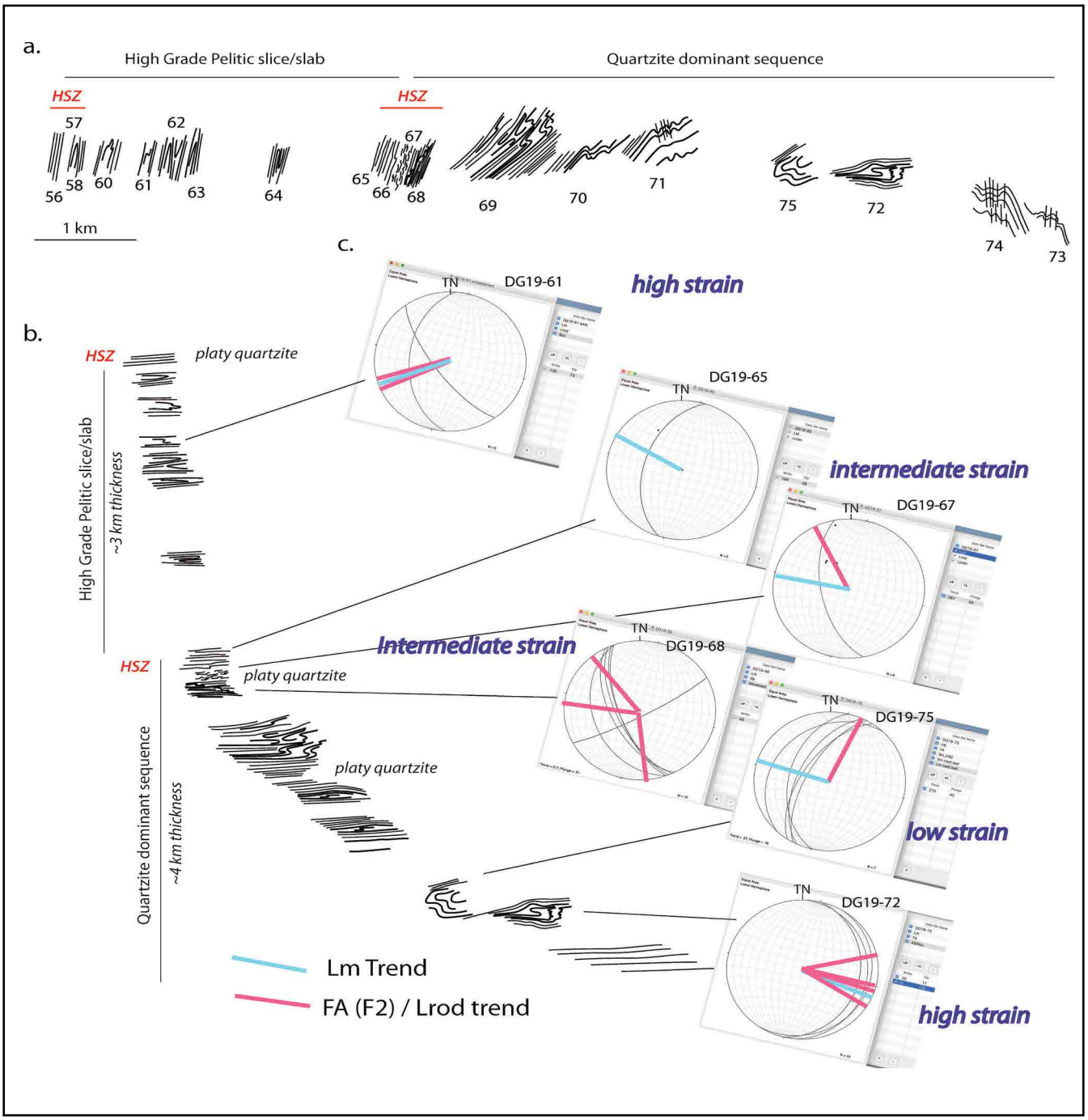

Figure 75. Fold axis versus mineral lineation (Lm) orientation shown on stereonets for different levels in the structural pile. Note high strain is inferred when the fold axis (FA) is at low angles or sub-parallel to Lm. Low strain is inferred when FA and Lm are at high angles approaching 90°.

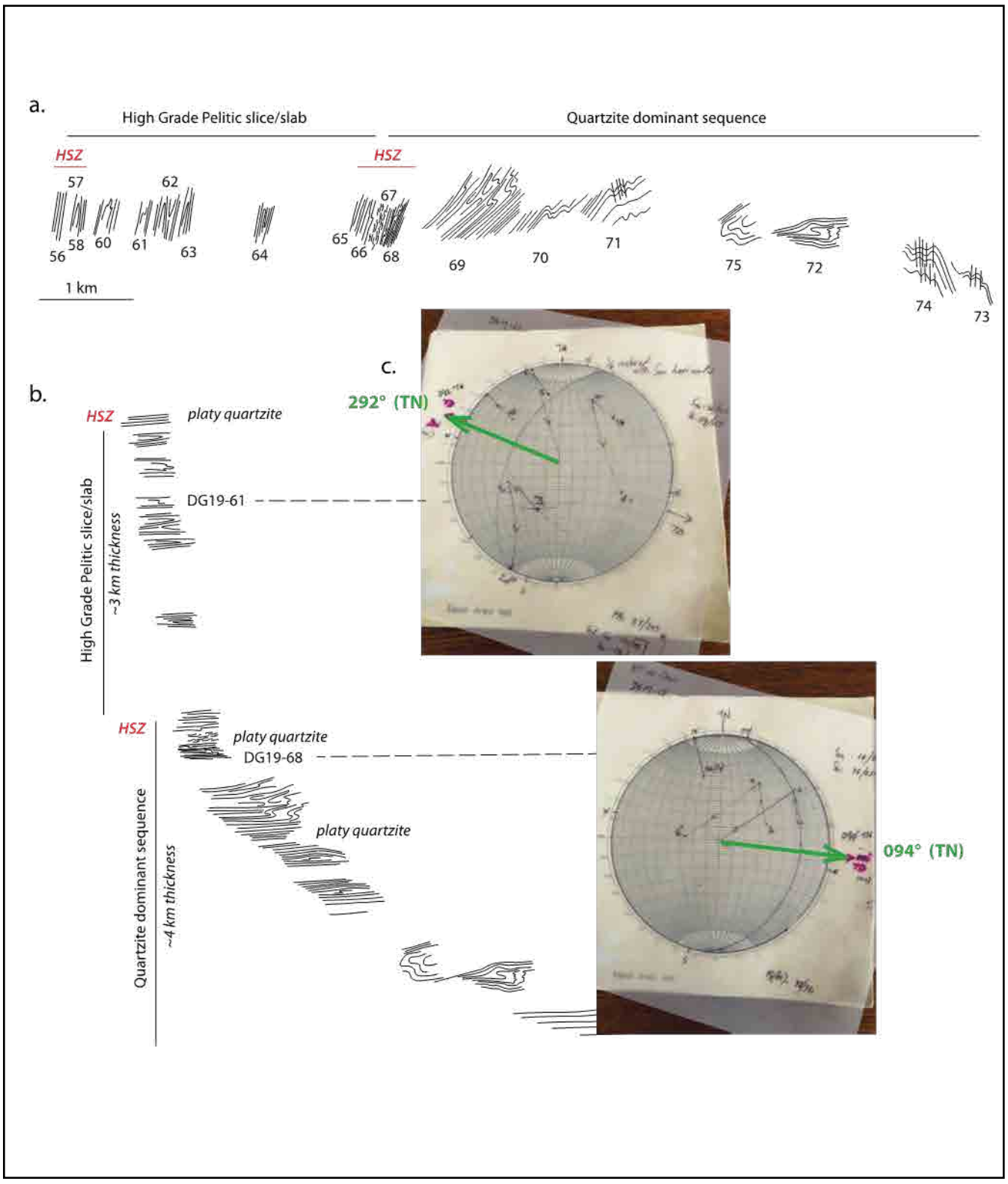

Figure 76. Transport direction vectors based on measured shear bands (Sb) in high-grade schist at DG19-61 and low-grade quartzite DG19-68. The shear band data have been restored by firstly removing the fold-plunge of the Devonian Mt McCall anticline, and secondly by rotating the foliation Sm to the horizontal. Dips on the restored shear bands with Sm horizontal are 50°NW (DG19-61) and 25°E (DG19-68).

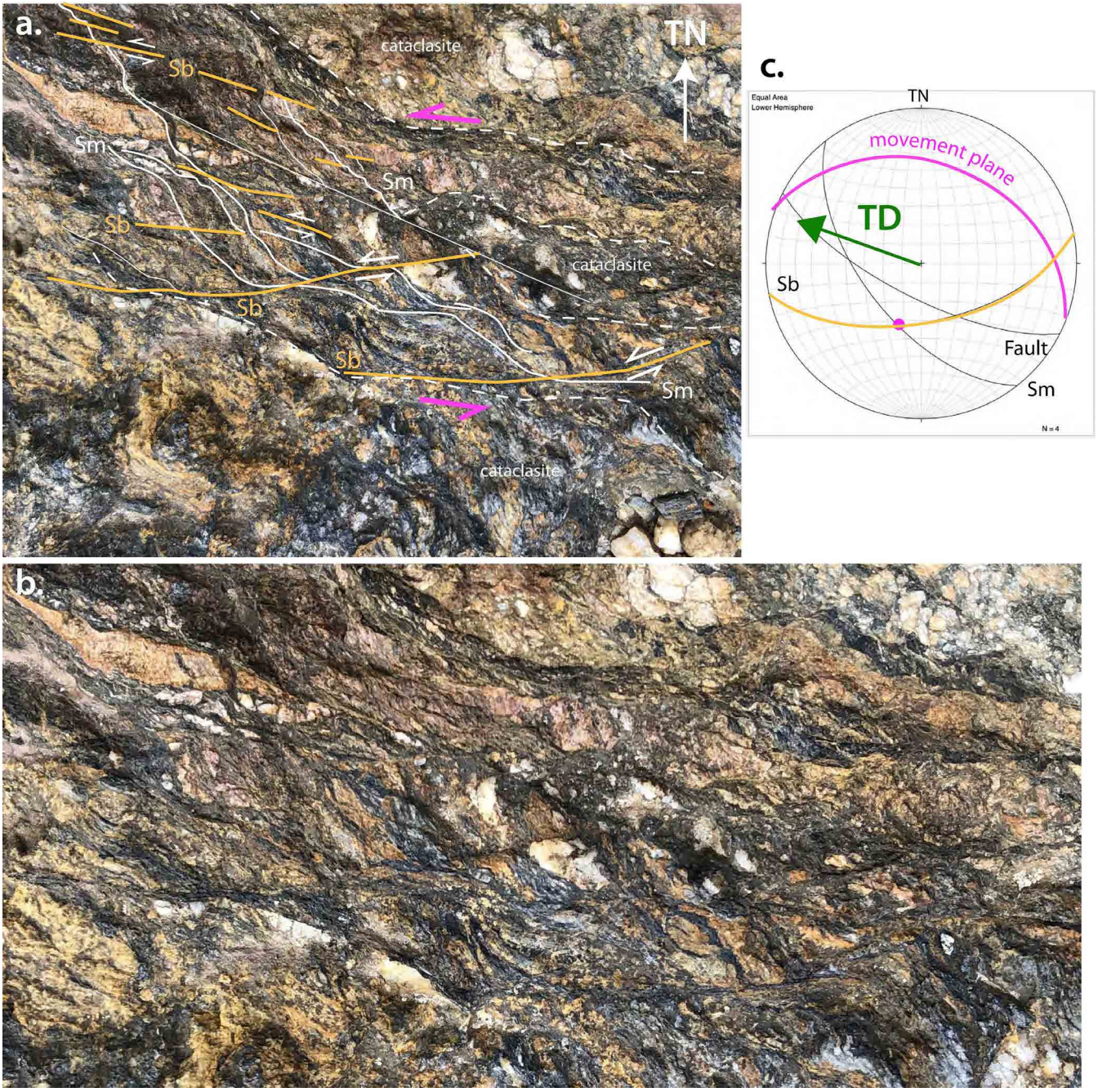

Figure 77. Sinistral (left lateral) shear bands (Sb) in high-grade schist within a brittle fault zone (DG19-61). The fault attitude is 117°/72°S. The intense foliation Sm has an attitude of 142°/59°SW, and the shear band an attitude of 079°/59S. b) Enlarged view of the shear bands in (a). c) Stereonet of the structural element attitudes including the dominant foliation (Sm,) the fault, and the shear bands (Sb). The nappe transport direction is shown by the green arrow-vector (towards 292°). This is defined by the strike of the non-restored movement plane (pink great circle), the plane perpendicular to the line of intersection of Sm and Sb (see also Figure 76).

6.0 CONCLUSIONS

As originally argued by Spry (1963a) the Central Tyennan region structure is a fold-nappe complex. The revised geometry of the fold-nappe complex presented here is not dissimilar to that of Spry (1963a) but the differences are in the closure sense of the fold-nappes and the overall continuity of the lower fold-nappes.

Central Tyennan structure is dominated by the major, regional-scale, south-closing, recumbent to reclined, isoclinal Franklin fold-nappe. It has a ~40 km axial surface strike-length, a maximum thickness of ~6-7 km and a minimum plunge extent of ~20 km. The fold-nappe has overall reclined geometry and is cored by the high-grade Franklin-Joyce metamorphic sheet. The fold-nappe complex consists of alternating south- and north-closing hinge zones with the structurally highest Franklin fold-nappe south-closing, the central Redan Hill fold-nappe north-closing and the structurally lowest Collingwood Plain fold-nappe south-closing.

The structurally lowest fold-nappe has been attenuated and segmented into a series of macro-fold pods as shown by the Collingwood Plain and Joyce Creek closures. These are high-grade garnet-quartzite and garnet-schist macro-fold pods (remnant macro-fold hinges) enveloped by intensely foliated and retrograded quartz-mica

phyllite. The fold-nappe complex structurally overlies the low-grade Scotchfire dolomitic phyllite. All units or sheets are internally isoclinally folded, show a consistent northwest-trending mineral/stretching lineation and marked rodding to mullion structure in fold hinges.

The Central Tyennan region consists of three metamorphic sheets, the structurally highest high-grade Franklin-Joyce metamorphic sheet, the sandwiched middle low-grade Fincham-Joyce metamorphic sheet and the lowest low-grade Scotchfire metamorphic sheet. All the metamorphic sheets were emplaced, stacked and in-folded with a west-over-east transport sense. Contacts between the sheets are high strain zones marked by transposition layering, mesoscopic isoclinal fold pods (augen) and multiple crenulation cleavages.

The map pattern of the Central Tyennan is further influenced by

1. Younger (Devonian?) northwest-trending and northwest-plunging open folds (The Collingwood syncline and Mary Anticline the largest of these folds)
2. A series of Late Silurian-Devonian west-northwest-trending and east-west trending oblique-slip brittle faults (dextral strike-slip component offset in plan and south-side up movement components in profile).

7.0 ACKNOWLEDGEMENTS

- Andrew McNeill for providing support through the 2016-2020 Geoscience Initiative, critically reviewing and editing the document and providing comments.
- Nic Turner and David Duncan for discussions and comments on the draft manuscript.
- Ron Berry for incisive and constructive comments on the draft manuscript.
- David Duncan for providing access to his Frenchmans Cap and Wards Bluff B/W photographs and negatives.
- Jason Bradbury DPIPWE for assistance with WHA and PWS permits for scientific research.
- Nic Deka PWS for assistance with access into Mt McCall and Frenchmans Cap.
- Rodney Smith (Rotorlift) for helicopter transport into Frenchmans Cap, skilled landings in difficult topography and access to his photographs.
- Rick Allmendinger and Nestor Cardozzo for use of OSX Stereonet.

8.0 REFERENCES

Alsop, G.I.; Holdsworth, R.E., 1999. Vergence and facing patterns in large scale sheath folds. *Journal of Structural Geology*, 21, 1335-1349.

Alsop, G.I.; Holdsworth, R.E., 2004. The geometry and topology of natural sheath folds: a new tool for structural analysis. *Journal of Structural Geology*, 26, 1561-1589.

Bell, T.D.; Rubenach, M.J.; Fleming, P.D.1986. Porphyroblast nucleation, growth and dissolution in regional metamorphic roournalcks as a function of deformation partitioning during foliation development. *Journal of Metamorphic Geology*, 4: 37-67.

Berry, R.F. 2014. Chapter 4.2 Cambrian Tectonics – The Tyennan Orogeny. In Corbett, K.D., Quilty, P.G & Calver, C.R. editors, Geological Evolution of Tasmania pp 95-110. *Geological Society of Tasmania Special Publication,* 24, Geological Society of Australia (Tasmania Division).

Berry,R.F. and Crawford, A.J. 1988. The tectonic significance of Cambrian allochthonous mafic-ultramafic complexes in Tasmania. *Australian Journal of Earth Sciences*, 35, 523-533.

Brown, D.A., Hand, M. and Morrissey, L.J., 2021. Zircon petrochronology and mineral equilibria of the eclogites from western Tasmania: interrogating the early Palaeozoic East Gondwana subduction record. *Gondwana Research*, 93, 252-274.

Calver, C. R., Baillie, P. W., Everard, J. L., Seymour, D. B., Williams, P. R., Forsyth, S. M., Turner, N. J., Williams, E. 1987. Geological Atlas 1:50 000 Series. Sheet 58 (8013N). *Lyell*. Department of Mines, Tasmania.

Carey, S.W. 1953. Geological structure of Tasmania in Relation to Mineralisation. *5th Empire Mining and Metallurgical Congress*, 1, pp 1108-1128.

Chmielowski, R.M. 2009. The Cambrian metamorphic history of Tasmania. PhD thesis, University of Tasmania.

Chmielowski, R.M. and Berry, R.F. 2009. A comparison of the monazite growth of the Tyennan Orogeny, Tasmania with earlier generations of monazite. Micro-Analysis, Processes, *Time (MAPT) Conference*, The Mineralogical Society.

Chmielowski, R.M. and Berry, R.F. 2012. The Cambrian Metamorphic History of Tasmania: The Metapelites. *Australian Journal of Earth Sciences,* 59, 1007-1019.

Duncan, D. McP. 1974. Reconnaissance geology of the Frenchmans Cap National Park. *Papers Proceedings of the Royal Society of Tasmania*, 107, 191-195.

Duncan, D. McP. 2021. *History of Structural Studies at Frenchmans Cap and Wards Bluff 1964/1965*. Mineral Resources Tasmania. Unpublished Report, UR2021_36, 4p.

Gee, D. 1962. *Structure and petrology of the Raglan Range*. B.Sc. (Hons), University of Tasmania.

Gee, D. 1963. Structure and Petrology of the Raglan Range. *Geological Survey Bulletin,* 47, Dept. of Mines, Tasmania.

Goscombe, B.D. 1990. *Equilibrium thermodynamics of the Lyell Highway eclogites*. Unpublished Report1990_19. Tasmania Department of Energy and Resources.

Gray, D.R. and Vicary, M.J. 2021. Structural Geology of Frenchmans Cap, Central Tyennan Domain, Tasmania. Mineral Resources Tasmania, *Geological Survey Paper,* 6, GSP6, 43p.

Green, D.C. and Everard, J.L. (compilers) 1998. Digital Geological Atlas 1:25 000 Scale Series. Sheet 3832 *Darwin*. Mineral Resources Tasmania.

Green, D.C. and Everard, J.L. (compilers) 2003. Digital Geological Atlas 1:25 000 Scale Series. Sheet 3833 *Owen*. Mineral Resources Tasmania.

Kamperman, M. 1984. *The Precambrian metamorphic geology of the Lyell Highway-Collingwood River area*. B.Sc (Hons) Thesis, University of Tasmania: Hobart.

Mather, R.P 1955. *The geology of the Andrew River area* (map square 3778). Hydro-Electric Commission of Tasmania unpubl. Rep.

McIntyre, E.B. 1964. *Structure and Petrology of the Collingwood area*. B.Sc. (Hons), University of Tasmania.

McLeod, I.R. 1955. *The geology of the Mt Fincham area* (map square 3780). Hydro-Electric Commission of Tasmania unpublished Report.

McLeod, I.R. 1956. *The geology of the Mt Maude area.* Hydro-Electric Commission of Tasmania unpublished Report.

Meffre, S., Berry, R. F. and Hall, M. 2000. Cambrian metamorphic complexes in Tasmania: tectonic implications. *Australian Journal of Earth Sciences,* 47, 971 – 985.

Palmeri, R.; Chmielowski, R.; Sandroni, S.; Talarico, F.; Ricci, C.A. 2009. Petrology of the eclogites from western Tasmania: Insights into the Cambro-Ordovician evolution of the paleo-Pacific margin of Gondwana. *Lithos,* 109, 223–239.

Raheim, A. 1976. Petrology of Eclogites and Surrounding Schists from the Lyell Highway - Collingwood River Area. *Journal of the Geological Society of Australia*, 23, 313-328.

Seymour, D.B., 2014. Chapoter 6.1 Middle Devonian Deformation. In Corbett, K.D., Quilty, P.G & Calver, C.R. (Editors), Geological Evolution of Tasmania pp 273-296. *Geological Society of Tasmania Special Publication,* 24, Geological Society of Australia (Tasmania Division).

Spry, A.H. 1957. Precambrian rocks of Tasmania, Part II- Mt. Mary area. *Papers and Proceedings of the Royal Society of Tasmania*, 91, 95-114.

Spry, A.H. 1962a. The Precambrian rocks, in The Geology of Tasmania Spry A. H. & Banks M. R. (Editors). *Journal of the Geological Society of Australia,* 9, 107-145.

Spry, A.H. 1962b. *Some aspects of the stratigraphy, structure and petrology of the Precambrian rocks of Tasmania.* PhD thesis, University of Tasmania.

Spry, A.H. 1963a. Precambrian rocks of Tasmania, Part V: Petrology and structure of the Frenchman's Cap area. *Papers and Proceedings of the Royal Society of Tasmania*, 97, 105-128.

Spry, A.H. 1963b. The Chronological Analysis of Crystallization and Deformation of some Tasmanian Precambrian Rocks. J*ournal of the Geological Society of Australia*, 10, 193-208.

Spry, A.H. 1963c. The occurrence of eclogite on the Lyell Highway, Tasmania. *Mineralogical Magazine,* 33, 589–593.

Spry, A.H. 1969. *Metamorphic Textures*. Pergamon Press Ltd.

Spry, A.H. and Gee, D. 1964. Some Effects of Palaeozoic Folding on the Pre-Cambrian Rocks of the Frenchmans Cap area, Tasmania. *Geological Magazine*, 101(5), pp. 385-396.

Spry, A.H. and Zimmerman, D. 1959. The Precambrian rocks of Tasmania, Part IV.-The Mt. Mullens area. *Papers and Proceedings of the Royal Society of Tasmania*, 93, 1-10.

Turner, N.J. 1971. *The Mt Madge - Mt Mary area*. B.Sc. (Hons), University of Tasmania.

Turner, N.J. 1986. Unpublished Field Notes - Lyell book 1(F_NJT_6). Department of Mines, Tasmania.

Turner, N.J. 1989. Precambrian. In: Burrett, C.F. and Martin, E.L. eds, Geology and Mineral Resources of Tasmania. *Geological Society of Tasmania Special Publication,* 15, 5-46.

Vicary, M.J. (compiler) 2004a. Digital Geological Atlas 1:25 000 Scale Series. Sheet 4033. *Collingwood*. Mineral Resources Tasmania.

Vicary, M.J. (compiler) 2004b. Digital Geological Atlas 1:25 000 Scale Series. Sheet 4032 *Loddon*. Mineral Resources Tasmania.

Williams, P.R. 1971. *The petrology and structure of the Mt McCall area*. B.Sc. (Hons), University of Tasmania.

APPENDIX 1

STRUCTURAL MAP OF THE CENTRAL TYENNAN REGION -A3

File Download

STRUCTURAL GEOLOGY OF THE CENTRAL TYENNAN REGION

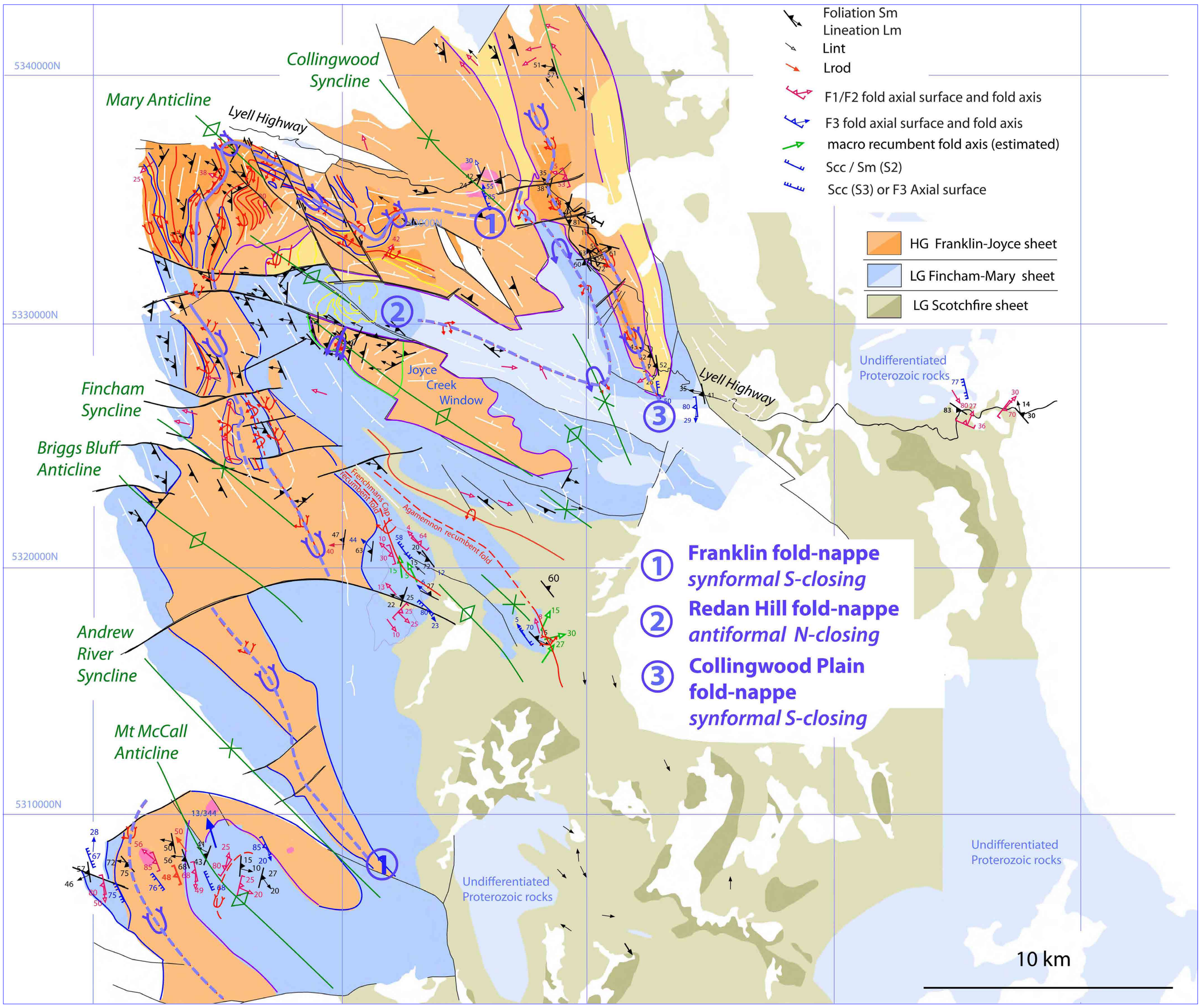

Central Tyennan structural map showing foliation Sm and lineation Lm data, and early recumbent (red traces) and late (green traces) fold axial surface traces, The high-grade rocks are shown as deep orange (garnet quartzite) and orange (garnet schist). The low-grade rocks are shown in blue (quartzite-schist/phyllite), khaki (phyllite/ dolomitic schist) and dark olive (dolomite). Map base is the 1:25000 and 1:250000 digital geological atlas from Mineral Resources Tasmania.

APPENDIX 2

TABULATED STRUCTURAL MEASUREMENTS

File Download

Central Tyennan Structural Measurements

Datum: GDA94 - MGA Zone 55

Projects	Structure	Structure Type	Dip	D/Direct	Reliability	Secondary Dip	Secondary Dip Direction	Comments	Originators	Chronostratigraphy	Collection Date	Field #	East	North	Accuracy	Location Method
Central Tyennan	Lineation	Laj	32	83.6	1 - Most reliable			Lcren	David Gray	Proterozoic	25/09/2019	DG19-44.1	427454	5326280	10m	GPS
Central Tyennan	Lineation	Lae	24	347.6	1 - Most reliable			Lm	David Gray	Proterozoic	25/09/2019	DG19-44.1	427454	5326280	10m	GPS
Central Tyennan	Metamorphic Foliation	Sag	30	50.6	1 - Most reliable			Sm	David Gray	Proterozoic	25/09/2019	DG19-44.1	427454	5326280	10m	GPS
Central Tyennan	Fold axis	Haa	30	38.6	1 - Most reliable			FA	David Gray	Proterozoic	25/09/2019	DG19-45.1	427029	5326496	10m	GPS
Central Tyennan	Crenulation Cleavage	Cai	70	127.6	1 - Most reliable			Scc/Sm	David Gray	Proterozoic	25/09/2019	DG19-45.1	427029	5326496	10m	GPS
Central Tyennan	Fold axis	Haa	83	148.6	1 - Most reliable			FA	David Gray	Proterozoic	25/09/2019	DG19-46.1	425047	5326230	10m	GPS
Central Tyennan	Crenulation Cleavage	Cai	83	212.6	1 - Most reliable			Scc	David Gray	Proterozoic	25/09/2019	DG19-46.1	425047	5326230	10m	GPS
Central Tyennan	Axial Surface	Pac			1 - Most reliable	77	258.6	AS/Scc	David Gray	Proterozoic	25/09/2019	DG19-46.2	425047	5326230	10m	GPS
Central Tyennan	Fold axis	Haa + Pac	36	348.6	1 - Most reliable	27	23.6	FA	David Gray	Proterozoic	25/09/2019	DG19-46.2	425047	5326230	10m	GPS
Central Tyennan	Fold axis	Haa	29	180.6	1 - Most reliable			FA	David Gray	Proterozoic	25/09/2019	DG19-47.1	414545	5327157	10m	GPS
Central Tyennan	Crenulation Cleavage	Cai	80	265.6	1 - Most reliable			Scc/As	David Gray	Proterozoic	25/09/2019	DG19-47.1	414545	5327157	10m	GPS
Central Tyennan	Lineation	Lae	35	279.6	1 - Most reliable			Lm	David Gray	Proterozoic	25/09/2019	DG19-47.2	414545	5327157	10m	GPS
Central Tyennan	Metamorphic Foliation	Sag	41	259.6	1 - Most reliable			Sm	David Gray	Proterozoic	25/09/2019	DG19-47.2	414545	5327157	10m	GPS
Central Tyennan	Lineation	Lae	6	83.6	1 - Most reliable			Lm	David Gray	Proterozoic	25/09/2019	DG19-47.3	414545	5327157	10m	GPS
Central Tyennan	Metamorphic Foliation	Sag	29	163.6	1 - Most reliable			Sm	David Gray	Proterozoic	25/09/2019	DG19-47.3	414545	5327157	10m	GPS
Central Tyennan	Lineation	Lae	26	193.6	1 - Most reliable			Lm/Lint	David Gray	Proterozoic	25/09/2019	DG19-48.1	412570	5328320		Topo Map
Central Tyennan	Crenulation Cleavage	Cai	50	83.6	1 - Most reliable			Scc	David Gray	Proterozoic	25/09/2019	DG19-48.1	412570	5328320		Topo Map
Central Tyennan	Metamorphic Foliation	Sag	52	253.6	1 - Most reliable			Sm	David Gray	Proterozoic	25/09/2019	DG19-48.1	412570	5328320		Topo Map

Projects	Structure	Structure Type	Dip	D/Direct	Reliability	Secondary Dip	Secondary Dip Direction	Comments	Originators	Chronostratigraphy	Collection Date	Field #	East	North	Accuracy	Location Method
Central Tyennan	Lineation	Lae	5	189.6	1 - Most reliable			Lint	David Gray	Proterozoic	25/09/2019	DG19-48.2	412550	5328320		Topo Map
Central Tyennan	Lineation	Lae	43	298.6	1 - Most reliable			Lm	David Gray	Proterozoic	25/09/2019	DG19-48.2	412550	5328320		Topo Map
Central Tyennan	Metamorphic Foliation	Sag	61	268.6	1 - Most reliable			Sm	David Gray	Proterozoic	25/09/2019	DG19-48.2	412550	5328320		Topo Map
Central Tyennan	Shear Band	Sau	72	193.6	1 - Most reliable			Sb (shear band-south block down)	David Gray	Proterozoic	25/09/2019	DG19-49.1	409720	5332674	10m	GPS
Central Tyennan	Metamorphic Foliation	Sag	60	238.6	1 - Most reliable			Sm	David Gray	Proterozoic	25/09/2019	DG19-49.1	409720	5332674	10m	GPS
Central Tyennan	Lineation	Lae	16	127.6	1 - Most reliable			Lm	David Gray	Proterozoic	25/09/2019	DG19-50.1	409065	5334152	10m	GPS
Central Tyennan	Shear Band	Sav	90	206.6	1 - Most reliable			Vertical Sb (shear band-south block down)	David Gray	Proterozoic	25/09/2019	DG19-50.1	409065	5334152	10m	GPS
Central Tyennan	Metamorphic Foliation	Sag	81	58.6	1 - Most reliable			Sm	David Gray	Proterozoic	25/09/2019	DG19-50.1	409065	5334152	10m	GPS
Central Tyennan	Lineation	Lae	5	208.6	1 - Most reliable			Lm	David Gray	Proterozoic	25/09/2019	DG19-51.1	409067	5334665	10m	GPS
Central Tyennan	Metamorphic Foliation	Sag	48	283.6	1 - Most reliable			Sm	David Gray	Proterozoic	25/09/2019	DG19-51.1	409067	5334665	10m	GPS
Central Tyennan	Fold axis	Haa + Pac	45	283.6	1 - Most reliable	53	258.6	F	David Gray	Proterozoic	25/09/2019	DG19-52.1	408460	5335313	10m	GPS
Central Tyennan	Lineation	Lae	35	313.6	1 - Most reliable			Lm	David Gray	Proterozoic	25/09/2019	DG19-52.1	408460	5335313	10m	GPS
Central Tyennan	Metamorphic Foliation	Sag	38	303.6	1 - Most reliable			Sm	David Gray	Proterozoic	25/09/2019	DG19-52.1	408460	5335313	10m	GPS
Central Tyennan	Lineation	Lae	53	193.6	1 - Most reliable			Lm	David Gray	Proterozoic	25/09/2019	DG19-52.2	408510	5335313	10m	GPS
Central Tyennan	Lineation	Laj	30	338.6	1 - Most reliable			Lcren	David Gray	Proterozoic	25/09/2019	DG19-53.1	405407	5335879	10m	GPS
Central Tyennan	Lineation	Lae	24	253.6	1 - Most reliable			Lm	David Gray	Proterozoic	25/09/2019	DG19-53.1	405407	5335879	10m	GPS
Central Tyennan	Metamorphic Foliation	Sag	42	296.6	1 - Most reliable			Sm	David Gray	Proterozoic	25/09/2019	DG19-53.1	405407	5335879	10m	GPS

Projects	Structure	Structure Type	Dip	D/Direct	Reliability	Secondary Dip	Secondary Dip Direction	Comments	Originators	Chronostratigraphy	Collection Date	Field #	East	North	Accuracy	Location Method
Central Tyennan	Fold axis	Haa + Pac	55	340.6	1 - Most reliable	85	68.6	F	David Gray	Proterozoic	25/09/2019	DG19-53.2	405407	5335879	10m	GPS
Central Tyennan	Fault	Fac	75	323.6	1 - Most reliable			Fault	David Gray	Ordovician	26/09/2019	DG19-54.1	389637	5307989	10m	GPS
Central Tyennan	Fault	Fac	70	323.6	1 - Most reliable			Fault	David Gray	Ordovician	26/09/2019	DG19-54.1	389637	5307989	10m	GPS
Central Tyennan	Fault	Fac	80	323.6	1 - Most reliable			Fault Pitch 80NE, HW down)	David Gray	Ordovician	26/09/2019	DG19-54.1	389637	5307989	10m	GPS
Central Tyennan	Bedding	Baf	74	106.6	1 - Most reliable			Sm	David Gray	Ordovician	26/09/2019	DG19-55	390230	5307965	10m	GPS
Central Tyennan	Fault	Fac	75	4	1 - Most reliable			Fault; sinistral movement	David Gray	Proterozoic	26/09/2019	DG19.56.1	390430	5308134	10m	GPS
Central Tyennan	Fault	Fac	81	2	1 - Most reliable			Fault; sinistral movement	David Gray	Proterozoic	26/09/2019	DG19.56.1	390430	5308134	10m	GPS
Central Tyennan	Metamorphic Foliation	Sag	80	62	1 - Most reliable			Sm	David Gray	Proterozoic	26/09/2019	DG19.56.1	390430	5308134	10m	GPS
Central Tyennan	Lineation	Laj	25	339	1 - Most reliable			Lcren	David Gray	Proterozoic	26/09/2019	DG19.57.1	390522	5308026	10m	GPS
Central Tyennan	Lineation	Lae	46	246	1 - Most reliable			Lm	David Gray	Proterozoic	26/09/2019	DG19.57.1	390522	5308026	10m	GPS
Central Tyennan	Metamorphic Foliation	Sag	57	262	1 - Most reliable			Sm	David Gray	Proterozoic	26/09/2019	DG19.57.1	390522	5308026	10m	GPS
Central Tyennan	Fold axis	Haa	27	4	1 - Most reliable			FA	David Gray	Proterozoic	26/09/2019	DG19.57.2	390522	5308026	10m	GPS
Central Tyennan	Fold axis	Haa	29	6	1 - Most reliable			FA	David Gray	Proterozoic	26/09/2019	DG19.57.2	390522	5308026	10m	GPS
Central Tyennan	Crenulation Cleavage	Cai	67	34	1 - Most reliable			Scc	David Gray	Proterozoic	26/09/2019	DG19.57.2	390522	5308026	10m	GPS
Central Tyennan	Crenulation Cleavage	Cai	71	80	1 - Most reliable			Scc/As	David Gray	Proterozoic	26/09/2019	DG19.57.3	390522	5308026	10m	GPS
Central Tyennan	Crenulation Cleavage	Cai	70	83	1 - Most reliable			Scc/As	David Gray	Proterozoic	26/09/2019	DG19.57.3	390522	5308026	10m	GPS
Central Tyennan	Crenulation Cleavage	Cai	67	84	1 - Most reliable			Scc/As	David Gray	Proterozoic	26/09/2019	DG19.57.3	390522	5308026	10m	GPS
Central Tyennan	Fold axis	Haa	32	6	1 - Most reliable			FA	David Gray	Proterozoic	26/09/2019	DG19.58.1	390756	5307813	10m	GPS
Central Tyennan	Metamorphic Foliation	Sag	77	227	1 - Most reliable			Sm	David Gray	Proterozoic	26/09/2019	DG19.58.1	390756	5307813	10m	GPS

Projects	Structure	Structure Type	Dip	D/Direct	Reliability	Secondary Dip	Secondary Dip Direction	Comments	Originators	Chronostratigraphy	Collection Date	Field #	East	North	Accuracy	Location Method
Central Tyennan	Axial Surface	Pac			1 - Most reliable	74	42	AS	David Gray	Proterozoic	26/09/2019	DG19.58.2	390756	5307813	10m	GPS
Central Tyennan	Axial Surface	Pac			1 - Most reliable	70	40	AS	David Gray	Proterozoic	26/09/2019	DG19.58.2	390756	5307813	10m	GPS
Central Tyennan	Crenulation Cleavage	Cai	76	267	1 - Most reliable			Scc	David Gray	Proterozoic	26/09/2019	DG19.58.3	390756	5307813	10m	GPS
Central Tyennan	Crenulation Cleavage	Cai	77	251	1 - Most reliable			Scc	David Gray	Proterozoic	26/09/2019	DG19.58.3	390756	5307813	10m	GPS
Central Tyennan	Crenulation Cleavage	Cai	75	246	1 - Most reliable			Scc	David Gray	Proterozoic	26/09/2019	DG19.58.4	390756	5307813	10m	GPS
Central Tyennan	Fold axis	Haa + Pac	41	182	1 - Most reliable	75	261	FA/AS	David Gray	Proterozoic	26/09/2019	DG19.58.5	390756	5307813	10m	GPS
Central Tyennan	Fold axis	Haa + Pac	50	169	1 - Most reliable	84	258	FA/AS	David Gray	Proterozoic	26/09/2019	DG19.58.5	390756	5307813	10m	GPS
Central Tyennan	Crenulation Cleavage	Cai	82	268	1 - Most reliable			Scc	David Gray	Proterozoic	26/09/2019	DG19.58.6	390756	5307813	10m	GPS
Central Tyennan	Axial Surface	Pac			1 - Most reliable	70	251	as	David Gray	Proterozoic	26/09/2019	DG19.60.1	391057	5308033	10m	GPS
Central Tyennan	Fold axis	Haa + Pac	34	184	1 - Most reliable	65	237	fa/as	David Gray	Proterozoic	26/09/2019	DG19.60.2	391057	5308033	10m	GPS
Central Tyennan	Metamorphic Foliation	Sag	66	256	1 - Most reliable			Sm	David Gray	Proterozoic	26/09/2019	DG19.60.3	391057	5308033	10m	GPS
Central Tyennan	Metamorphic Foliation	Sag	67	242	1 - Most reliable			Sm	David Gray	Proterozoic	26/09/2019	DG19.60.4	391057	5308033	10m	GPS
Central Tyennan	Fold axis	Haa	50	194	1 - Most reliable			FA	David Gray	Proterozoic	26/09/2019	DG19.60.5	391057	5308033	10m	GPS
Central Tyennan	Metamorphic Foliation	Sag	75	234	1 - Most reliable			Sm	David Gray	Proterozoic	26/09/2019	DG19.60.6	391057	5308033	10m	GPS
Central Tyennan	Shear Band	Sau	59	169	1 - Most reliable			Sb	David Gray	Proterozoic	26/09/2019	DG19.61.1	391331	5308040	10m	GPS
Central Tyennan	Metamorphic Foliation	Sag	56	229	1 - Most reliable			Sm	David Gray	Proterozoic	26/09/2019	DG19.61.1	391331	5308040	10m	GPS
Central Tyennan	Fault	Fac	72	207	1 - Most reliable			F	David Gray	Proterozoic	26/09/2019	DG19.61.2	391331	5308040	10m	GPS
Central Tyennan	Metamorphic Foliation	Sag	67	230	1 - Most reliable			Sm	David Gray	Proterozoic	26/09/2019	DG19.61.2	391331	5308040	10m	GPS
Central Tyennan	Fault	Fac	72	195	1 - Most reliable			F	David Gray	Proterozoic	26/09/2019	DG19.61.3	391331	5308040	10m	GPS
Central Tyennan	Lineation	Lae	39	249	1 - Most reliable			Lm	David Gray	Proterozoic	26/09/2019	DG19.61.4	391331	5308040	10m	GPS
Central Tyennan	Metamorphic Foliation	Sag	45	274	1 - Most reliable			Sm	David Gray	Proterozoic	26/09/2019	DG19.61.4	391331	5308040	10m	GPS

Projects	Structure	Structure Type	Dip	D/Direct	Reliability	Secondary Dip	Secondary Dip Direction	Comments	Originators	Chronostratigraphy	Collection Date	Field #	East	North	Accuracy	Location Method
Central Tyennan	Lineation	Lag	39	257	1 - Most reliable			Lrod	David Gray	Proterozoic	26/09/2019	DG19.61.5	391331	5308040	10m	GPS
Central Tyennan	Lineation	Lag	35	248	1 - Most reliable			Lrod	David Gray	Proterozoic	26/09/2019	DG19.61.5	391331	5308040	10m	GPS
Central Tyennan	Crenulation Cleavage	Cai	76	234	1 - Most reliable			Scc	David Gray	Proterozoic	26/09/2019	DG19.61.6	391331	5308040	10m	GPS
Central Tyennan	Axial Surface	Pac			1 - Most reliable	53	239	As/S1	David Gray	Proterozoic	26/09/2019	DG19.62.1	391603	5308123	10m	GPS
Central Tyennan	Compositional Layering	Sak	75	235	1 - Most reliable			Sm	David Gray	Proterozoic	26/09/2019	DG19.62.1	391603	5308123	10m	GPS
Central Tyennan	Compositional Layering	Sak	79	243	1 - Most reliable			So/Sm	David Gray	Proterozoic	26/09/2019	DG19.62.1	391603	5308123	10m	GPS
Central Tyennan	Axial Surface	Pac			1 - Most reliable	73	244	As/S1	David Gray	Proterozoic	26/09/2019	DG19.62.2	391603	5308123	10m	GPS
Central Tyennan	Compositional Layering	Sak	70	238	1 - Most reliable			So/Sm	David Gray	Proterozoic	26/09/2019	DG19.62.2	391603	5308123	10m	GPS
Central Tyennan	Compositional Layering	Sak	80	258	1 - Most reliable			So/Sm	David Gray	Proterozoic	26/09/2019	DG19.62.2	391603	5308123	10m	GPS
Central Tyennan	Lineation	Lae	72	281	1 - Most reliable			Lm	David Gray	Proterozoic	26/09/2019	DG19.63.1	391729	5308220	10m	GPS
Central Tyennan	Metamorphic Foliation	Sag	75	230	1 - Most reliable			Sm	David Gray	Proterozoic	26/09/2019	DG19.63.1	391729	5308220	10m	GPS
Central Tyennan	Metamorphic Foliation	Sag	75	258	1 - Most reliable			Sm; NE Limb	David Gray	Proterozoic	26/09/2019	DG19.64.1	392749	5308579	10m	GPS
Central Tyennan	Compositional Layering	Sak	80	250	1 - Most reliable			So/Sm; SW Limb	David Gray	Proterozoic	26/09/2019	DG19.64.2	392749	5308579	10m	GPS
Central Tyennan	Lineation	Laj	35	331	1 - Most reliable			Lcren	David Gray	Proterozoic	26/09/2019	DG19.65.1	393392	5309027	10m	GPS
Central Tyennan	Lineation	Lae	43	302	1 - Most reliable			Lm	David Gray	Proterozoic	26/09/2019	DG19.65.1	393392	5309027	10m	GPS
Central Tyennan	Metamorphic Foliation	Sag	48	288	1 - Most reliable			Sm	David Gray	Proterozoic	26/09/2019	DG19.65.1	393392	5309027	10m	GPS
Central Tyennan	Fold axis	Haa + Pac	49	170	1 - Most reliable	68	259	FA	David Gray	Proterozoic	26/09/2019	DG19.66.1	393596	5309039	10m	GPS
Central Tyennan	Metamorphic Foliation	Sag	77	257	1 - Most reliable			Sm	David Gray	Proterozoic	26/09/2019	DG19.66.1	393596	5309039	10m	GPS
Central Tyennan	Metamorphic Foliation	Sag	60	259	1 - Most reliable			Sm	David Gray	Proterozoic	26/09/2019	DG19.67.1	393641	5308905	10m	GPS
Central Tyennan	Lineation	Lae	50	281	1 - Most reliable			Lm	David Gray	Proterozoic	26/09/2019	DG19.67.2	393641	5308905	10m	GPS
Central Tyennan	Lineation	Lag	50	321	1 - Most reliable			Lrod	David Gray	Proterozoic	26/09/2019	DG19.67.3	393641	5308905	10m	GPS

Projects	Structure	Structure Type	Dip	D/Direct	Reliability	Secondary Dip	Secondary Dip Direction	Comments	Originators	Chronostratigraphy	Collection Date	Field #	East	North	Accuracy	Location Method
Central Tyennan	Lineation	Lag	49	324	1 - Most reliable			Lrod	David Gray	Proterozoic	26/09/2019	DG19.67.3	393641	5308905	10m	GPS
Central Tyennan	Lineation	Lag	57	317	1 - Most reliable			Lrod	David Gray	Proterozoic	26/09/2019	DG19.67.3	393641	5308905	10m	GPS
Central Tyennan	Lineation	Laj	8	349	1 - Most reliable			Lcren; 5 pitch	David Gray	Proterozoic	26/09/2019	DG19.67.4	393641	5308905	10m	GPS
Central Tyennan	Lineation	Lae	48	177	1 - Most reliable			Lm	David Gray	Proterozoic	26/09/2019	DG19.68.1	393843	5308703	10m	GPS
Central Tyennan	Metamorphic Foliation	Sag	65	245	1 - Most reliable			Sm	David Gray	Proterozoic	26/09/2019	DG19.68.1	393843	5308703	10m	GPS
Central Tyennan	Lineation	Lae	52	274	1 - Most reliable			Lm	David Gray	Proterozoic	26/09/2019	DG19.68.2	393843	5308703	10m	GPS
Central Tyennan	Metamorphic Foliation	Sag	68	250	1 - Most reliable			Sm	David Gray	Proterozoic	26/09/2019	DG19.68.2	393843	5308703	10m	GPS
Central Tyennan	Lineation	Lae	65	270	1 - Most reliable			Lm	David Gray	Proterozoic	26/09/2019	DG19.68.3	393843	5308703	10m	GPS
Central Tyennan	Metamorphic Foliation	Sag	68	248	1 - Most reliable			Sm	David Gray	Proterozoic	26/09/2019	DG19.68.3	393843	5308703	10m	GPS
Central Tyennan	Lineation	Lae	30	320	1 - Most reliable			Lm	David Gray	Proterozoic	26/09/2019	DG19.68.4	393843	5308703	10m	GPS
Central Tyennan	Metamorphic Foliation	Sag	59	243	1 - Most reliable			Sm	David Gray	Proterozoic	26/09/2019	DG19.68.4	393843	5308703	10m	GPS
Central Tyennan	Shear Band	Sau	38	250	1 - Most reliable			Sb	David Gray	Proterozoic	26/09/2019	DG19.68.5	393843	5308703	10m	GPS
Central Tyennan	Metamorphic Foliation	Sag	64	250	1 - Most reliable			Sm	David Gray	Proterozoic	26/09/2019	DG19.68.5	393843	5308703	10m	GPS
Central Tyennan	Metamorphic Foliation	Sag	48	336	1 - Most reliable			Sm	David Gray	Proterozoic	26/09/2019	DG19.69.1	394069	5308449	10m	GPS
Central Tyennan	Lineation	Lae	45	304	1 - Most reliable			Lm	David Gray	Proterozoic	26/09/2019	DG19.69.2	394069	5308449	10m	GPS
Central Tyennan	Metamorphic Foliation	Sag	48	314	1 - Most reliable			Sm	David Gray	Proterozoic	26/09/2019	DG19.69.2	394069	5308449	10m	GPS
Central Tyennan	Crenulation Cleavage	Cai	72	60	1 - Most reliable			Scren	David Gray	Proterozoic	26/09/2019	DG19.69.3	394069	5308449	10m	GPS
Central Tyennan	Metamorphic Foliation	Sag	33	367	1 - Most reliable			Sm	David Gray	Proterozoic	26/09/2019	DG19.70.1	394527	5308336	10m	GPS
Central Tyennan	Metamorphic Foliation	Sag	49	357	1 - Most reliable			Sm	David Gray	Proterozoic	26/09/2019	DG19.70.2	394527	5308336	10m	GPS
Central Tyennan	Crenulation Cleavage	Cai	68	57	1 - Most reliable			Scren	David Gray	Proterozoic	26/09/2019	DG19.70.3	394527	5308336	10m	GPS
Central Tyennan	Metamorphic Foliation	Sag	64	298	1 - Most reliable			Sm	David Gray	Proterozoic	26/09/2019	DG19.70.3	394527	5308336	10m	GPS

Projects	Structure	Structure Type	Dip	D/Direct	Reliability	Secondary Dip	Secondary Dip Direction	Comments	Originators	Chronostratigraphy	Collection Date	Field #	East	North	Accuracy	Location Method
Central Tyennan	Fold axis	Haa + Pac	47	257	1 - Most reliable	46	288	FA	David Gray	Proterozoic	26/09/2019	DG19.70.4	394527	5308336	10m	GPS
Central Tyennan	Metamorphic Foliation	Sag	55	296	1 - Most reliable			Sm	David Gray	Proterozoic	26/09/2019	DG19.70.5	394527	5308336	10m	GPS
Central Tyennan	Fold axis	Haa	33	228	1 - Most reliable			FA	David Gray	Proterozoic	26/09/2019	DG19.70.6	394527	5308336	10m	GPS
Central Tyennan	Lineation	Laj	34	368	1 - Most reliable			Lcren	David Gray	Proterozoic	26/09/2019	DG19.70.6	394527	5308336	10m	GPS
Central Tyennan	Lineation	Lae	47	340	1 - Most reliable			Lm	David Gray	Proterozoic	26/09/2019	DG19.70.6	394527	5308336	10m	GPS
Central Tyennan	Metamorphic Foliation	Sag	38	270	1 - Most reliable			Sm	David Gray	Proterozoic	26/09/2019	DG19.71.1	394640	5308432	10m	GPS
Central Tyennan	Metamorphic Foliation	Sag	15	20	1 - Most reliable			Sm	David Gray	Proterozoic	26/09/2019	DG19.71.2	394640	5308432	10m	GPS
Central Tyennan	Metamorphic Foliation	Sag	33	270	1 - Most reliable			Sm	David Gray	Proterozoic	26/09/2019	DG19.71.3	394640	5308432	10m	GPS
Central Tyennan	Lineation	Lae	41	297	1 - Most reliable			Lm	David Gray	Proterozoic	26/09/2019	DG19.71.4	394640	5308432	10m	GPS
Central Tyennan	Metamorphic Foliation	Sag	43	290	1 - Most reliable			Sm	David Gray	Proterozoic	26/09/2019	DG19.71.4	394640	5308432	10m	GPS
Central Tyennan	Lineation	Lae	32	297	1 - Most reliable			Lm	David Gray	Proterozoic	26/09/2019	DG19.71.5	394640	5308432	10m	GPS
Central Tyennan	Metamorphic Foliation	Sag	35	277	1 - Most reliable			Sm	David Gray	Proterozoic	26/09/2019	DG19.71.5	394640	5308432	10m	GPS
Central Tyennan	Fold axis	Haa + Pac	20	114	1 - Most reliable	25	104	FA	David Gray	Proterozoic	26/09/2019	DG19.72.1	396476	5307669	10m	GPS
Central Tyennan	Fold axis	Haa	10	114	1 - Most reliable			FA	David Gray	Proterozoic	26/09/2019	DG19.72.2	396476	5307669	10m	GPS
Central Tyennan	Lineation	Lae	10	104	1 - Most reliable			Lm	David Gray	Proterozoic	26/09/2019	DG19.72.3	396476	5307669	10m	GPS
Central Tyennan	Metamorphic Foliation	Sag	15	94	1 - Most reliable			Sm	David Gray	Proterozoic	26/09/2019	DG19.72.3	396476	5307669	10m	GPS
Central Tyennan	Fold axis	Haa	20	124	1 - Most reliable			FA	David Gray	Proterozoic	26/09/2019	DG19.72.4	396476	5307669	10m	GPS
Central Tyennan	Fold axis	Haa	30	114	1 - Most reliable			FA	David Gray	Proterozoic	26/09/2019	DG19.72.5	396476	5307669	10m	GPS
Central Tyennan	Crenulation Cleavage	Cai	11	124	1 - Most reliable			Scren	David Gray	Proterozoic	26/09/2019	DG19.72.6	396476	5307669	10m	GPS
Central Tyennan	Fold axis	Haa	22	104	1 - Most reliable			FA	David Gray	Proterozoic	26/09/2019	DG19.72.7	396476	5307669	10m	GPS
Central Tyennan	Fold axis	Haa	5	79	1 - Most reliable			FA	David Gray	Proterozoic	26/09/2019	DG19.72.8	396476	5307669	10m	GPS

Projects	Structure	Structure Type	Dip	D/Direct	Reliability	Secondary Dip	Secondary Dip Direction	Comments	Originators	Chronostratigraphy	Collection Date	Field #	East	North	Accuracy	Location Method
Central Tyennan	Fold axis	Haa + Pac	6	202	1 - Most reliable	85	72	FA	David Gray	Proterozoic	26/09/2019	DG19.73.1	397313	5307904	10m	GPS
Central Tyennan	Metamorphic Foliation	Sag	66	94	1 - Most reliable			Sm	David Gray	Proterozoic	26/09/2019	DG19.73.1	397313	5307904	10m	GPS
Central Tyennan	Fold axis	Haa + Pac	20	159	1 - Most reliable	85	244	FA	David Gray	Proterozoic	26/09/2019	DG19.74.1	396985	5307608	10m	GPS
Central Tyennan	Lineation	Lae	24	144	1 - Most reliable			Lm	David Gray	Proterozoic	26/09/2019	DG19.74.1	396985	5307608	10m	GPS
Central Tyennan	Metamorphic Foliation	Sag	27	124	1 - Most reliable			Sm	David Gray	Proterozoic	26/09/2019	DG19.74.1	396985	5307608	10m	GPS
Central Tyennan	Metamorphic Foliation	Sag	65	299	1 - Most reliable			Sm	David Gray	Proterozoic	26/09/2019	DG19.75.1	395915	5307977	10m	GPS
Central Tyennan	Bedding	Baf	55	286	1 - Most reliable			Sm	David Gray	Proterozoic	26/09/2019	DG19.75.2	395915	5307977	10m	GPS
Central Tyennan	Fold axis	Haa + Pac	25	34	1 - Most reliable	80	304	FA	David Gray	Proterozoic	26/09/2019	DG19.75.3	395915	5307977	10m	GPS
Central Tyennan	Bedding	Baf	24	314	1 - Most reliable			Sm	David Gray	Proterozoic	26/09/2019	DG19.75.4	395915	5307977	10m	GPS
Central Tyennan	Metamorphic Foliation	Sag	45	284	1 - Most reliable			Sm	David Gray	Proterozoic	26/09/2019	DG19.75.5	395915	5307977	10m	GPS
Central Tyennan	Lineation	Lae	40	289	1 - Most reliable			Lm	David Gray	Proterozoic	26/09/2019	DG19.75.6	395915	5307977	10m	GPS
Central Tyennan	Fold axis	Haa + Pac	35	203.6	1 - Most reliable	90	281.6	FA	David Gray	Proterozoic	11/11/2020	DG20.46.1	425050	5326226	10m	GPS
Central Tyennan	Compositional Layering	Sak	80	293.6	1 - Most reliable			So/Sm	David Gray	Proterozoic	11/11/2020	DG20.46.2	425050	5326226	10m	GPS
Central Tyennan	Metamorphic Foliation	Sag	85	33.6	1 - Most reliable			Sm	David Gray	Proterozoic	11/11/2020	DG20.46.3	425050	5326226	10m	GPS
Central Tyennan	Reverse Fault	Fae	38	293.6	1 - Most reliable			Reverse Fault	David Gray	Proterozoic	11/11/2020	DG20.46.4	425050	5326226	10m	GPS
Central Tyennan	Fold axis	Haa	45	323.6	1 - Most reliable			FA	David Gray	Proterozoic	11/11/2020	DG20.46.5	425050	5326226	10m	GPS
Central Tyennan	Fold axis	Haa + Pac	50	283.6	1 - Most reliable	74	232.6	FA	David Gray	Proterozoic	11/11/2020	DG20.47.1	425003	5326196	10m	GPS
Central Tyennan	Fold axis	Haa + Pac	50	338.6	1 - Most reliable	74	228.6	FA	David Gray	Proterozoic	11/11/2020	DG20.47.2	425003	5326196	10m	GPS
Central Tyennan	Shear Band	Sau	0	93.6	1 - Most reliable			Sb	David Gray	Proterozoic	11/11/2020	DG20.47.3	425003	5326196	10m	GPS
Central Tyennan	Metamorphic Foliation	Sag	70	143.6	1 - Most reliable			Sm	David Gray	Proterozoic	11/11/2020	DG20.47.3	425003	5326196	10m	GPS

Projects	Structure	Structure Type	Dip	D/Direct	Reliability	Secondary Dip	Secondary Dip Direction	Comments	Originators	Chronostratigraphy	Collection Date	Field #	East	North	Accuracy	Location Method
Central Tyennan	Lineation	Lae	53	253.6	1 - Most reliable			Lm	David Gray	Proterozoic	11/11/2020	DG20.47.4	425003	5326196	10m	GPS
Central Tyennan	Metamorphic Foliation	Sag	56	238.6	1 - Most reliable			Sm	David Gray	Proterozoic	11/11/2020	DG20.47.4	425003	5326196	10m	GPS
Central Tyennan	Lineation	Lae	30	289.6	1 - Most reliable			Lm	David Gray	Proterozoic	11/11/2020	DG20.48.1	411974	5327887	10m	GPS
Central Tyennan	Metamorphic Foliation	Sag	40	253.6	1 - Most reliable			Sm	David Gray	Proterozoic	11/11/2020	DG20.48.1	411974	5327887	10m	GPS
Central Tyennan	Fold axis	Haa + Pac	48	273.6	1 - Most reliable	55	188.6	FA	David Gray	Proterozoic	11/11/2020	DG20.48.2	411974	5327887	10m	GPS
Central Tyennan	Fold axis	Haa	35	198.6	1 - Most reliable			FA	David Gray	Proterozoic	11/11/2020	DG20.48.3	411974	5327887	10m	GPS
Central Tyennan	Shear Band	Sau	45	283.6	1 - Most reliable			Sb	David Gray	Proterozoic	11/11/2020	DG20.48.4	411974	5327887	10m	GPS
Central Tyennan	Metamorphic Foliation	Sag	50	278.6	1 - Most reliable			Sm	David Gray	Proterozoic	11/11/2020	DG20.48.4	411974	5327887	10m	GPS
Central Tyennan	Lineation	Lae	25	323.6	1 - Most reliable			Lm	David Gray	Proterozoic	11/11/2020	DG20.48.5	411974	5327887	10m	GPS
Central Tyennan	Metamorphic Foliation	Sag	45	248.6	1 - Most reliable			Sm	David Gray	Proterozoic	11/11/2020	DG20.48.5	411974	5327887	10m	GPS
Central Tyennan	Lineation	Lae	20	243.6	1 - Most reliable			Lm	David Gray	Proterozoic	11/11/2020	DG20.48.6	411974	5327887	10m	GPS
Central Tyennan	Metamorphic Foliation	Sag	22	253.6	1 - Most reliable			Sm	David Gray	Proterozoic	11/11/2020	DG20.48.6	411974	5327887	10m	GPS
Central Tyennan	Lineation	Lae	35	263.6	1 - Most reliable			Lm	David Gray	Proterozoic	11/11/2020	DG20.49.1	412041	5327847	10m	GPS
Central Tyennan	Metamorphic Foliation	Sag	45	268.6	1 - Most reliable			Sm	David Gray	Proterozoic	11/11/2020	DG20.49.1	412041	5327847	10m	GPS
Central Tyennan	Fold axis	Haa + Pac	50	243.6	1 - Most reliable	54	243.6	FA	David Gray	Proterozoic	11/11/2020	DG20.49.2	412041	5327847	10m	GPS
Central Tyennan	Metamorphic Foliation	Sag	25	258.6	1 - Most reliable			Sm	David Gray	Proterozoic	11/11/2020	DG20.49.2	412041	5327847	10m	GPS
Central Tyennan	Lineation	Lae	33	308.6	1 - Most reliable			Lm	David Gray	Proterozoic	11/11/2020	DG20.49.3	412041	5327847	10m	GPS
Central Tyennan	Metamorphic Foliation	Sag	40	258.6	1 - Most reliable			Sm	David Gray	Proterozoic	11/11/2020	DG20.49.3	412041	5327847	10m	GPS
Central Tyennan	Lineation	Lae	40	311.6	1 - Most reliable			Lm	David Gray	Proterozoic	11/11/2020	DG20.50.1	412446	5328187	10m	GPS
Central Tyennan	Metamorphic Foliation	Sag	55	275.6	1 - Most reliable			Sm	David Gray	Proterozoic	11/11/2020	DG20.50.1	412446	5328187	10m	GPS

Projects	Structure	Structure Type	Dip	D/Direct	Reliability	Secondary Dip	Secondary Dip Direc-tion	Comments	Originators	Chronostra-tigraphy	Collection Date	Field #	East	North	Accu-racy	Location Method
Central Tyennan	Metamorphic Foliation	Sag	83	243.6	1 - Most reliable			Sm	David Gray	Proterozoic	11/11/2020	DG20.51.1	424130	5325672	10m	GPS
Central Tyennan	Shear Band	Sau	50	88.6	1 - Most reliable			Sb	David Gray	Proterozoic	11/11/2020	DG20.51.2	424130	5325672	10m	GPS
Central Tyennan	Metamorphic Foliation	Sag	65	93.6	1 - Most reliable			Sm	David Gray	Proterozoic	11/11/2020	DG20.51.2	424130	5325672	10m	GPS
Central Tyennan	Fold axis	Has + Par	35	178.6	1 - Most reliable	80	263.6	F3 fold	David Gray	Proterozoic	11/11/2020	DG20.51.3	424130	5325672	10m	GPS
Central Tyennan	Compositional Layering	Sak	85	358.6	1 - Most reliable			So/Sm	David Gray	Proterozoic	11/11/2020	DG20.52.1	424089	5325670	10m	GPS
Central Tyennan	Compositional Layering	Sak	80	353.6	1 - Most reliable			So/Sm	David Gray	Proterozoic	11/11/2020	DG20.52.2	424089	5325670	10m	GPS
Central Tyennan	Fold axis	Haa + Pac	70	355.6	1 - Most reliable	80	278.6	FA	David Gray	Proterozoic	11/11/2020	DG20.52.3	424089	5325670	10m	GPS
Central Tyennan	Fold axis	Hal	44	263.6	1 - Most reliable			FA Early	David Gray	Proterozoic	11/11/2020	DG20.52.4	424089	5325670	10m	GPS
Central Tyennan	Metamorphic Foliation	Sag	85	273.6	1 - Most reliable			Sm	David Gray	Proterozoic	11/11/2020	DG20.52.5	424089	5325670	10m	GPS

Tasmanian
Government

Mineral Resources Tasmania
PO Box 56 Rosny Park
Tasmania Australia 7018
Ph: +61 3 6165 4800

info@mrt.tas.gov.au www.mrt.tas.gov.au